

NASA CR-169, 146

NASA-CR-169146
19820021468

FILTER FAILURE DETECTION FOR
SYSTEMS WITH LARGE SPACE
STRUCTURE DYNAMICS

Craig R. Carignan

June, 1982

SSL#1-82

(Under NASA Grant #NAG1-126)



LIBRARY COPY

AUG 30 1984

LANGLEY RESEARCH CENTER
LIBRARY, NASA
HAMPTON, VIRGINIA

SPACE SYSTEMS LABORATORY
DEPT. OF AERONAUTICS AND ASTRONAUTICS
MASSACHUSETTS INSTITUTE OF TECHNOLOGY
CAMBRIDGE, MA 02139

FILTER FAILURE DETECTION FOR
SYSTEMS WITH LARGE SPACE
STRUCTURE DYNAMICS

Craig R. Carignan

June, 1982

SSL#1-82

(Under NASA Grant #NAG1-126)

FILTER FAILURE DETECTION FOR SYSTEMS
WITH LARGE SPACE STRUCTURE DYNAMICS

by

CRAIG RAYMOND CARIGNAN

Submitted to the Department of Aeronautics and
Astronautics on May 14, 1982 in partial
fulfillment of the requirements for the
Degree of Master of Science in
Aeronautics and Astronautics

ABSTRACT

A failure detection filter is applied to the detection of actuator and sensor failures on a free-free beam. Computer simulation tests are used to verify the filter design and study the effect of unmodeled modes on filter performance.

In actuator tests, the failure signal to spillover noise ratio was found to be greatest when the filter bandwidth was 5 rad/sec beyond the input frequency. Observation spillover, however, was found to vary widely in tests run under similar conditions (same input frequency and filter poles) but with different detector gains.

In sensor tests, the maximum signal-to-noise ratio for varying filter bandwidth depended upon the initial conditions placed on the unmodeled modes; the performance was good even for initial amplitudes on the first unmodeled mode 7.5% of that on the last modeled mode.

Data-sampling tests on filters designed for continuous data processing but employed in a sampled data mode revealed that adequate filter performance could be achieved only when the sampling rate was considerably beyond the natural frequency of the last system mode. Stability problems were encountered when the filter bandwidth became too high relative to the sampling rate.

The failure simulation tests suggest high sampling rates and sensor post-filtering to deal with the problems posed by sampling phase lag and observation spillover.

Thesis Supervisor: Wallace E. Vander Velde
Professor of Aeronautics and Astronautics

ACKNOWLEDGMENTS

This thesis is not the result of one person's work, but rather the result of advice and help from many people. In view of this, I would like to express my gratitude and thanks to the following people: my thesis advisor, Professor Wally Vander Velde, for his expert help and guidance throughout this thesis, Professor Rene Miller for his advice and encouragement in this and previous work, and Barbara for typing this thesis. My acknowledgments would not be complete without thanking my friends in the Space Systems Lab and my family for their encouragement and support.

I would also like to express my appreciation to the National Aeronautics and Space Administration for sponsoring this work under NASA Grant #NAG1-126, "Reliability Issues in Active Control of Flexible Space Structures."

Table of Contents

	<u>Page</u>
1. Introduction	7
2. Detection Filter Theory	11
2.1 Detection filter structure	11
2.2 Failure models	14
2.3 Detection filter design	17
2.3.1 Fully measurable systems	18
2.3.2 Partially measurable systems	19
2.3.2.1 Detection generator	20
2.3.2.2 Detector gain	22
2.3.2.3 Detection space	24
2.3.3 Sensor detectability	26
2.3.4 Sets of events	30
2.3.4.1 Actuator set	31
2.3.4.2 Sensor set	31
2.4 Two-mode Design Example	33
3. Computational Design of Filter	38
3.1 Orthogonal Reduction	38
3.2 Input Failure Event Design	41
3.2.1 Subroutine SEPDET	42
3.2.2 Subroutine DETGEN	44
3.2.3 Subroutine DGAIN	46
3.3 Measurement failure event design	48

	<u>Page</u>
4. Application to Flexible Beam	51
4.1 NASA LaRC Experimental Beam	51
4.2 State equations for beam model	53
4.3 Failure detection filter design for the beam	56
4.4 Computer simulation of beam	58
4.4.1 Effect of model error	61
4.4.2 Sampled-data systems	75
5. Summary and Conclusions	81
Appendix A: Failure Detection Filter program (FDFIL)	84
Appendix B: Beam Simulation Program (FDSIM)	99
References	105

List of Illustrations	<u>Page</u>
2.1 Failure detection filter block diagram	12
2.2 Eigenvalue assignment for detection filter	12
3.1 Flowchart for ORTRED	39
3.2 Flowchart for SEPDET	43
3.3 Flowchart for DETGEN	45
3.4 Flowchart for DGAIN	47
3.5 Sensor design process schematic	49
4.1 LaRC experimental beam set-up	52
4.2 SPAR beam modal frequencies and shapes	54
4.3 Output error transformation for sensor case	60
4.4 Sampled-data system/filter	60
4.5 Actuator failure for matched models	64
4.6 Model error effect for different filter models	65
4.7 Actuator tests for $\lambda^+ = -10$ and $\omega_u^+ = 5, 20, 50$	68
4.8 Actuator tests for $\lambda = -15$ and $\omega_u = 5, 20, 50$	69
4.9 Actuator tests for $\lambda = -20$ and $\omega_u = 5, 20, 50$	70
4.10 Sensor tests for various initial conditions	73
4.11 Sensor tests for various filter bandwidths	74
4.12 Data sampling tests for various sampling rates	78
4.13 Data sampling tests for various filter bandwidths	79

$+\lambda$ denotes filter poles (rad/sec)

ω_u denotes input frequencies (rad/sec)

CHAPTER I

INTRODUCTION

With the advent of the space shuttle, aerospace engineers are contemplating the assembly and deployment of some very large space structures. Some structures under consideration include antennas and reflectors 100 meters in diameter and solar power satellites as large as 20 x 10 kilometers. Unlike the spacecraft of previous decades, these large structures have little inherent rigidity due to their low mass and large size. If the natural damping is not somehow increased, periodic disturbances such as gravity gradient and solar pressure which are close to the low natural frequencies of the structure will cause large dynamic overstresses that will eventually tear the structure apart.

The solar power satellite provides a good example of the types of overwhelming issues one would typically encounter in designing a control system for a large space structure. In order to adequately damp the many vibrational modes of the satellite, hundreds of thrusters and control moment gyros may be required to supplement passive damping. The system designer will have to decide how many actuators and sensors to use and where to place them on the structure. For example, rate gyro sensors and control moment gyros could be located almost anywhere on a truss-like structure. The control engineer will then have to decide what kind of control law to implement in order to maintain satisfactory structural rigidity. Obviously,

the control system cannot incorporate all the structural modes in its model, so care must be taken when controlling the disturbance-induced vibrations in the low frequency modes that the control does not spillover into the higher frequency unmodeled modes.

One factor which should not be overlooked in either the design or operation of the control system is the likelihood of some failures among actuators and sensors. For example, if the interval between maintenance visits is three years and the control system utilizes a total of 400 sensors and actuators each with an exponential distribution of time to failure with a mean time to failure of 100,000 hours, the expected number of failures in this interval is 92, and the probability that there will be no failures is 2×10^{-46} . Thus even with a very optimistic mean time to failure, it is virtually certain that failures will occur.

One of the major issues in dealing with component unreliability in control systems is how to detect a failure and identify the failed component. This thesis is concerned with one method of doing failure detection and identification (FDI).

Many approaches to FDI have been used, the simplest of which involves triplication of components: a discrepancy between the signals of two like sensors signifies a failure, and comparison with the third determines which of the two has failed. Though simple, this method rapidly becomes costly and

even bulky for certain applications.

There are several approaches to FDI which require specification of failure modes ahead of time, but one which does not is generalized parity relations.⁵ This method uses sensor data from several time steps to detect failures rather than data from duplicate sensors at the same time instant. This approach has the obvious advantage of requiring fewer components, but it turns out to be very susceptible to plant disturbances and sensor noise. This detection routine also performs poorly when there is model error present, whether it be in the form of modal truncation or frequency errors.

A closed-loop method, the failure detection filter, can simultaneously monitor many different types of components, including sensors, actuators, and dynamic elements of the system. As with any other observer, the detection filter incorporates a linear-dynamic model of the system to estimate the true states of the system. Since the model receives the same control inputs as the true system, the outputs of the system and filter will normally match resulting in an output error of zero. However, when a component fails, the output error will no longer be zero, signifying that a failure has occurred. The failed component can then be identified by the fixed line or plane to which the output error is restricted by the detection filter.

The failure detection filter was first proposed by

Beard (1) in 1971 for deterministic systems. The theory was later expanded by Jones (2) to stochastic and sampled-data systems. Though not strictly valid for sampled-data systems, the detection filter will behave satisfactorily for sufficiently high sampling rates. Besides the application by Jones to a lateral mode autopilot, the failure detection filter was applied by VanderVelde (8) and Gerard (9) to the computer control of a guideway vehicle, and by Meserole (3) to fault-tolerant control of a turbofan engine. In neither of these previous applications was the filter designed to detect a sensor failure when the sensor output was not measuring a state directly. This is also the first time model error has been introduced into the filter.

The next chapter summarizes the main concepts of failure detection theory along with an analytic design procedure for the filter. Chapter 3 proposes a computational design procedure for the deterministic filter based mainly upon algorithms suggested in Appendix A of Beard (1). In Chapter 4, simulation results of actuator and sensor failures in deterministic systems are presented along with some results on data-sampling. Finally, some conclusions are outlined in Chapter 5.

CHAPTER II

FAILURE DETECTION FILTER THEORY

Detection filter theory is based upon vector-space concepts involving the state estimation errors generated by the filter following component failures. The major feature of the failure detection filter is that the output error is small while the system is functioning normally, and following the failure of a system component that error is significantly larger and appears only in a single direction or plane—that direction or plane indicating which component has failed. Thus the filter provides the basis for both detection of component failures and isolation of the faulty component. It is not necessary to specify in advance the possible modes of component failures.

In this chapter, the structure of the failure detection filter is first presented along with failure models for both actuator and sensor malfunctions and plant dynamics changes. The concept of failure "detectability" will then be introduced followed by the filter design theory for both fully measurable systems ($\text{rank } C=n$) and partially measurable systems ($\text{rank } C < n$). Finally, a two-mode beam example is used to illustrate the analytic design procedure.

2.1 Detection Filter Structure

The structure of the failure detection filter depicted in Fig. 2.1 is the same as that of any other state estimation

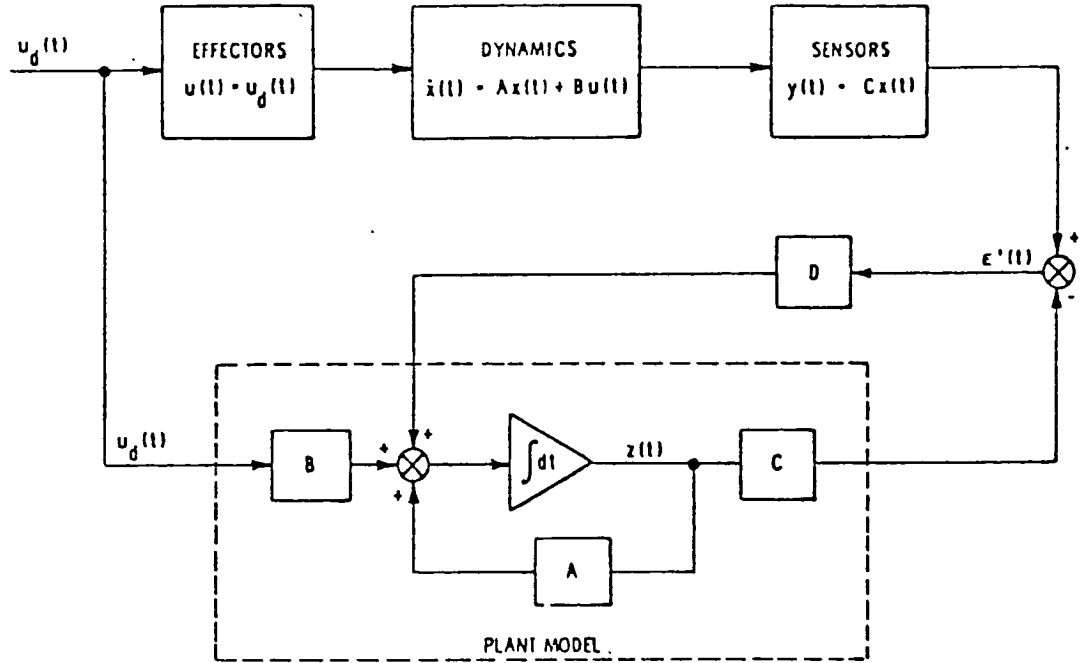


Fig. 2.1: Failure detection filter block diagram.
(taken from reference[1])

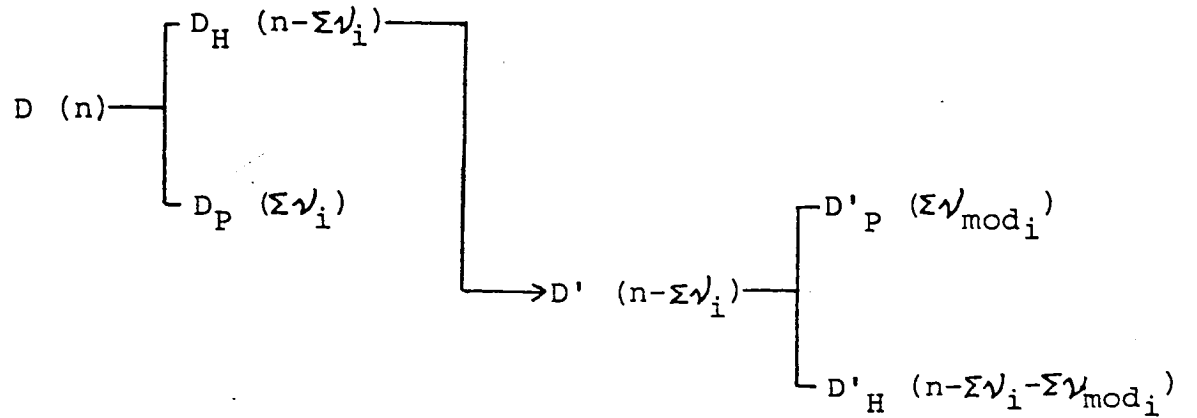


Fig. 2.2: Eigenvalue assignment for detection filter
(number in parentheses indicates the number of
eigenvalues of $[A-DC]$ assigned with that gain).

filter monitoring a linear time invariant system. The difference is in the feedback gain D which is designed so that the output error will be held to a fixed direction or plane depending upon what component has failed. If D were the Kalman gain, the filter would minimize the mean square error between the states $\underline{x}(t)$ and the filter estimates $\hat{\underline{x}}(t)$ when noise is introduced into the system. For the case of an observer, $\hat{\underline{x}}(t)$ approaches $\underline{x}(t)$ asymptotically since no noise is present.

The system being monitored by the detection filter must be linear, time-invariant, and observable. The consequences of unobservability will be pointed out as they are encountered. In this work, mainly continuous inputs and measurements are considered.

The system is represented by the linear equations:

$$\begin{aligned}\dot{\underline{x}}(t) &= A \underline{x}(t) + B \underline{u}(t) \\ \underline{y}(t) &= C \underline{x}(t)\end{aligned}\tag{2.1-1}$$

where the state vector $\underline{x}(t)$ has dimension n , the control vector $\underline{u}(t)$ has m inputs, and the measurement vector $\underline{y}(t)$ has p outputs.

The filter incorporates the model:

$$\begin{aligned}\dot{\hat{\underline{x}}}(t) &= A \hat{\underline{x}}(t) + B \underline{u}(t) + D [\underline{y}(t) - \hat{\underline{y}}(t)] \\ \hat{\underline{y}}(t) &= C \hat{\underline{x}}(t)\end{aligned}\tag{2.1-2}$$

where $\hat{\underline{x}}$ is the filter state vector and $\hat{\underline{y}}(t)$ the predicted measurement vector.

The state and measurement error dynamics are

$$\begin{aligned}\dot{\underline{e}}(t) &= [A - DC] \underline{e}(t) \\ \underline{e}(t) &= C \underline{e}(t)\end{aligned}\tag{2.1-3}$$

where $\underline{e}(t) \triangleq \underline{x}(t) - \hat{\underline{x}}(t)$ and $\underline{\epsilon}(t) = \underline{y}(t) - \hat{\underline{y}}(t)$. If the eigenvalues of $A-DC$ have negative real parts, the steady state error will be zero so $\hat{\underline{x}}(t)$ will track $\underline{x}(t)$. Equation 2.1-3 is valid, however, only when $\{A,B,C\}$ of the filter in (2.1-2) match that of the true system represented by (2.1-1).

2.2 Failure Models

As mentioned above, (2.1-3) is valid only when the triplets $\{A,B,C\}$ characterizing the system and filter match. If there is a component failure or change in plant dynamics, (2.1-1) will no longer represent the true system.

Consider an actuator j that has either failed completely or gone awry. The control vector, $\underline{u}(t)$, is given by

$$\underline{u}(t) = \underline{u}_c(t) + \hat{\underline{e}}_{m_j} n(t) \quad (2.2-1)$$

where $\underline{u}_c(t)$ is the commanded input (and filter input), $\hat{\underline{e}}_{m_j}$ is a unit vector in the j^{th} direction of dimension m , and $n(t)$ is a scalar time function depending upon the type of failure. The new state equation becomes

$$\dot{\underline{x}}(t) = A\underline{x}(t) + B\underline{u}_c(t) + \underline{b}_j n(t) \quad (2.2-2)$$

where \underline{b}_j is the column of B corresponding to the j^{th} actuator and $n(t)$ is some scalar time function. If the actuator fails completely in the off mode, $n(t)$ is simply minus the j^{th} input, $-\underline{u}_{c_j}(t)$, and the control effectiveness matrix for the true system is the same as for the filter except that the j^{th} column of B is deleted.

Subtracting (2.1-2) from (2.2-2), the error equations become

$$\begin{aligned}\dot{\underline{e}}(t) &= [A-DC] \underline{e}(t) + \underline{b}_j n(t) \\ \underline{\xi}(t) &= \underline{C} \underline{e}(t)\end{aligned}\tag{2.2-3}$$

The vector \underline{b}_j is called the "event vector" because it is the driving vector in the event of failure of the j^{th} actuator. Detection filter theory will show that for any event vector \underline{f} , it is possible to find a D such that $\underline{\xi}(t)$ maintains a fixed direction in response to $\underline{f}n(t)$.

Similarly, consider a sensor failure represented by the new measurement relation

$$\underline{y}(t) = \underline{C} \underline{x}(t) + \hat{\underline{e}}_{p_j} n(t)\tag{2.2-4}$$

where $\hat{\underline{e}}_{p_j}$ is a unit vector in the j^{th} direction and $n(t)$ is an arbitrary scalar function of time. Complete failure of the j^{th} sensor in the zero-output mode is modeled by letting $n(t) = -\underline{C}_j^T \underline{x}(t)$, the predicted sensor output, and the measurement matrix for the true system is that of the filter with the j^{th} row deleted.

The new error equations are generated analogously with (2.2-4) replacing $\underline{y}(t)$ in (2.1-1):

$$\begin{aligned}\dot{\underline{e}}(t) &= [A-DC] \underline{e}(t) - \underline{d}_j n(t) \\ \underline{\xi}(t) &= \underline{C} \underline{e}(t) + \hat{\underline{e}}_{p_j} n(t)\end{aligned}\tag{2.2-5}$$

Unlike the actuator case, the output error in the sensor failure

mode will have two directions: \hat{e}_{p_j} due directly to the sensor failure and another component caused by the measurement error effect in the filter feedback loop. Even though D can be chosen to make $\underline{e}(t)$ due to \underline{d}_j unidirectional, this direction will usually not be \hat{e}_{p_j} , and therefore the output error will span a plane rather than lie in a fixed direction.

Finally, let us consider changes in plant dynamics. Let the ij^{th} element of A , for instance, change by the amount Δa_{ij} . The new state equation is:

$$\dot{\underline{x}}(t) = A\underline{x}(t) + B\underline{u}(t) + \Delta a_{ij}x_j(t)\hat{e}_{n_i} \quad (2.2-6)$$

This model represents the effect of an alteration in the derivative of $x_i(t)$ due to dynamics involving $x_j(t)$. The error equations become

$$\begin{aligned} \dot{\underline{e}}(t) &= [A - DC]\underline{e}(t) + \Delta a_{ij}x_j(t)\hat{e}_{n_i} \\ \underline{e}(t) &= C\underline{e}(t) \end{aligned} \quad (2.2-7)$$

Comparing this with Eq. (2.2-3), we see that the two pairs of equations have the same form with the scalar time function in this case being $\Delta a_{ij}x_j(t)$ and the new event vector as the n -dimensional i^{th} unit vector.

Actuator and plant dynamics failure models are, in fact, called "input failure models" since both can be represented as extraneous additive inputs to the system. When the failure term also appears in the measurement equation [as in Eq. (2.2-5) for sensor failures], the error equations are referred to as

the "measurement failure models." Only the actuator input and measurement failures will be considered in this work.

2.3 Detection Filter Design

The preceding discussion of failure models motivates the following definition of "detectability" found in Beard [1]: The event associated with the vector \underline{f} in the state error equation

$$\dot{\underline{e}}(t) = [A - DC]\underline{e}(t) + \underline{f}n(t) \quad (2.3-1)$$

is "detectable" if there exists a gain matrix D such that:

- (i) $C\underline{e}_p(t)$ maintains a fixed direction in the output space ($\underline{e}_p(t)$ is the settled-out solution of Eq. 2.3-1)
- (ii) All the eigenvalues of $(A - DC)$ can be arbitrarily specified (this condition may be relaxed for fixed but stable eigenvalues).

If \underline{f} is detectable, then one can identify the failed component by checking the direction of the output error. For a measurement failure, the definition of detectability must be revised (see Section 2.3.3) and the output error is confined to a plane.

In the next several sections, the design of D for both fully measurable systems ($\text{rank } C = n$) and partially measurable systems ($\text{rank } C < n$) will be presented. Finding D for the first case is simple since the state vector $\underline{x}(t)$ can be solved uniquely given $\underline{y}(t)$. However, when the state vector is not fully measurable, the design of D is much more difficult and generates the need for a more advanced methodology.

2.3.1 Fully Measurable Systems

Let NS be the number of sensors or rows of C . To satisfy condition (ii) of detectability, choose $A-DC$ to equal $-\sigma I$ where σ is a positive scalar constant. Then the eigenvalues of $A-DC$ are all $-\sigma$ and D is given uniquely by

$$D = (A + \sigma I) C^{-1} \quad (2.3-2)$$

for $\text{rank} C = n = NS$ and nonuniquely as

$$D = (A + \sigma I) (C^T C)^{-1} C^T \quad (2.3-3)$$

for $\text{rank} C = n < NS$.

For an actuator failure, $\underline{f} = \underline{b}_i$ and the solution of Eq. (2.2-3) is

$$\begin{aligned} \underline{e}(t) = & e^{-\sigma(t-t_0)} \underline{e}(t_0) \\ & + \int_{t_0}^t e^{-\sigma(t-\tau)} \underline{b}_i n(\tau) d\tau \end{aligned} \quad (2.3-4)$$

The first term on the right is due to the initial conditions of the filter and will asymptotically approach zero for $\sigma > 0$. The second term is the driven or settled solution—it comes about because the filter models the i^{th} actuator as working properly ($\underline{u}(t) = \underline{u}_c(t)$) whereas in actuality it is not.

Since \underline{b}_i is constant, the settled-out solution is

$$\underline{e}_s(t) = \underline{b}_i \int_{t_0}^t e^{-\sigma(t-\tau)} n(\tau) d\tau \quad (2.3-5)$$

Therefore, $\underline{e}_s(t)$ lies in the direction \underline{b}_i and a settled output error in the direction $C\underline{b}_i$ indicates a malfunction of the i^{th}

actuator.

Now consider a failure in the i^{th} sensor as modeled by (2.2-4). Retaining the same choice for A-DC, the solution to (2.2-5) is

$$\underline{e}(t) = e^{-\sigma(t-t_0)} \underline{e}(t_0) - D \hat{\underline{e}}_{pi} \int_{t_0}^t e^{-\sigma(t-\tau)} n(\tau) d\tau \quad (2.3-6)$$

The settled output error is given by

$$\underline{e}_s(t) = -CD \hat{\underline{e}}_{pi} \int_{t_0}^t e^{-\sigma(t-\tau)} n(\tau) d\tau + \hat{\underline{e}}_{pi} n(t)$$

Therefore, an output error lying in the plane spanned by $CD \hat{\underline{e}}_{pi}$ and $\hat{\underline{e}}_{pi}$ indicates a failure of the i^{th} sensor.

Thus we see that finding D in the fully measurable case is indeed trivial and given by (2.3-2) for A-DC = $-\sigma I$. Choosing A-DC = $-\sigma I$ enabled the assignment of eigenvalues directly and also produced readily identifiable output error directions for component malfunctions because of the simple form of the state error transition matrix.

2.3.2 Partially Measurable Systems

Because C is not invertible in partially measurable systems, D cannot be solved by a simple relation like (2.3-2). What this means physically is that when an event occurs, an actuator failure for instance, the output error which results will not be uniquely associated with the state error caused by the event. Thus since the output error is the only accessible

signal, D will not be unique in satisfying the conditions of detectability. It will therefore be necessary to explore the relation of D to the space spanned by state errors during an event.

2.3.2.1 Detection Generator

Consider the system equations (2.1-1) for the case of a single actuator:

$$\dot{\underline{x}}(t) = A\underline{x}(t) + \underline{b}_i u(t) \quad (2.3-7)$$

From linear systems theory, the controllable space of $u(t)$, [the space of states which are possible to reach from the origin using $u(t)$] is the range space of

$$W_i \triangleq [\underline{b}_i \mid A\underline{b}_i \mid \cdots \mid A^{n-1}\underline{b}_i] \quad (2.3-8)$$

The event vector \underline{f} has a similar meaning with respect to the error space $\underline{e}(t)$ of (2.3-1). In this case, the error space that can be reached in the event of a failure is the range space of

$$W_f = [\underline{f} \mid (A-DC)\underline{f} \mid \cdots \mid (A-DC)^{n-1}\underline{f}] \quad (2.3-9)$$

or the "detection space" of \underline{f} . The output error space therefore spans CW_f , and condition (i) of detectability is satisfied only if the rank of CW_f is 1. Any matrix D which satisfies this condition is called a "detector gain" for \underline{f} .

Associated with \underline{f} is another vector also in W_f defined by the following theorem proven in Beard:

Detection generator theorem -

If (i) (A, C) is an observable pair

(ii) $\text{rank } W_f = k$

(iii) $\text{rank } CW_f = 1$

Then there exists an n -vector \underline{g} in W_f such that

$$[C \mid CA \mid \cdots \mid CA^{k-2}] \underline{g} = \underline{0} \quad (2.3-10)$$

and

$$CA^{k-1} \underline{g} \neq \underline{0}$$

The latter relation in (2.3-10) guarantees that the controllable space of \underline{g} with respect to $(A-DC)$ is of dimension k and so matches the controllable space of \underline{f} . Note also that the first equation in (2.3-10) yields

$$\begin{aligned} & [\underline{g} \mid (A-DC)\underline{g} \mid \cdots \mid (A-DC)^{k-1}\underline{g}] \\ &= [\underline{g} \mid A\underline{g} \mid \cdots \mid A^{k-1}\underline{g}] \end{aligned} \quad (2.3-11)$$

so the set of vectors $\{\underline{g}, A\underline{g}, \dots, A^{k-1}\underline{g}\}$ form a basis for the controllable space of \underline{f} .

Since \underline{f} is the generator of W_f , it can be expressed as

$$\underline{f} = \alpha_1 \underline{g} + \alpha_2 A\underline{g} + \cdots + \alpha_k A^{k-1} \underline{g} \quad (2.3-12)$$

where the α_i are scalars. Premultiplying by C and using (2.3-10),

$$C\underline{f} = \alpha_k CA^{k-1} \underline{g} \quad (2.3-13)$$

If $C\underline{f} \neq 0$, then $\alpha_k \neq 0$, and since the magnitude of \underline{g} is not restricted by (2.3-10), we are free to choose $\alpha_k = 1$.

If in general, for some nonnegative integer μ ,

$$\begin{aligned} CA^j \underline{f} &= \underline{0} & j = 0, \dots, \mu-1 \\ CA^\mu \underline{f} &\neq \underline{0} \end{aligned} \quad (2.3-14)$$

then

$$\begin{aligned} \alpha_{k-j} &= 0 & \text{for } j = 0, \dots, \mu-1 \\ \alpha_{k-\mu} &\neq 0 \end{aligned} \quad (2.3-15)$$

and \underline{g} is chosen so that $\alpha_{k-\mu} = 1$. The fact that (A, C) is an observable pair will guarantee that (2.3-14) holds for $\mu \leq k-1$. Using (2.3-15) in (2.3-12) yields

$$\underline{f} = \alpha_1 \underline{g} + \dots + \alpha_{k-\mu-1} A^{k-\mu-2} \underline{g} + A^{k-\mu-1} \underline{g} \quad (2.3-16)$$

where μ satisfies (2.3-14).

The n-vector \underline{g} which satisfies (2.3-10) and (2.3-16) is called a k^{th} order "detection generator" for \underline{f} . The detection generator theorem has shown that as long as (A, C) is an observable pair, there always exists a detection generator associated with a detector gain.

2.3.2.2 Detector Gain

The preceding development of the detection generator serves as a prelude to the following theorem from which D can be found:

Detector gain theorem -

If (i) (A, C) is an observable pair

(ii) $\text{rank } W_f = k$

(iii) $\text{rank } CW_f = 1$

and k eigenvalues of $[A-DC]$ associated with W_f

are given by the roots of

$$S^k + p_k S^{k-1} + \dots + p_2 S + p_1 = 0 \quad (2.3-17)$$

Then D is a solution of

$$DCA^{k-1}\underline{f} = p_1 \underline{g} + p_2 A\underline{g} + \dots + p_k A^{k-1}\underline{g} + A^k \underline{g} \quad (2.3-18)$$

where p_i are scalars and \underline{g} is a k^{th} order detection generator for \underline{f}

Conversely, any D satisfying (2.3-18) is a detector gain for \underline{f} and k eigenvalues of $[A-DC]$ associated with W_f are given by the roots of (2.3-17).

This theorem is perhaps the main result of detection filter theory and follows mainly from the Cayley-Hamilton Theorem applied to $[A-DC]$ and invoking (2.3-11).

Premultiplying (2.3-16) by CA^μ and using (2.3-10) yields

$$CA^\mu \underline{f} = CA^{k-1} \underline{g} \quad (2.3-19)$$

which when substituted into (2.3-18) gives

$$DCA^\mu \underline{f} = p_1 \underline{g} + \dots + p_k A^{k-1} \underline{g} + A^k \underline{g} \quad (2.3-20)$$

where $\mu = 0$ corresponds to the condition $C\underline{f} \neq 0$. The rest of the results will be derived for $\mu = 0$, but the corresponding general results can be obtained by simply replacing \underline{f} by $A^\mu \underline{f}$.

The general solution of (2.3-20) is expressible in the form

$$D = D_p + D_h$$

where

$$\begin{aligned} D_p &= q_D [(C\underline{f})^T C\underline{f}]^{-1} (C\underline{f})^T \\ D_h &= D' [I - C\underline{f} [(C\underline{f})^T C\underline{f}]^{-1} (C\underline{f})^T] \end{aligned} \quad (2.3-21)$$

with q_D being the right side of (2.3-20) and D' an arbitrary

matrix the same dimensions as D . D_p is the particular solution of D and satisfies (2.3-20). Therefore, D_p is alone sufficient to guarantee condition (i) of detectability and specify k eigenvalues of $[A-DC]$. D_H is the homogeneous solution of D , i.e., $D_H C \underline{f} = \underline{0}$, and represents the freedom left in D after having satisfied (2.3-20). Condition (ii) of detectability will be satisfied only if the remaining $n-k$ eigenvalues of $[A-DC]$ can be assigned using D' .

2.3.2.3 Detection Space

Beard proposes the following auxiliary lemma to show that the remaining eigenvalues of $[A-DC]$ can be assigned (the actual assignment of these remaining eigenvalues is discussed in Chapter 3):

Auxiliary detector gain lemma —

For A' , C' , and D' given by

$$\begin{aligned} A' &= A - q_0 [(C \underline{f})^T C \underline{f}]^{-1} (C \underline{f})^T C \\ C' &= C - C \underline{f} [(C \underline{f})^T C \underline{f}]^{-1} (C \underline{f})^T C \\ D' &\text{ arbitrary} \end{aligned} \quad (2.3-22)$$

The number of eigenvalues of $[A'-D'C'] = [A-DC]$ that can be specified by D' is $q' = \text{rank } M'$ where

$$M' = [C' \mid C'A' \mid \cdots \mid C'A'^{n-1}]^T \quad (2.3-23)$$

This lemma shows that the total number of eigenvalues of $[A-DC]$ that can be specified while constraining D to be a detector gain is $k + q'$. Therefore, condition (ii) of detectability will be satisfied only if $n = k + q'$.

The next lemma shows that M' does not depend upon the particular detection generator used or its order k even though it

appears to through A' :

Detection space theorem —

For K defined by

$$K = A - A \underline{f} [(\underline{C} \underline{f})^T \underline{C} \underline{f}]^{-1} (\underline{C} \underline{f})^T \underline{C}$$

M' is also equivalent to

$$M' = [C' | C'K | \dots | C'K^{n-1}]^T \quad (2.3-24)$$

Since C' and K depend only on A , C , and \underline{f} , M' is the same regardless of what detection generator is used. Thus the number of eigenvalues of $[A-DC]$ that can be specified while constraining D to be a detector gain is always the same no matter what \underline{g} is used to find D_p . The null space of M' is called the "detection space" of \underline{f} and corresponds to the controllable space of \underline{f} with respect to $[A-DC]$. The dimension of the detection space is called the "detection order" ν , and a detection generator of order ν is called the "maximal generator" for \underline{f} .

The rank of the null space of M' is $\nu = n - q'$, so if q' eigenvalues of $[A-DC]$ are assignable using D' , then a detection generator of order $k = \nu$ is needed to assign all the eigenvalues and satisfy condition (ii) of detectability. Beard shows that if (A,C) is an observable pair, \underline{f} will have a maximal generator and it is unique. Thus, the event \underline{f} is guaranteed detectable if (A,C) is observable. Beard also shows that although observability is necessary to satisfy condition (ii) of detectability, it is not necessary to satisfy condition (i) if \underline{f} is in the observable space. The number of assignable eigenvalues in this case is the rank of the observability matrix M defined by (2.3-23) without

the primes. Therefore, if one is willing to accept n -rank M unassignable eigenvalues, every observable event is detectable in this weaker sense for the unobservable pair (A,C) .

The following theorem summarizes the conditions for detectability:

Detectability Theorem —

Every vector in the state space R^n is detectable if and only if (A,C) is an observable pair.

2.3.3 Sensor Detectability

In deriving (2.2-5), we noted a fundamental difference between measurement and input failures; whereas an actuator failure only drives the state error through the event vector \underline{b}_j , a sensor failure drives the state error through the output feedback term as well as the event vector \underline{d}_j . Consequently, the best the filter can do is constrain the output error to a two-dimensional plane. Even though this was shown only for the fully measurable case, Beard proves this is true for partially measurable systems as well.

Because the event vector \underline{d}_j is at the discretion of the designer and is not related at all to the sensor itself, the theorems in the previous sections are not directly applicable. Instead, the i^{th} row of C will be associated with a sensor failure just as the i^{th} column of B was associated with an actuator failure. This motivates the following modified definition of detectability for sensor failures:

The i^{th} row of C , \underline{c}_i^T , is "sensor-detectable" if there exists a gain matrix D such that:

- (i) $\underline{\epsilon}_p(t)$ is constrained to a 2D-plane (where $\underline{\epsilon}_p(t)$ is the settled-out solution of (2.2-5))
- (ii) the eigenvalues of $[A-DC]$ can be specified arbitrarily

The following theorem is the sensor counterpart to the Detectability Theorem:

Sensor Detectability Theorem —

If (A,C) is an observable pair and \underline{c}_i^T is linearly independent of all the other rows of C , then \underline{c}_i^T is sensor detectable.

The filter design procedure for sensors is stated in two steps which also serve as a basis for the proof of this theorem:

- (1) first choose D to be a detector gain for \underline{f} , by making it a solution of (2.3-20), where

$$C\underline{f}_i = \hat{\underline{e}}_{p_i} \quad (2.3-25)$$

- (2) then make D' a detector gain for \underline{d}_i with respect to the pair (A',C')

Before proving the theorem, we first outline two implications of (2.3-25). First, the existence of \underline{f} is guaranteed because \underline{c}_i^T is linearly independent of the other rows of C (pseudo-inverse of C exists). Therefore by the detectability theorem, \underline{f} is detectable. Second, \underline{d}_i is now fixed because (2.3-20) becomes

$$\underline{d}_i = p_1 \underline{g} + \dots + p_\nu A^{\nu-1} \underline{g} + A^\nu \underline{g} \quad (2.3-26)$$

where ν is the detection order of \underline{f} , and \underline{g} is its maximal generator.

Assume for the moment that \underline{d}_i lies in the observable space of (A',C') and prove that condition (i) of sensor detectability

holds. This assumption plus the detectability theorem guarantee that the detector gain D' exists for the event \underline{d}_i with respect to (A', C') . Furthermore, $C' \underline{e}'_s(t)$ lies in a fixed direction where $\underline{e}'_s(t)$ is the settled-out solution of

$$\dot{\underline{e}}'(t) = (A' - D'C') \underline{e}'(t) - \underline{d}_i n(t) \quad (2.3-27)$$

Since $A' - D'C'$ is equal to $A - DC$, $\underline{e}'_s(t)$ is the settled state error for the pair (A, C) using the gain D as well. This fixed direction can therefore be expressed as

$$C' \underline{e}'_s(t) = \underline{y}_d m_d(t) \quad (2.3-28)$$

where \underline{y}_d is this fixed direction and $m_d(t)$ is a scalar function depending upon $n(t)$.

From (2.3-22), C' is given by

$$C' = C - \hat{\underline{e}}_{p_i} \underline{c}_i^T \quad (2.3-29)$$

so that

$$C \underline{e}'_s(t) = \underline{y}_d m_d(t) + \hat{\underline{e}}_{p_i} \underline{c}_i^T \underline{e}'_s(t) \quad (2.3-30)$$

From (2.2-5), the output error is

$$\underline{\xi}(t) = \underline{y}_d m_d(t) + \hat{\underline{e}}_{p_i} [\underline{c}_i^T \underline{e}'_s(t)] \quad (2.3-31)$$

Since the quantity in brackets is a scalar, $\underline{\xi}(t)$ lies in the plane spanned by \underline{y}_d and $\hat{\underline{e}}_{p_i}$. Beard shows that \underline{y}_d can be broken up into a component in the $\hat{\underline{e}}_{p_i}$ direction and the $CK^{\lambda} A \underline{f}$ direction, where K is given in (2.3-24) and λ is the lowest integer such that $CK^{\lambda} A \underline{f} \neq 0$. Thus the output error lies in the plane formed by $\hat{\underline{e}}_{p_i}$ and $CK^{\lambda} A \underline{f}$.

Let us now relax the assumption that \underline{d}_i lies in the observable space of (A', C') . The observability matrix is given by M' defined

by (2.3-23), so if \underline{d}_i is unobservable, $M' \underline{d}_i = \underline{0}$. Therefore, \underline{d}_i lies in the nullspace of M' , or equivalently, in the detection space of \underline{f} . As Beard shows, every vector contained in the detection space of \underline{f} has the same detection order and detection space as \underline{f} , so D is a detector gain for \underline{d}_i as well as for \underline{f} (i.e., \underline{d}_i is detectable in the traditional sense). Therefore, the second step of making D' a detector gain for \underline{d}_i is unnecessary, and $Ce'_s(t)$ will lie in a fixed direction.

Finally, it remains to show that all the eigenvalues of $A-DC$ are assignable. When making D a detector gain for \underline{f} , ν eigenvalues can be assigned using (2.3-17) since (A,C) is an observable pair. If \underline{d}_i is unobservable with respect to (A',C') , then D' is unconstrained, and the remaining $n-\nu$ eigenvalues are assignable by the free choice of D' by the auxiliary detector gain lemma. Now if \underline{d}_i is observable for (A',C') , a total of only $n-\text{rank } M'$ eigenvalues can be assigned while making D' a detector gain for \underline{d}_i and using D'' , the auxiliary detector gain for D' (D' is the auxiliary detector gain for D). The remaining ν eigenvalues are associated with the unobservable space of (A',C') which coincides with the detection space of \underline{f} and have already been specified by making D a detector gain for \underline{f} . Thus all the eigenvalues are assignable.

One last remark helps to simplify the computation of D' . D' can be made a detector gain for $A\underline{f}$ instead of \underline{d}_i because $A\underline{f} \equiv \underline{d}_i \pmod{E}$, where E denotes the unobservable space of (A',C') . This means that the difference $A\underline{f} - \underline{d}_i$ lies in E . With this substitution, the need to compute (2.3-26) is avoided.

2.3.4 Sets of Events

Up to this point, we have only concerned ourselves with detectability of a single event. Now consider the set of event vectors $\{\underline{f}_1, \dots, \underline{f}_r\}$. The set is considered "mutually detectable" if there exists a D that satisfies the conditions of detectability for all r events. If the set of vectors satisfy

$$\text{rank } CF = r$$

$$F \triangleq [A^{\mu_1} \underline{f}_1, \dots, A^{\mu_r} \underline{f}_r] \quad (2.3-32)$$

with μ defined for each \underline{f}_i as in (2.3-14), then the events are called "output separable." Two events are not output separable if the output error for both events lie in the same direction. All sets of events considered in this work were output separable.

A necessary and sufficient condition for a set of output separable events to be mutually detectable is given by the following theorem:

Group Detection Theorem —

The output separable vectors $\{\underline{f}_1, \dots, \underline{f}_r\}$ are mutually detectable if and only if the sum of the individual detection orders of the \underline{f}_i is equal to the group detection order given by the dimension of the nullspace of M'_G , $(n - \text{rank } M'_G)$, where M'_G is defined as M' in (2.3-24) with \underline{f} replaced by F .

The basic outline of the proof proceeds as follows. Since the set of events $\{\underline{f}_1, \dots, \underline{f}_r\}$ are output separable, the events have nonintersecting subspaces (shown by Beard), and thus ν_i eigenvalues can be specified for each \underline{f}_i while satisfying (2.3-20). An additional $q'_G = \text{rank } M'_G$ eigenvalues can be specified

by free choice of D' . Therefore, condition (ii) of detectability is satisfied if and only if $\sum \nu_i = n - q'_G$. If the set is not mutually detectable, $n - q'_G - \sum \nu_i$ eigenvalues cannot be controlled.

2.3.4.1 Actuator Set

The design of the detection filter for a set of actuator events proceeds as follows:

- (1) determine the maximal generator for each \underline{b}_i using (2.3-10)
- (2) form F as defined in (2.3-32) and divide the set up into output separable subsets
- (3) subdivide the set further, if necessary, until the subsets are also mutually detectable
- (4) solve (2.3-20) for each \underline{b}_i to make D a detector gain for F while using the p_i 's to specify $\sum \nu_i$ eigenvalues
- (5) specify the remaining eigenvalues of $A-DC$ using D'

Step 3 is unnecessary if the uncontrollable eigenvalues resulting from nonmutual detectability are satisfactory. Beard generates an algorithm that aids in finding these fixed eigenvalues and can also expedite step 3.

2.3.4.2 Sensor Set

One design method for a filter detecting sensor failures proceeds as follows:

- (1) for each \underline{c}_i^T , determine \underline{f}_i such that $C\underline{f}_i = \hat{\underline{e}}_{p_i}$ where the sensors are linearly independent
- (2) form F as in (2.3-32) and subdivide into mutually detectable sets (events are automatically output separable by step 1)

(3) form the set of vectors $\{A\underline{f}_1, \dots, A\underline{f}_{k_1}\}$ where $F_{k_1} = \{\underline{f}_1, \dots, \underline{f}_{k_1}\}$ is the set resulting from step 2; let A' and C' be defined as in (2.3-22) with \underline{f} replaced by F_{k_1} ; categorize the $A\underline{f}_i$ as follows, and remove those events falling under (iii):

$$(i) M_F' A\underline{f}_i \neq \underline{0}$$

$$(ii) M_F' A\underline{f}_i = \underline{0} ; \text{rank}\{CA\underline{f}_i, CA'A\underline{f}_i, \dots, CA'^{n-1}A\underline{f}_i\} = 1$$

$$(iii) M_F' A\underline{f}_i = \underline{0} ; \text{rank}\{CA\underline{f}_i, CA'A\underline{f}_i, \dots, CA'^{n-1}A\underline{f}_i\} > 1$$

(4) let $F_{k_2} = \{\underline{f}_1, \dots, \underline{f}_{k_2}\}$ be the set resulting from step 3; let A' and C' be defined as in (2.3-22) with \underline{f} replaced by F_{k_2} ; repeat step 2 with A , C , and \underline{f}_i replaced by A' , C' , and the $A\underline{f}_i$ in category (i); remove $A\underline{f}_i$'s until the $A\underline{f}_i$ are mutually detectable with respect to (A', C') ; if any $A\underline{f}_i$ are removed, some $A\underline{f}_i$ may move from category (ii) to (i) and mutual detectability with the new members must be rechecked

(5) solve (2.3-20) for each \underline{f}_i in the set F_{k_3} resulting from step 4 to make D a detector gain for F_{k_3} while specifying $\sum \nu_i$ eigenvalues

(6) solve (2.3-20) for each $A\underline{f}_i$ in the set F_{k_3} to make D' a detector gain for AF_{k_3} with respect to (A', C') while specifying $\sum \nu_{i_{\text{mod}}}$ eigenvalues ($\nu_{i_{\text{mod}}}$ denotes the maximum order a detection generator for $A\underline{f}_i$ can have)

(7) use D'' to specify the remaining eigenvalues of

$$(A' - D'C') = A - DC \quad [D'' \text{ is to } D' \text{ as } D' \text{ is to } D \text{ in section 2.3.4.1.}]$$

A few remarks concerning step 3 are in order. If category (i) is the case, $A\bar{f}_i$ does not lie in the unobservable space of C' with respect to A' and thus $A\bar{f}_i$ is detectable. For categories (ii) and (iii), $A\bar{f}_i$ does lie in the unobservable space so $A\bar{f}_i$ is not detectable; this is of no consequence, however, if D is a detector gain for $A\bar{f}_i$ as well as \bar{f}_i as is the case for category (ii) (see end of Section 2.3.3). The rank test given in step 3 determines whether the given sequence of vectors lie in a fixed direction—if they do, category (ii) applies.

The assignment of eigenvalues in the last three steps is depicted in Fig. 2.2: $\sum \nu_i$ eigenvalues are assigned using D_p and $n - \sum \nu_i$ are specified using D' ; of the $n - \sum \nu_i$, $\sum \nu_{i_{\text{mod}}}$ are assigned using D'_p and the rest using D'_H which depends on D'' (subscripts P and H denote particular and homogeneous solutions, respectively).

2.4 Two-mode Design Example

As a simple example of the analytic design procedure for the failure detection filter, consider the normal mode equations

$$\ddot{\psi}_r(t) + \omega_r^2 \psi_r(t) = G_r u(t) \quad r=1,2,\dots \quad (2.4-1)$$

where ψ_r represents the amplitude of the r^{th} mode, ω_r its natural frequency, and G_r the amplitude of the input u . In a single degree of freedom mass-spring system, for instance, ψ is just the displacement x and ω^2 is the spring constant k divided by the mass m .

In particular, consider the system of equations for two flexible modes of a beam given in the form (2.1-1):

$$\begin{bmatrix} \dot{\psi}_1 \\ \ddot{\psi}_1 \\ \dot{\psi}_2 \\ \ddot{\psi}_2 \end{bmatrix} = \begin{bmatrix} 0 & 1 & 0 & 0 \\ -\omega_1^2 & 0 & 0 & 0 \\ 0 & 0 & 0 & 1 \\ 0 & 0 & -\omega_2^2 & 0 \end{bmatrix} \begin{bmatrix} \psi_1 \\ \dot{\psi}_1 \\ \psi_2 \\ \dot{\psi}_2 \end{bmatrix} + \begin{bmatrix} 0 & 0 \\ \frac{1}{M}\phi_1(\epsilon_1) & \frac{1}{M}\phi_1(\epsilon_2) \\ 0 & 0 \\ \frac{1}{M}\phi_2(\epsilon_1) & \frac{1}{M}\phi_2(\epsilon_2) \end{bmatrix} \begin{bmatrix} u_1 \\ u_2 \end{bmatrix} \quad (2.4-2)$$

$$\begin{bmatrix} \gamma_1 \\ \gamma_2 \end{bmatrix} = \begin{bmatrix} 0 & \phi_1(\alpha_1) & 0 & \phi_2(\alpha_1) \\ 0 & \phi_1(\alpha_2) & 0 & \phi_2(\alpha_2) \end{bmatrix} \begin{bmatrix} \psi_1 \\ \dot{\psi}_1 \\ \psi_2 \\ \dot{\psi}_2 \end{bmatrix}$$

where force actuators at ϵ_1, ϵ_2 and translation rate sensors at α_1, α_2 are used $[\phi_i(x_j)]$ represents value of the i^{th} mode shape at x_j .

To simplify the design procedure, Beard shows that if the matrix A is replaced by

$$\bar{A} = A - \bar{D}C \quad (2.4-3)$$

with \bar{D} arbitrary, the detector gain is unaffected. Following this suggestion, let's replace A by the simpler form

$$\bar{A} = \begin{bmatrix} 0 & 0 & 0 & 0 \\ -\omega_1^2 & 0 & 0 & 0 \\ 0 & 0 & 0 & 0 \\ 0 & 0 & -\omega_2^2 & 0 \end{bmatrix} \quad (2.4-4)$$

Now let's proceed to design a detection filter that can detect failures of either actuator #1 or actuator #2. The two event vectors for this case are \underline{b}_1 and \underline{b}_2 , the two columns of B. If the two actuators are not both at the same location or placed symmetrically about the center (for a free-free beam), the directions $C\underline{b}_1$ and $C\underline{b}_2$ will be linearly independent and thus output separable. To determine mutual detectability, the detection order for each \underline{f} must be found.

For an appropriate choice of D, K is found from (2.3-24) to be equal to \bar{A} , and C' using (2.3-22) becomes

$$C' = \begin{bmatrix} 0 & C_1 & 0 & C_3 \\ 0 & C_2 & 0 & C_4 \end{bmatrix} \quad (2.4-5)$$

where the C_i 's are functions of the elements of $C\underline{b}$ and C. Now form

$$M' = \begin{bmatrix} C' \\ \hline C'K \\ \hline C'K^2 \\ \hline C'K^3 \end{bmatrix} = \begin{bmatrix} 0 & C_1 & 0 & C_3 \\ \hline 0 & C_2 & 0 & C_4 \\ -\omega_1^2 C_1 & 0 & -\omega_1^2 C_3 & 0 \\ \hline -\omega_1^2 C_2 & 0 & -\omega_1^2 C_4 & 0 \\ 0 & 0 & 0 & 0 \\ \hline 0 & 0 & 0 & 0 \\ 0 & 0 & 0 & 0 \end{bmatrix} \quad (2.4-6)$$

The two rows of C' are linearly dependent so that the rank of M' is 2 and thus the detection order of \underline{f} is 2 for both \underline{b}_1 and \underline{b}_2 . Since M'_G is the null matrix, the group detection order is four and the events are mutually detectable.

The maximal generator for \underline{f} is second order in this case and so must satisfy the set (2.3-10):

$$\begin{aligned} C\underline{g} &= \underline{0} \\ CA\underline{g} &= \underline{0} \end{aligned} \quad (2.4-7)$$

If \underline{g} is represented by $[g_a \ g_b \ g_c \ g_d]^T$, the first of (2.4-7) becomes

$$\begin{aligned} \phi_{11} g_b + \phi_{21} g_d &= 0 \\ \phi_{12} g_b + \phi_{22} g_d &= 0 \end{aligned} \quad (2.4-8)$$

where ϕ_{ij} is used to denote $\phi_i(\alpha_j)$. Since we have assumed linear independence of the sensors,

$$\begin{vmatrix} \phi_{11} & \phi_{21} \\ \phi_{12} & \phi_{22} \end{vmatrix} \neq 0 \quad (2.4-9)$$

and we must accept the trivial solution $g_b = g_d = 0$. The second equation in (2.4-7) transforms into

$$\begin{bmatrix} g_a \\ g_c \end{bmatrix} = \begin{bmatrix} -\omega_1^2 \phi_{11} & -\omega_2^2 \phi_{21} \\ -\omega_1^2 \phi_{12} & -\omega_2^2 \phi_{22} \end{bmatrix}^{-1} \begin{bmatrix} \phi_{11} & \phi_{21} \\ \phi_{12} & \phi_{22} \end{bmatrix} \begin{bmatrix} \beta_1 \\ \beta_2 \end{bmatrix} \quad (2.4-10)$$

with β_1 and β_2 denoting the nonzero elements of \underline{b} , and (2.4-9) guaranteeing existence of the inverted matrix.

All that remains is to solve (2.3-20) with $k = 2$ for each event. If λ is chosen for all the filter eigenvalues, $p_1 = \lambda^2$ and $p_2 = -2\lambda$. The particular solution of D is found to be

$$D_p = \begin{bmatrix} (p_1 - \omega_1^2)g_{1a} & (p_1 - \omega_1^2)g_{2a} \\ -p_2\omega_1^2 g_{1a} & -p_2\omega_1^2 g_{2a} \\ (p_1 - \omega_2^2)g_{1c} & (p_1 - \omega_2^2)g_{2c} \\ -p_2\omega_2^2 g_{1c} & -p_2\omega_2^2 g_{2c} \end{bmatrix} \begin{bmatrix} \phi_{11}\beta_{11} + \phi_{21}\beta_{12} & \phi_{11}\beta_{21} + \phi_{21}\beta_{22} \\ \phi_{12}\beta_{11} + \phi_{22}\beta_{12} & \phi_{12}\beta_{21} + \phi_{22}\beta_{22} \end{bmatrix} \quad (2.4-11)$$

where β_{ij} denotes β_j for \underline{b}_i . [Note that the original A is used in obtaining this result.]

Since all four eigenvalues have been assigned using (2.3-20), $D=D_p$ and the design is complete. If the gain were being designed for only one actuator, the remaining two eigenvalues would have to be assigned by some other means. This is often not easy to do analytically using determinants, and is best done computationally using D' , especially for higher order systems.

CHAPTER III

COMPUTATIONAL DESIGN OF FILTER

For systems of order four and greater, the analytic design approach outlined in the previous chapter becomes very cumbersome. The design example was actually a relatively simple case facilitated by the fact that the same types of sensors were used and the filter was designed to detect two events. In most cases, it is not possible to solve for the detection generator explicitly nor is it possible to assign all filter eigenvalues using D_p alone (definitely not for sensor failure events). This chapter will present a design alternative based upon a process called "orthogonal reduction" which is best implemented on a computer. All of these algorithms were first proposed by Beard but also appear in Jones as well.

3.1 Orthogonal Reduction

Many of the processes involved in the filter design involve finding the rank of a matrix or finding a vector in the nullspace of a certain matrix. The detection generator, for example, is in the nullspace of M' , the detection space of \underline{f} , and the detection order is $n - \text{rank} M'$. The orthogonal reduction procedure is an iterative process which generates a positive semi-definite matrix, the range space of which coincides with the nullspace of a given matrix V , $N(V)$.

Let V be an $m \times n$ matrix given by

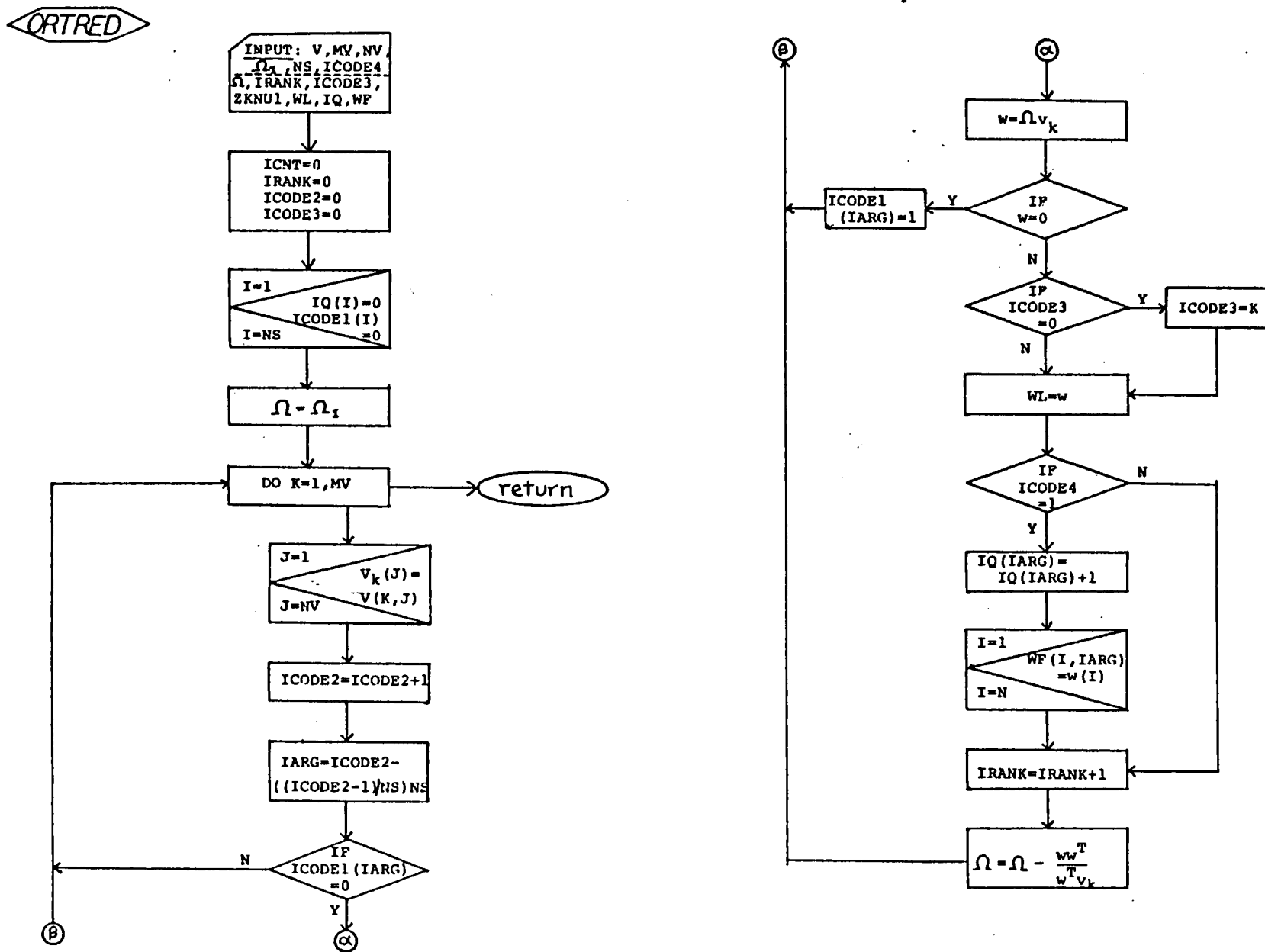


Fig. 3.1: Flowchart for ORTRED.

$$V = \begin{bmatrix} \underline{v}_1^T \\ \vdots \\ \underline{v}_m^T \end{bmatrix} \quad (3.1-1)$$

where \underline{v}_i^T are the rows of V . Let Ω denote the symmetric matrix whose range space is to coincide with the nullspace of V . Each row of V is then tested to see whether it is orthogonal to the range space of V (the rows of V span $N^\perp(V)$) by defining the auxiliary vector

$$\underline{w}_i = \Omega \underline{v}_i \quad (3.1-2)$$

If $\underline{w}_i \neq \underline{0}$, \underline{v}_i is not perpendicular to the columns of Ω (Ω is symmetric) and Ω is reduced so that $\underline{w}_i = \underline{0}$. This is repeated until the columns of Ω , $R(\Omega)$, are all orthogonal to the rows of V , $N^\perp(V)$.

The reduction algorithm proceeds as follows:

- (i) with Ω_i from the previous iteration, form the auxiliary vector

$$\underline{w}_i = \Omega_i \underline{v}_i$$

- (ii) if $\underline{w}_i = \underline{0}$, set

$$\Omega_{i+1} = \Omega_i$$

- if $\underline{w}_i \neq \underline{0}$, set

$$\Omega_{i+1} = \Omega_i - \frac{\underline{w}_i \underline{w}_i^T}{\underline{w}_i^T \underline{v}_i} \quad (3.1-3)$$

The procedure must begin with Ω_1 positive definite to ensure Ω remains positive semi-definite and $\underline{w}_i^T \underline{v}_i \neq 0$. The rank of

the matrix is equal to the number of reductions performed.

The algorithm for subroutine ORTRED is presented in Fig. 3.1 with several modifications tailored to the types of matrices we will be dealing with. First of all, a row can be skipped in the reduction process if it is known that it is linearly dependent on the preceding rows. This is especially useful for matrices such as M' in (2.3-24) which are generated cyclically. When the auxiliary vector for a particular row of M' , $(\underline{c}_j^T \ K^l)^T$ for example, is zero, then this row is linearly dependent on the preceding rows of M' . Also, the remaining rows of M' that depend upon \underline{c}_j , $(\underline{c}_j^T \ K^i)^T$ for $i > l$, are also dependent upon the preceding rows of M' . Thus, after the appearance of the first zero auxiliary vector, the rest of the rows that depend on \underline{c}_j needn't be considered. [ICODE1(J) is set equal to one at this termination point.] When the termination points for all \underline{c}_j 's have been reached, M' is completely reduced.

ICODE3 and WL are used when computing the maximal generator. ICODE3 is the row of C associated with the last nonzero auxiliary vector WL. The arrays IQ and WF are used when calculating D' . IQ stores the orders of K associated with the termination points for each row of C, and WF stores the last nonzero auxiliary vector for each row.

3.2 Input failure event design

The computation of D for actuators is accomplished by calling three subroutines: SEPDET, DETGEN, and DGAIN. Subroutine SEPDET first determines whether the events are output separable—it then determines whether the events are mutually detectable.

In the process of determining mutual detectability, SEPDET calls subroutine DETGEN to find the maximal generator for each event. Finally, subroutine DGAIN is called to calculate D using the detection orders and generators from SEPDET. Inputs to the main program FDFIL (see Appendix A) are the system matrix A and its order N , the measurement matrix C and number of sensors NS , the number of actuators NA , the matrix of event vectors $FALL$ and number of events NF , and the filter eigenvalues EV .

3.2.1 Subroutine SEPDET

The flowchart for SEPDET appears in Fig. 3.2. The program first computes μ_i for each f_i according to (2.3-14) and replaces f_i by $A^\mu f_i$ in $FALL$ and CF . The rank of CF is found using ORTRED to see whether the events are separable. If not, the error message 'NOT SEPARABLE' is printed and the designer must remove the dependent events from $FALL$ and start again.

Once the events are output separable, the program proceeds to determine whether the events are mutually detectable. The matrix M' in (2.3-24) is generated using C' and K for the full set of events and the rank is found using ORTRED to determine the group detection order, $\nu_G = N - \text{rank} M'_F$. The call to DETGEN yields the individual detection orders ν_i . If $\nu_G \neq \sum \nu_i$, the events are not mutually detectable, and one or more events will have to be removed and the process started over.

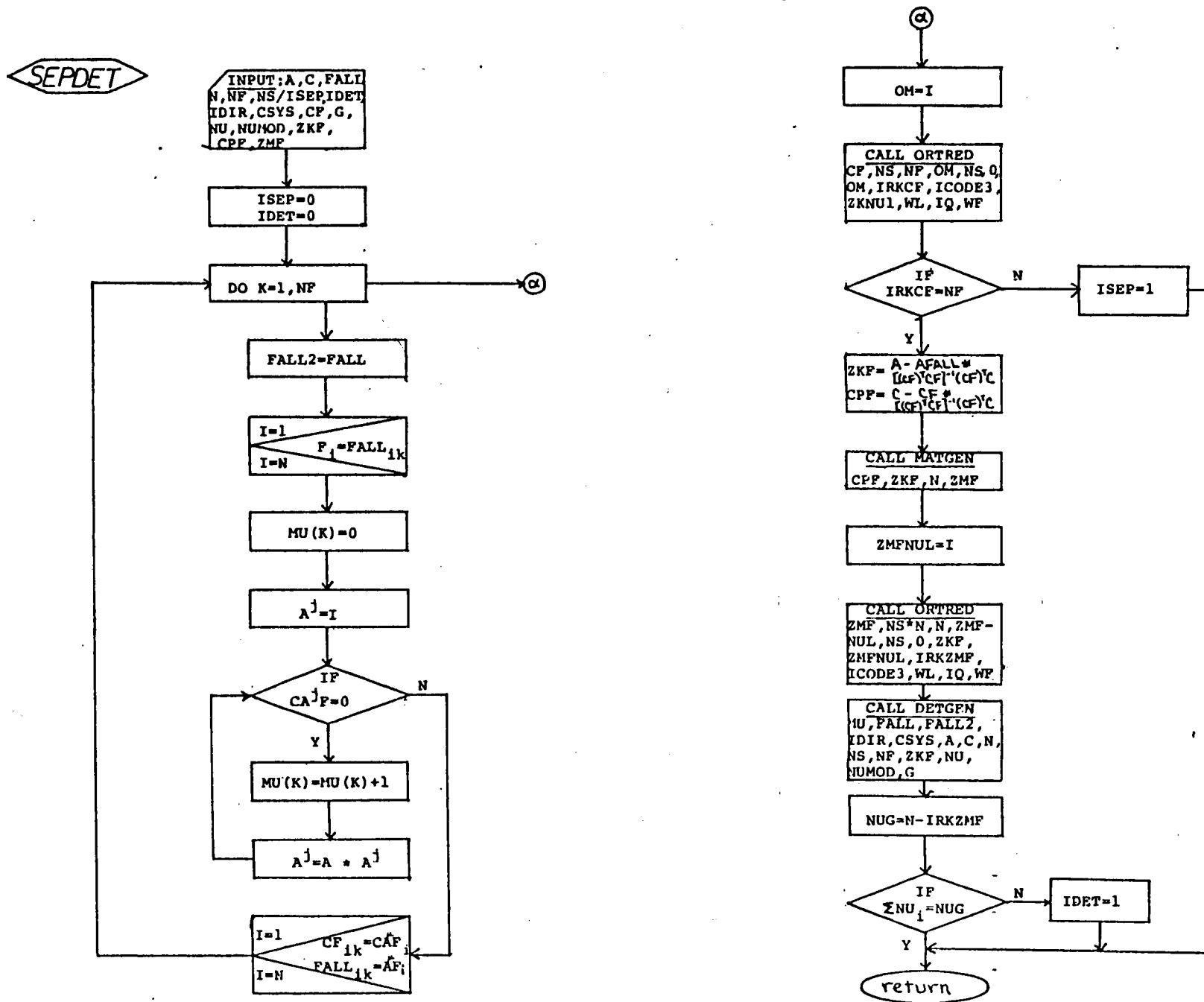


Fig. 3.2: Flowchart for SEPDET.

3.2.2 Subroutine DETGEN

This routine will calculate the "maximal" generator and detection order ν for an event, or alternatively, the "maximum" generator and its order ν_{mod} if (C,A) is an unobservable pair. The process is illustrated in Fig. 3.3 and begins with calculating M' in (2.3-24) for the single event and then using ORTRED to find the detection order, $\nu = N - \text{rank } M'$. The resulting nullspace in this case is the detection space of \underline{f} and coincides with the range space of the final Ω .

In addition to being in the detection space of \underline{f} , the detection generator must satisfy (2.3-10). This is accomplished by applying ORTRED to the matrix

$$M_K = [C \mid CK \mid \cdots \mid CK^{\nu-1}] \quad (3.1-4)$$

starting with the final Ω_f from the first step. Since C spans a subspace one dimension greater than C' and the process is started with Ω_f which is orthogonal to C' , only one row of C will not be terminated when first encountered. If \underline{w}_l is the last nonzero auxiliary vector for this row \underline{c}_j , the maximal generator is given by

$$\underline{g} = \begin{pmatrix} \underline{c}_j^T A^\mu \underline{f} \\ \underline{c}_j^T K^{\nu-1} \underline{w}_l \end{pmatrix} \underline{w}_l \quad (3.1-5)$$

As stated earlier, if (C,A) is not observable, the detection generator found in (3.1-5) is not maximal (order is not ν), but it is the generator of maximum possible order; this

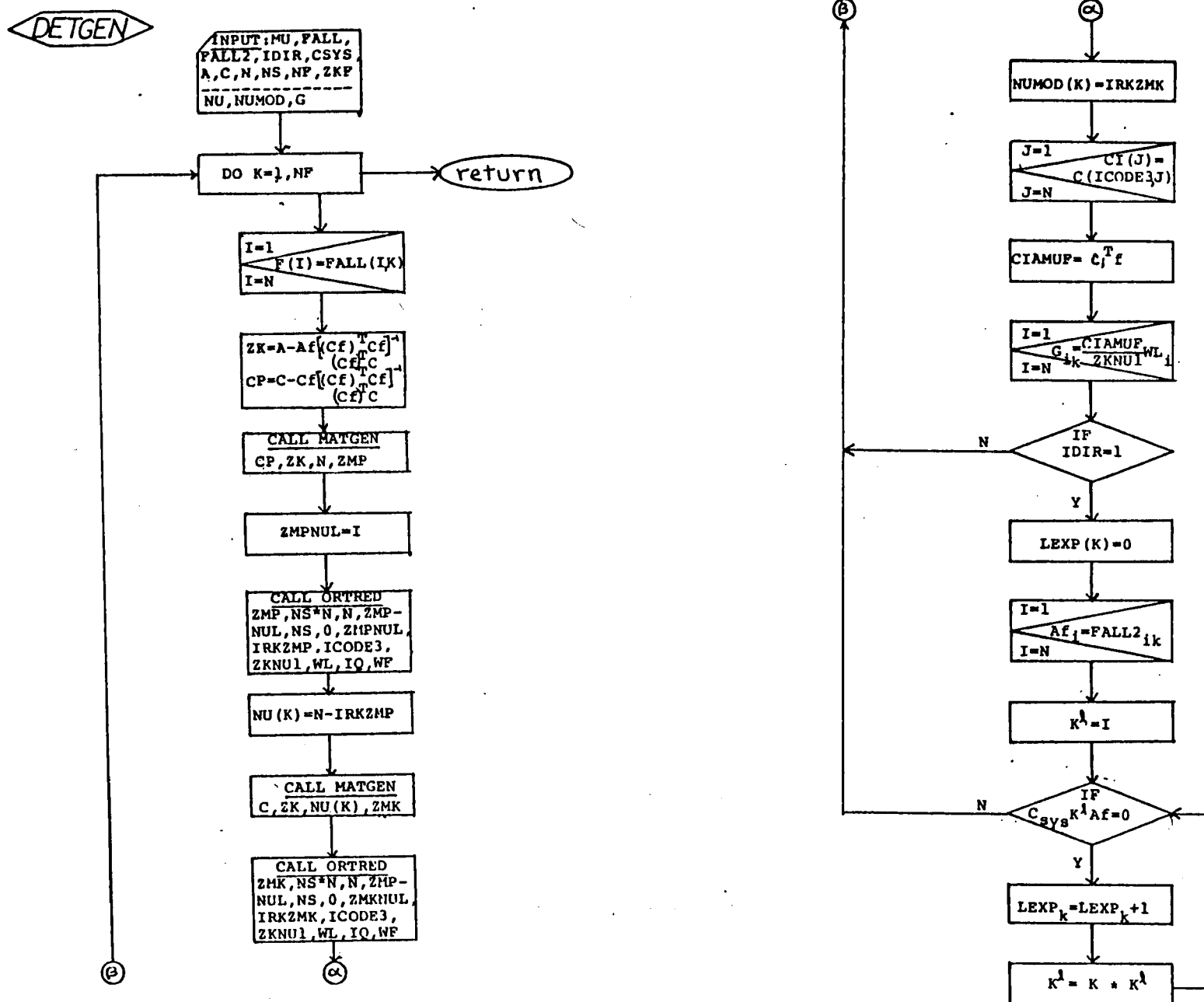


Fig. 3.3: Flowchart for DETGEN.

generator will be referred to as the "modified" generator and has order $\nu_{\text{mod}} = \text{rank } M_k$. If (C, A) is an observable pair, ν_{mod} will equal ν . The rest of the algorithm computes the vector $CK^{\lambda} A \underline{f}$ which is one component of the output error for sensor failures.

3.2.3 Subroutine DGAIN

This subroutine will finally compute the detector gain D while assigning the filter eigenvalues. The process begins (see Fig. 3.4) by finding the particular solution of D for

$$DCF = Q_D \quad (3.1-5)$$

where

$$Q_D = [q_1, \dots, q_{NF}]$$

$$q_{D_i} = p_i g_i + \dots + p_{\nu_{\text{mod}_i}} A^{\nu_{\text{mod}_i}-1} g_i + A^{\nu_{\text{mod}_i}} g_i$$

and ν_{mod_i} and g_i have already been calculated by SEPDET. The coefficients p_i are found by calling EVAS which computes the coefficients in (2.3-17) generated by $(s-\lambda)^{\nu_{\text{mod}_i}}$ where λ is the chosen filter eigenvalue (all are same).

If $\sum \nu_{\text{mod}_i} = n$, all eigenvalues are assigned and the detector gain is simply D_p . Otherwise, the remaining eigenvalues must be assigned using D' . Calculating D' is very similar to the procedure used in calculating D_p except that instead of using maximal generators, the last nonzero auxiliary vectors before termination found in reducing M'_F are used. Jones refers to this process as "completion of the state space" because one is assigning eigenvalues associated with that portion of the

DGAIN

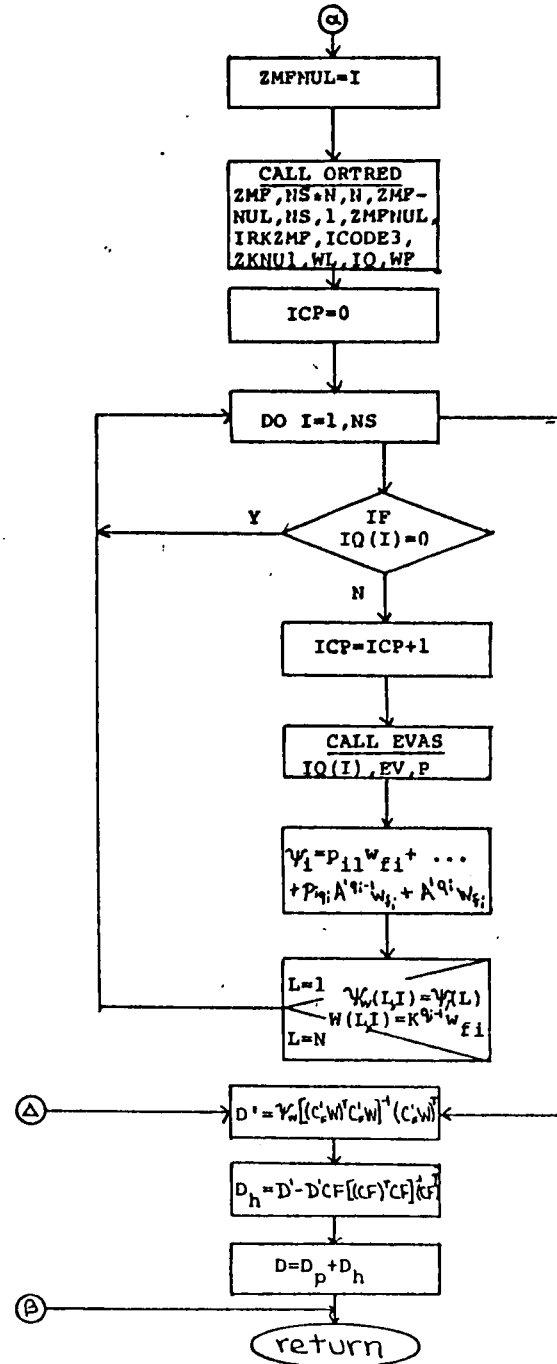
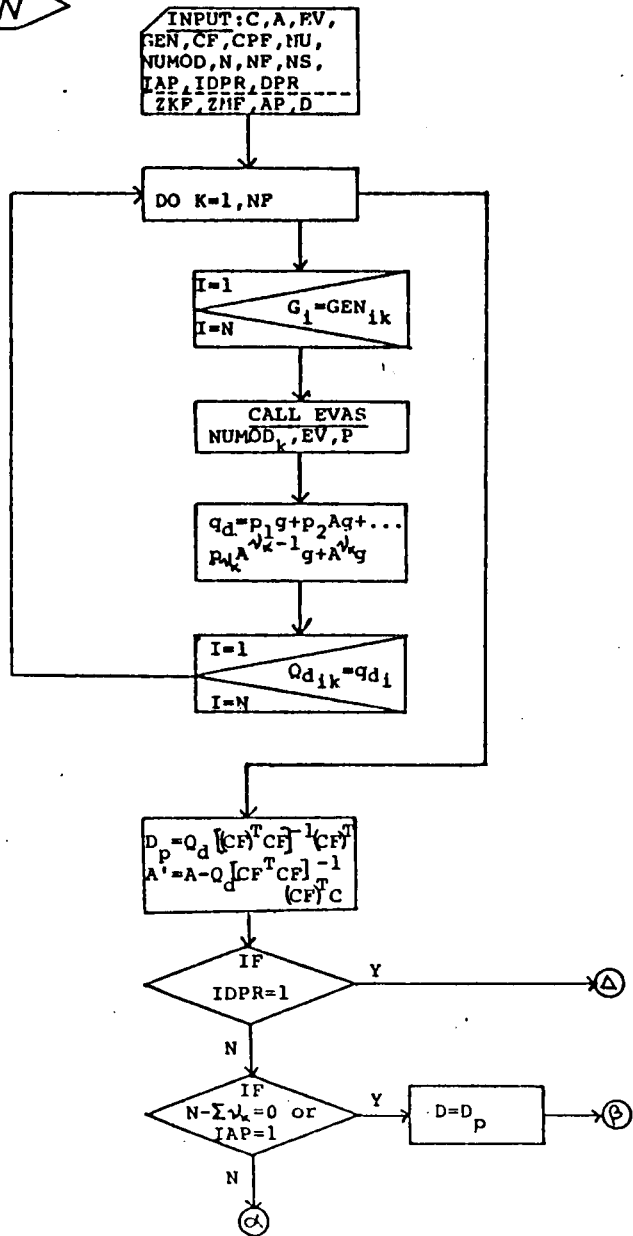


Fig. 3.4: Flowchart for DGAIN.

state space not covered by a detection space.

Finding D' begins by applying ORTRED to M'_F (M' for the full set F) to obtain IQ and WF as explained in section 3.1. D' is then any solution satisfying

$$D' C'_F W = \Psi_w \quad (3.1-6)$$

where

$$W = [K^{q_1-1} \underline{w}_{f_1}, \dots, K^{q_{ICP}-1} \underline{w}_{f_{ICP}}]$$

$$q_i \neq 0 \quad i = 1, \dots, NS$$

$$\Psi_w = [\underline{\psi}_1, \dots, \underline{\psi}_{ICP}]$$

$$\underline{\psi}_i = p_{i1} \underline{w}_{f_1} + \dots + p_{iq_i} A'^{(q_i-1)} \underline{w}_{f_i} + A'^{q_i} \underline{w}_{f_i}$$

The \underline{w}_{f_i} are the columns of WL corresponding to the rank C' nonzero q_i , and A'_F , C'_F correspond to A' , C' in (2.3-22) for the full set F . The coefficients p_{ij} are found by calling EVAS for q_i eigenvalues. One solution of (3.1-6) is simply the particular solution

$$D' = \Psi_w [(C'_F W)^T C'_F W]^{-1} (C'_F W)^T \quad (3.1-7)$$

The general solution for D is found by applying (2.3-21) to the full set F .

3.3 Measurement failure event design

The algorithm for sensor filter design does not use any new subroutines (except SENSOR which calls the routines) but the order and implementation are different. A schematic for the sensor design process is given in Fig. 3.5. SEPDET is called first for (A, C, F) to determine whether the set is

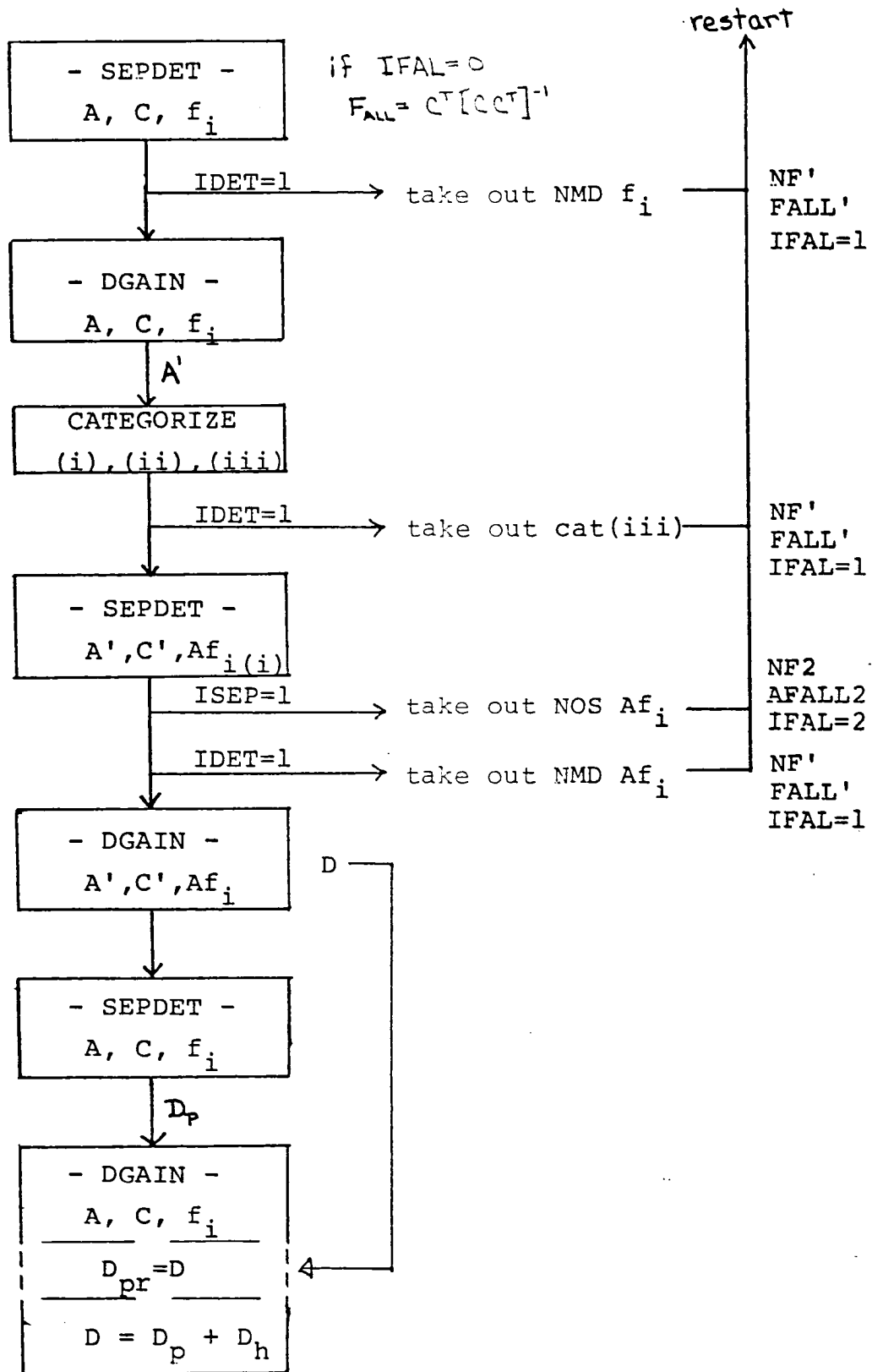


Fig. 3.5: Sensor design process schematic.

mutually detectable (since $C\bar{f}_i = \hat{e}_i$, $i = 1, \dots, NF$, it is automatically separable). If the set is not mutually detectable, events must be removed from F until it is and NF (no. events) set accordingly (F must now be inputted directly into the program instead of being calculated in SENSOR).

DGAIN is now called to calculate A'_F (set $IAP=1$) for use in computing M'_F , the observable space of (C', A') (this has been denoted W_0 in the program). The $A\bar{f}_i$ are then generated (recall that \bar{f} is actually $A^\mu \bar{f}$ when $\mu \neq 0$) and categorized according to step 3 in Section 2.3.4.2. The \bar{f}_i corresponding to the $A\bar{f}_i$ falling in category (iii) are then removed from F , and the process begins again with the new F and NF until no $A\bar{f}_i$ falls under (iii).

The next step is to call SEPDET for $(A', C', A\bar{f}_i)$. If the $A\bar{f}_i$ are not separable, there is no problem since we still have the output error directions \hat{e}_i from the events \bar{f}_i to distinguish between sensor failures. Removing the dependent $A\bar{f}_i$ from the set $A\bar{f}_1$ we only need make D' a detector gain for this new set $A\bar{f}_2$ of NF_2 events. [The program can be easily modified to handle this case by inputting $A\bar{f}_2$ and NF_2 into SENSOR and bypassing the statements $NF_2=NF$ and $A\bar{f}_2=A\bar{f}$.] If the $A\bar{f}_i$ are not mutually detectable, however, the corresponding \bar{f}_i will have to be removed from F and the whole process restarted with the new F .

Once the $A\bar{f}_i$ are separable/detectable, DGAIN is called to calculate D' (D' is the output D of DGAIN in this case). SEPDET is recalled to regenerate ν_i and g_i for the original \bar{f}_i to be used in calculating D_p . Now DGAIN is called a final time for (A, C, \bar{f}_i) with the input D' calculated above to compute D .

CHAPTER IV

APPLICATION TO FLEXIBLE BEAM

In demonstrating various control and failure detection algorithms for large space structures, researchers often use a long beam or rectangular plate as a typical structural element. A beam is usually chosen because of its simplicity and resemblance to a long truss, though plates find their usefulness in simulating the closely spaced frequencies of a flat solar array. In this chapter, the experimental beam at NASA Langley Research Center will be described along with the design of the filter using the finite element description of the beam. The effectiveness of the filter in detecting failures of force actuators on the beam will then be tested using various input frequencies and filter bandwidths in mismatched filter-system models. A position sensor failure will also be simulated for the case where there is only an initial condition on modal amplitudes present. The effect of data sampling will also be investigated.

4.1 NASA LaRC Experimental Beam

In all the failure detection simulation tests, the dynamics model and actuator/sensor types and locations were chosen to correspond to those of the experimental beam at NASA LaRC to predict the performance of the filter in subsequent tests using the actual beam. The Langley beam is made of aluminum ($M=0.502$ slugs) and is twelve feet long with a 6" x 3/16" cross section (see reference 4). Actuation is provided by electro-

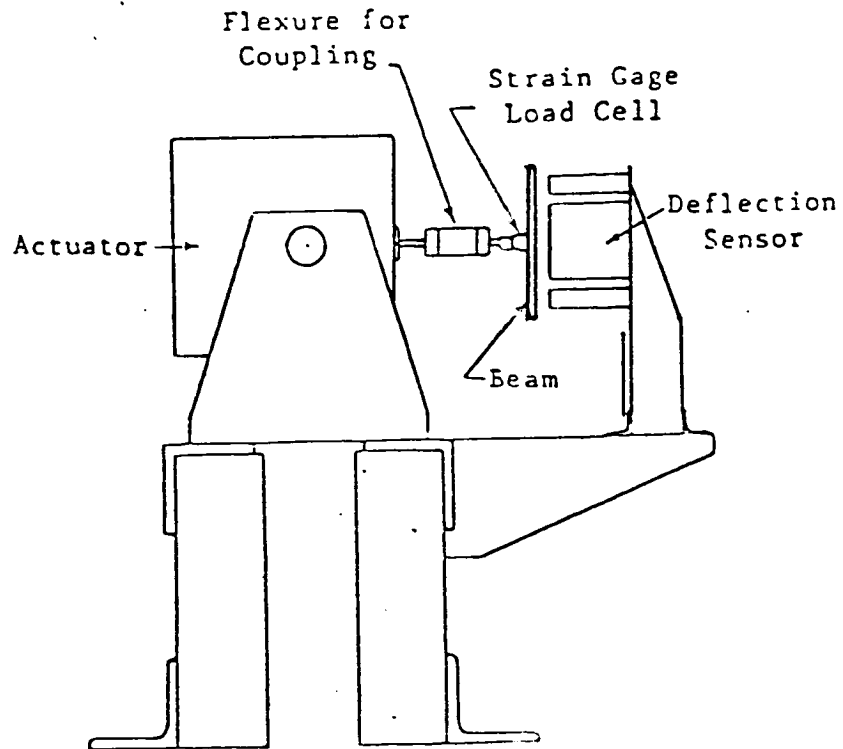


Fig. 4.1: End view of NASA LaRC experimental beam set-up. (taken from reference[4])

TABLE 4.1: Modal frequencies and shapes for first eight modes of LaRC beam (taken from reference[4]).

MODE #	MODAL FREQUENCY (rad/sec)	MODE SHAPE VALUE		
		x=0.5ft	x=2.5ft	x=6.0ft
1	0	7.06	6.18	4.64
2	0	-5.83	-3.15	1.53
3	11.418	-7.83	-0.60	5.91
4	31.360	6.45	-4.28	0.00
5	61.258	5.07	-6.36	6.90
6	100.900	-3.68	5.31	0.00
7	150.185	-2.27	1.74	6.84
8	209.004	-0.88	-2.70	0.00

magnetic shakers at four discrete locations along the beam, and the horizontal deflections are measured by nine Kaman KD-2300 probes, four of which are colocated with the actuators (see Fig. 4.1). All of the deflections of interest to us will take place in the horizontal plane of the beam.

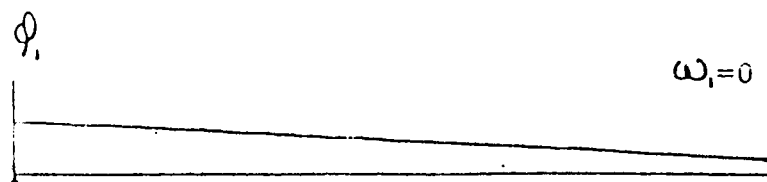
Because the beam is supported in a gravity field and the actuator dynamics are significant, the experimental beam does not behave exactly as a uniform beam would. Researchers at Langley have therefore found it convenient to perform their structural analysis using a finite element model. The beam model consists of 24 sections, each of which is constrained so that it can translate and rotate in only one degree of freedom. The SPAR program was then used to obtain the natural frequencies and orthogonal mode shapes for the first ten modes of the beam (see Fig. 4.2a-h for first eight modes). The SPAR generated mode shape values at positions 0.5 ft, 2.5 ft, and 6.0 ft from the end of the beam are given in Table 4.1 for the two rigid body modes (translation and rotation) and first six flex modes along with the modal frequencies.

4.2 State equations for beam model

In order to obtain the modal equations for the beam, we begin with the series expansion for the beam displacement

$$y(\epsilon, t) = \sum_{i=1}^{\infty} \phi_i(\epsilon) \psi_i(t) \quad (4.2-1)$$

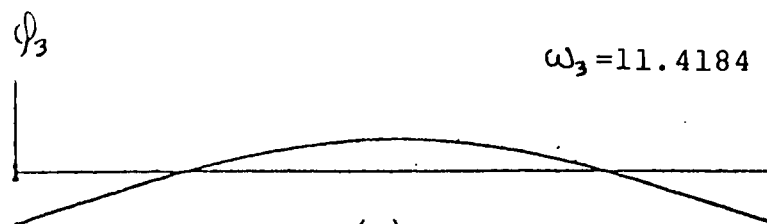
where $\phi_i(\epsilon)$ is an orthogonal set of mode shapes and $\psi_i(t)$ are



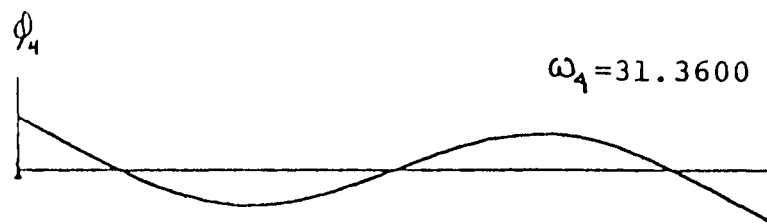
(a)



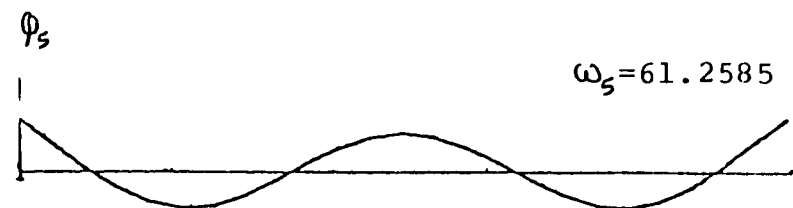
(b)



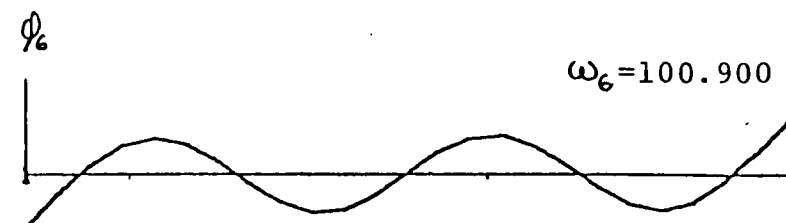
(c)



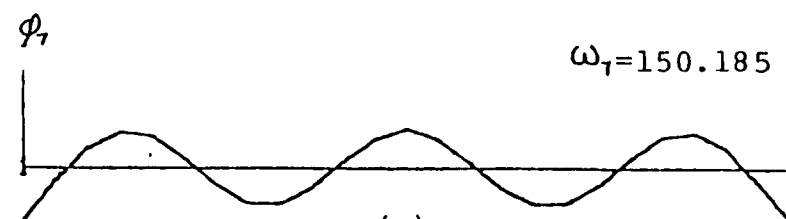
(d)



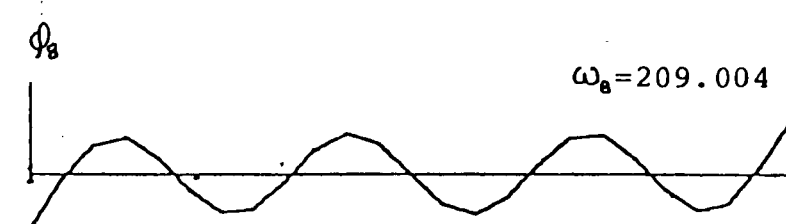
(e)



(f)



(g)



(h)

Fig. 4.2: SPAR beam modal frequencies and shapes (frequencies in rad/sec).
(taken from reference[4])

the modal amplitudes. Next substitute this into the governing differential equation for the undamped beam

$$EI \frac{\partial^4 y}{\partial \epsilon^4} + m \frac{\partial^2 y}{\partial t^2} = f(\epsilon, t) \quad (4.2-2)$$

where f is the forcing term and m , E , and I are the beam mass (M) per unit length, modulus, and cross-section inertia, respectively. Assuming the use of m point force actuators,

$$f(\epsilon, t) = \sum_{j=1}^m \delta(\epsilon - \epsilon_j) u_j(t) \quad (4.2-3)$$

with ϵ_j being the actuator positions and $u_j(t)$ the control magnitudes, one obtains the set of relations

$$\omega_i^2 \psi_i(t) + \frac{d^2 \psi_i}{dt^2} - \frac{1}{M} \sum_{j=1}^m \phi_i(\epsilon_j) u_j(t) = 0 \quad (4.2-4)$$

where ω_i is the natural frequency of the i^{th} mode and ϕ_i is the normalized mode shape (for ϕ_i not normalized, the input amplitudes must be scaled).

Next, consider casting (4.2-4) in the state-space form

$$\begin{aligned} \dot{\underline{x}} &= A \underline{x} + B \underline{u} \\ y &= C \underline{x} \end{aligned} \quad (4.2-5)$$

where

$$\underline{x}^T = [\psi_1 \quad \dot{\psi}_1 \quad \psi_2 \quad \dot{\psi}_2 \quad \dots \quad \psi_N \quad \dot{\psi}_N]$$

$$A = \begin{bmatrix} \circ & 1 & & & \\ -\omega_1^2 & \circ & & & \\ & & \circ & 1 & \\ & & -\omega_2^2 & \circ & \\ & & & & \ddots & \\ & \circ & & & & \circ & 1 \\ & & & & & & -\omega_N^2 & \circ \end{bmatrix}$$

$$B = \begin{bmatrix} \circ & \circ & \cdot & \cdot & \cdot & \circ \\ \frac{1}{M} \phi_1(\epsilon_1) & \frac{1}{M} \phi_1(\epsilon_2) & \cdot & \cdot & \cdot & \frac{1}{M} \phi_1(\epsilon_m) \\ \circ & \circ & \cdot & \cdot & \cdot & \circ \\ \frac{1}{M} \phi_2(\epsilon_1) & \frac{1}{M} \phi_2(\epsilon_2) & \cdot & \cdot & \cdot & \frac{1}{M} \phi_2(\epsilon_m) \\ \vdots & \vdots & & & & \vdots \\ \circ & \circ & \cdot & \cdot & \cdot & \circ \\ \frac{1}{M} \phi_N(\epsilon_1) & \frac{1}{M} \phi_N(\epsilon_2) & \cdot & \cdot & \cdot & \frac{1}{M} \phi_N(\epsilon_m) \end{bmatrix}$$

$$C = \begin{bmatrix} \phi_1(\alpha_1) & \circ & \phi_2(\alpha_1) & \circ & \cdot & \cdot & \cdot & \phi_N(\alpha_1) \\ \phi_1(\alpha_2) & \circ & \phi_2(\alpha_2) & \circ & \cdot & \cdot & \cdot & \phi_N(\alpha_2) \\ \vdots & & & & & & & \\ \phi_1(\alpha_p) & \circ & \phi_2(\alpha_p) & \circ & \cdot & \cdot & \cdot & \phi_N(\alpha_p) \end{bmatrix}$$

where the number of modes has been truncated at N , and the use of m force actuators at positions ϵ_j and p translation deflection sensors at positions ϵ_i have been assumed.

4.3 Failure detection filter design for the beam

For all the beam simulations that will appear later

in this chapter, the actuators and sensors located, at 0.5 ft, 2.5 ft, and 6.0 ft from the end of the beam were used. The co-location was chosen simply as a matter of convenience, whereas the sensor located at 9.5 ft was not used since it is not output separable from the one located at 2.5 ft. In order for the state equations (4.2-5) to be a true representation of the beam, normalized mode shapes must be used. Thus, the orthogonal mode shapes in Table 4.1 were normalized according to (L = beam length)

$$\int_0^L \phi_i^2(x) dx = L \quad (4.3-1)$$

before being used to compute A , B , and C . The orthogonal mode shape values at the actuator locations appear in Table 4.3.

For actuator failure detection, it was always possible to design a filter that could detect a failure of two actuators, but never for all three. This is because the individual detection orders are always two, but the group detection order for the three events is always n (the system order) making the events nonmutually detectable. The events are always output separable since the actuators are not symmetrically opposed with respect to the center of the beam. By extrapolation, it will be possible to detect up to $p-1$ input failure events with a single filter where p is the number of position sensors.

The design for sensor failures was made somewhat more difficult by the fact that when designing for two sensors, it was found that $Af_{\underline{1}}$ and $Af_{\underline{2}}$ were not output separable, with

respect to (C', A') . This simply meant that D' only needed to be made a detector gain for either $Af_{\underline{1}}$ or $Af_{\underline{2}}$ and would automatically be a detector gain for the other. The rest of the design proceeded normally resulting in a filter that could detect two failure events. As in the actuator case, it was not possible to detect three sensor events with a single filter.

4.4 Computer simulation of beam

In order to simulate the dynamics of the system and filter, a fifth order Runge-Kutta integration routine was used. The step size was always maintained at a sufficiently small size compared to the period of the highest frequency mode being simulated in order not to misrepresent the continuity of the system dynamics. A listing of the beam simulation program appears in Appendix B.

The program accepts as input the detector gain D calculated by FDFIL and the nominal system (filter) matrix A , actuator effectiveness matrix BF , and measurement matrix CF used in computing D . BS and CS for the system are also initially set equal to the nominal matrices BF and CF , respectively. When the failure time, T_{FAIL} , is reached, the column of BS associated with the failed actuator, or correspondingly, the row of CS associated with the failed sensor, is zeroed out to represent a failure in the off position. The values of BF and CF retain the nominal system values thus creating the driving term in the state error equation.

To easily verify whether the steady-state output error lies in the direction $C\underline{b}_i$ subsequent to the failure of the i^{th} actuator, the output is transformed so that any vector lying in the direction $C\underline{b}_i$ is changed to the direction $\hat{\underline{e}}_{p_i}$. The desired transformation then is

$$R = [(CF)^T(CF)]^{-1}(CF)^T \quad (4.4-1)$$

where F is the full matrix of event vectors \underline{b}_i . It is easily verified by direct substitution of (4.4-1) that $RC\underline{b}_i = \hat{\underline{e}}_{p_i}$ for $i=1,2,3$.

Similarly, it would be desirable to transform the output error for the i^{th} sensor event so that an error in the plane spanned by $\hat{\underline{e}}_{p_i}$ and $CK^{\lambda}A\underline{f}_i$ will lie in an easily identifiable plane. Fortunately, the use of three sensors permits a geometrical construction of the desired transformation. Consider the plane spanned by $\hat{\underline{e}}_1$ and $\underline{w} = CK^{\lambda}A\underline{f}_1$ in Fig. 4.3. This is the plane in which the output error is constrained to lie in the event of a sensor #1 failure. Now if the xyz coordinate system is rotated counterclockwise about the x-axis through the angle Υ (the angle that the projection of \underline{w} on the y-z plane makes with the y-axis), the ξ - η plane coincides with the plane spanned by $\hat{\underline{e}}_1$ and \underline{w} . Thus under the transformation

$$R = \begin{bmatrix} 1 & 0 & 0 \\ 0 & \cos\Upsilon & \sin\Upsilon \\ 0 & -\sin\Upsilon & \cos\Upsilon \end{bmatrix} \quad (4.4-2)$$

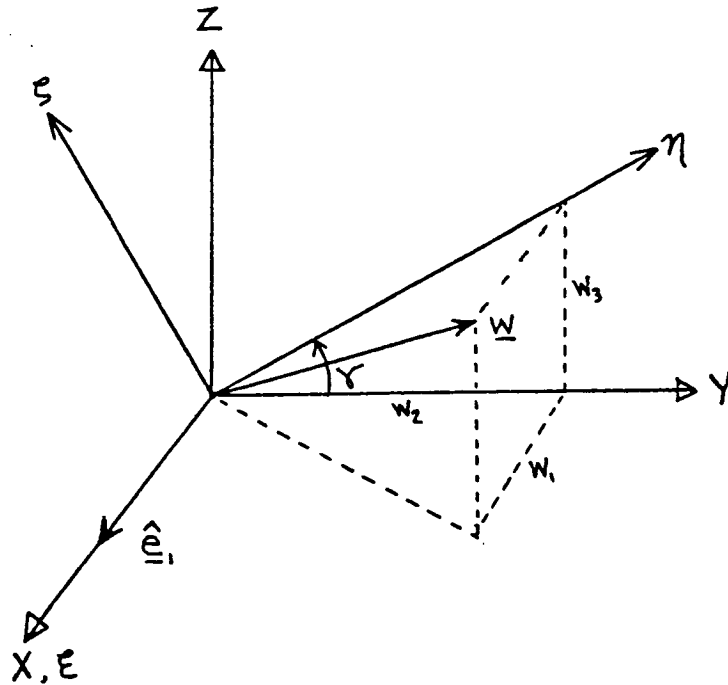


Fig. 4.3: Transformation of output error for sensor #1 failures.

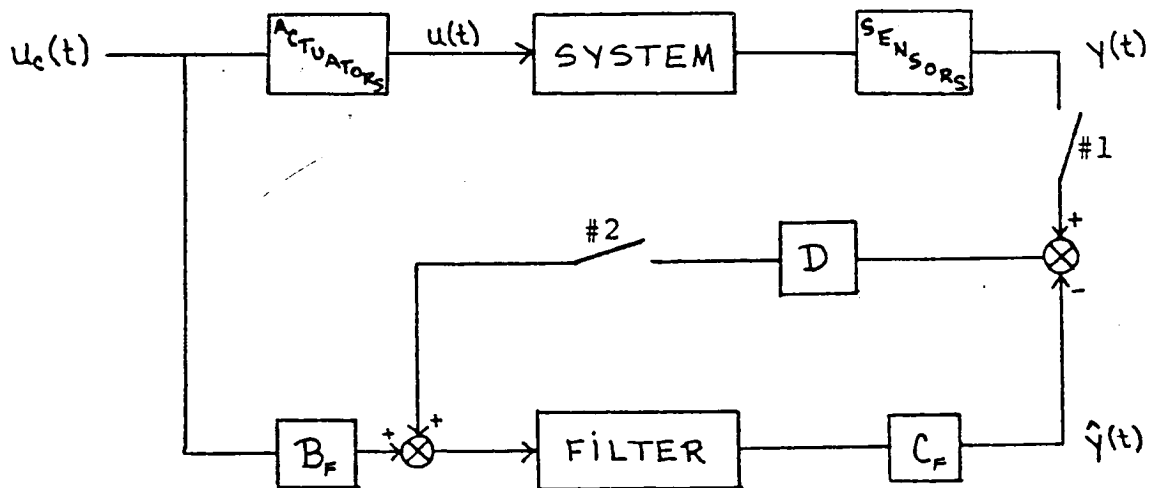


Fig. 4.4: Sampled-data system.

an error in the plane spanned by \hat{e}_1 and \underline{w} will have a first and second component but no third.

In the next two sections, the effect of model error in the filter and data sampling of the output will be investigated for the deterministic system. These two effects will be of the greatest concern in actual tests of the beam since the filter must necessarily incorporate a truncated model and data processor capability limits the sampling frequency. The effect of actuator, sensor, and plant noise will not be investigated here because they enter the realm of stochastic filter design which is beyond the scope of this work. Even after satisfying the requirements of being a detector gain, there is usually some freedom left in D that can be used to make the behavior of the detection filter approach that of the Kalman filter. Since no attempt was made here to optimize D for noisy systems under the constraints of being a detector gain, results of noise simulations would not reflect the true capabilities of the detection filter.

4.4.1 Effect of model error

Consider the case where the filter model contains fewer modes than the system model—this will always be the case for the actual beam. Let the state and output equations for the system be

$$\begin{bmatrix} \dot{\underline{x}}_M \\ \dot{\underline{x}}_U \end{bmatrix} = \begin{bmatrix} A_M & 0 \\ 0 & A_U \end{bmatrix} \begin{bmatrix} \underline{x}_M \\ \underline{x}_U \end{bmatrix} + \begin{bmatrix} B_M \\ B_U \end{bmatrix} \underline{u} \quad (4.4-3)$$

$$\underline{y} = \begin{bmatrix} C_M & C_U \end{bmatrix} \begin{bmatrix} \underline{x}_M \\ \underline{x}_U \end{bmatrix}$$

and for the filter

$$\begin{aligned} \dot{\hat{\underline{x}}}_M &= A_M \hat{\underline{x}}_M + B_M \underline{u} + D(\underline{y} - \hat{\underline{y}}) \\ \hat{\underline{y}} &= C_M \hat{\underline{x}}_M \end{aligned} \quad (4.4-4)$$

where the subscripts M and U denote modeled and unmodeled modes, respectively.

The new state error equations for the modeled modes are

$$\dot{\underline{e}}_M = (A_M - DC_M) \underline{e}_M - DC_U \underline{x}_U \quad (4.4-5)$$

and the coupled equations for the system and filter become

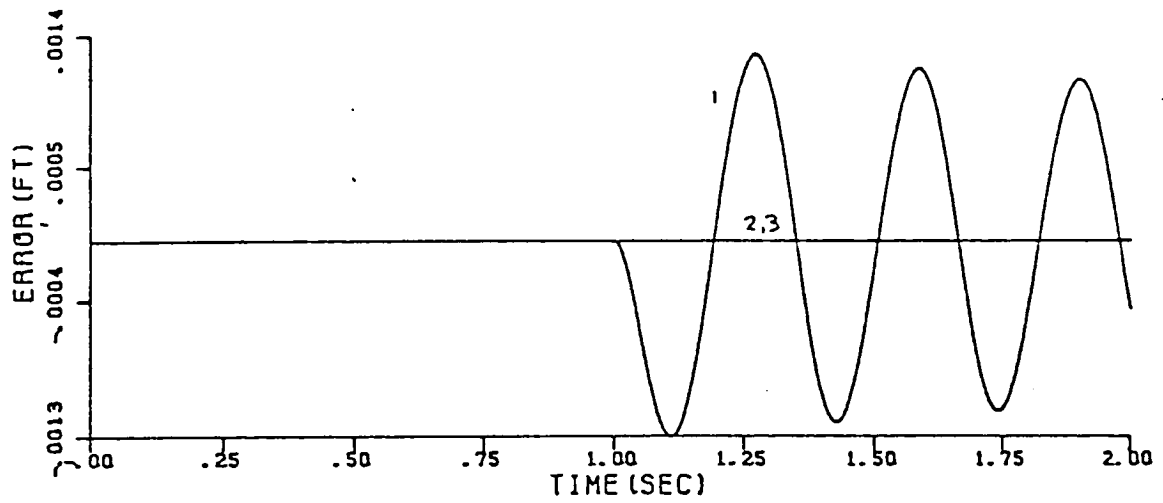
$$\begin{bmatrix} \dot{\underline{x}}_M \\ \dot{\underline{x}}_U \\ \dot{\underline{e}} \end{bmatrix} = \begin{bmatrix} A_M & 0 & 0 \\ 0 & A_U & 0 \\ 0 & -DC_U & A_M - DC_M \end{bmatrix} \begin{bmatrix} \underline{x}_M \\ \underline{x}_U \\ \underline{e} \end{bmatrix} + \begin{bmatrix} B_M \\ B_U \\ 0 \end{bmatrix} \underline{u} \quad (4.4-6)$$

The effect of B_U and C_U on the system of (4.4-3) are known as control and observation spillover, respectively. Spillover was first pointed out by Balas (7) in his work on active control of flexible structures. B_U in (4.4-3) has the effect of

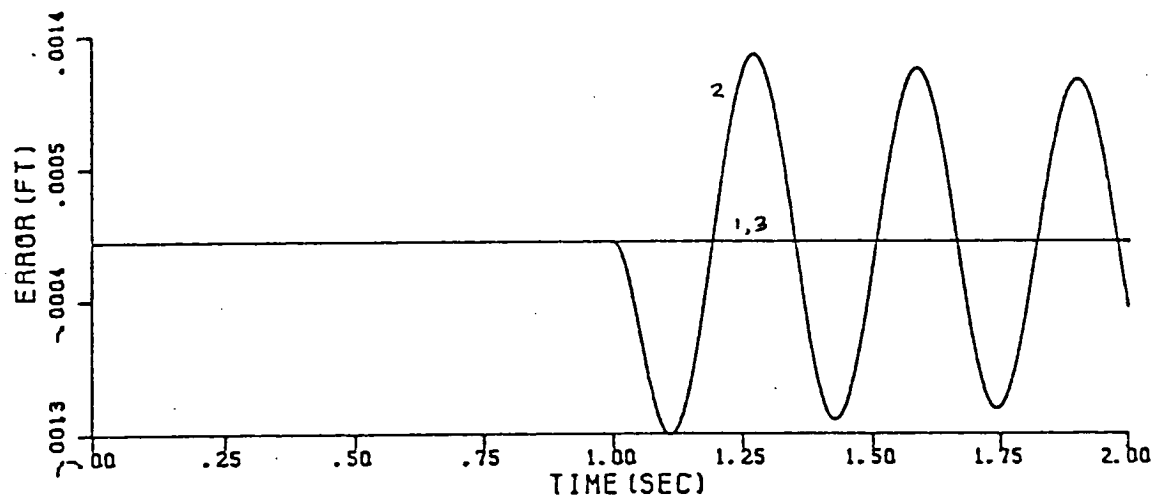
driving the unmodeled modes, and C_u creates an extra driving term in the state error equation (4.4-5)—however, neither type of spillover can cause filter instability since the triangularity of the dynamics matrix in (4.4-6) is preserved.

The first two simulations performed were for a perfectly matched system and filter (no spillover present) in order to verify the filter design. The detection filter was set up to detect a failure of either actuator #1 at 0.5 ft from the end of the beam, or actuator #2 at 2.5 ft. Results for the simulation of failures of both actuators at 1.0 sec are shown in Fig. 4.5 for a five-mode model and 15 rad/sec filter bandwidth. All three actuators were driving the system with an exponentially decaying sinusoid of the form, $e^{-0.2t} \sin \omega_u t$, with an input frequency of $\omega_u = 20$ rad/sec. The three transformed output errors are plotted on the same graph with the nonzero-signal in Fig. 4.5a representing the failure signal corresponding to the direction \hat{e}_1 and, in Fig. 4.5b, the direction \hat{e}_2 . The verification is good to within the number of significant figures in the detector gain used in the simulation.

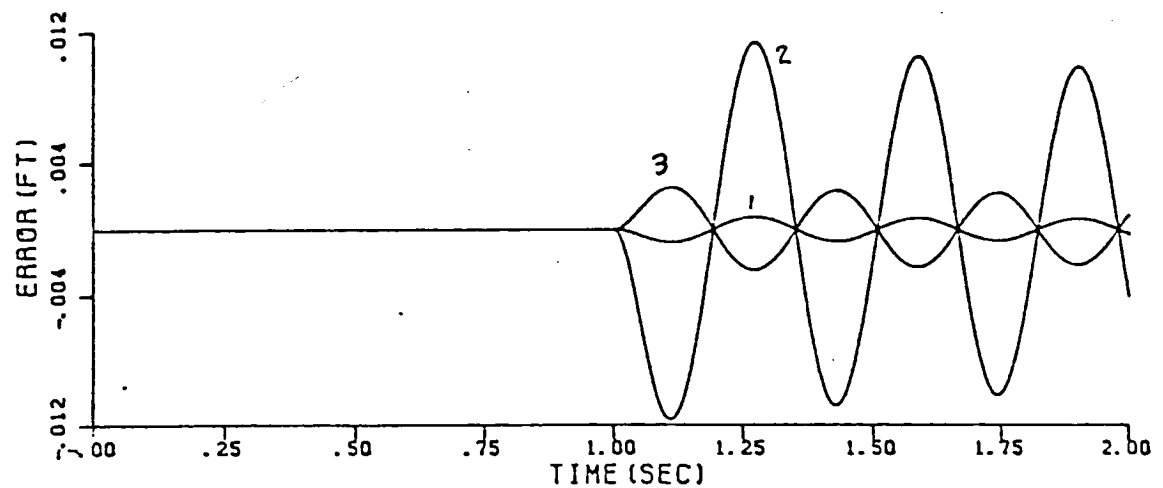
The effect of model error is dramatically illustrated in Fig. 4.6 for failure of the first actuator. Actuators #1,2,3 were operating at 20, 5, and 50 rad/sec, respectively, and the filter bandwidth was 15 rad/sec. Figure 4.6a is for a four-mode filter model and eight-mode system. The failure signal is not distinguishable from the other signals because



(a) transformed output error for actuator #1 failure.

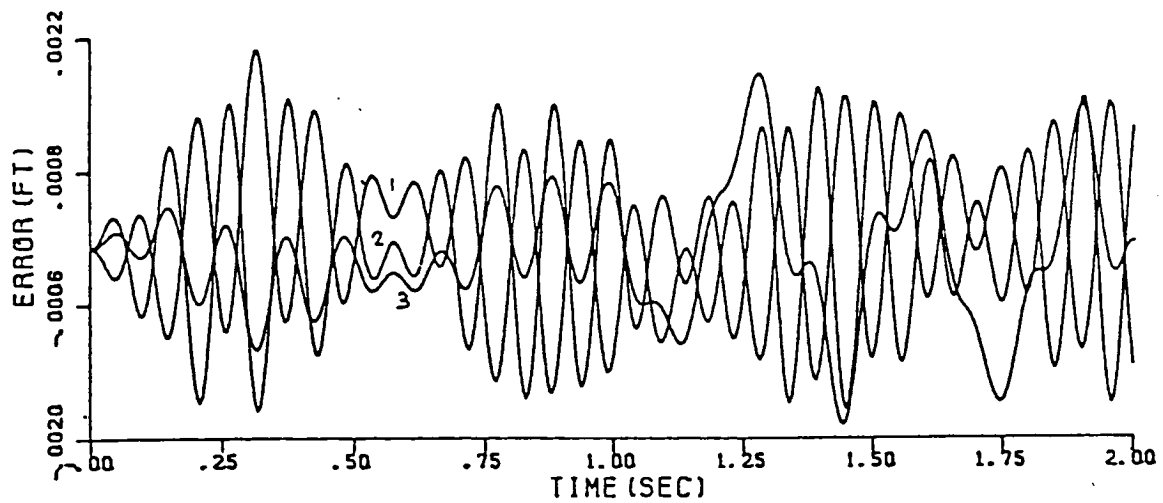


(b) transformed output error for actuator #2 failure.

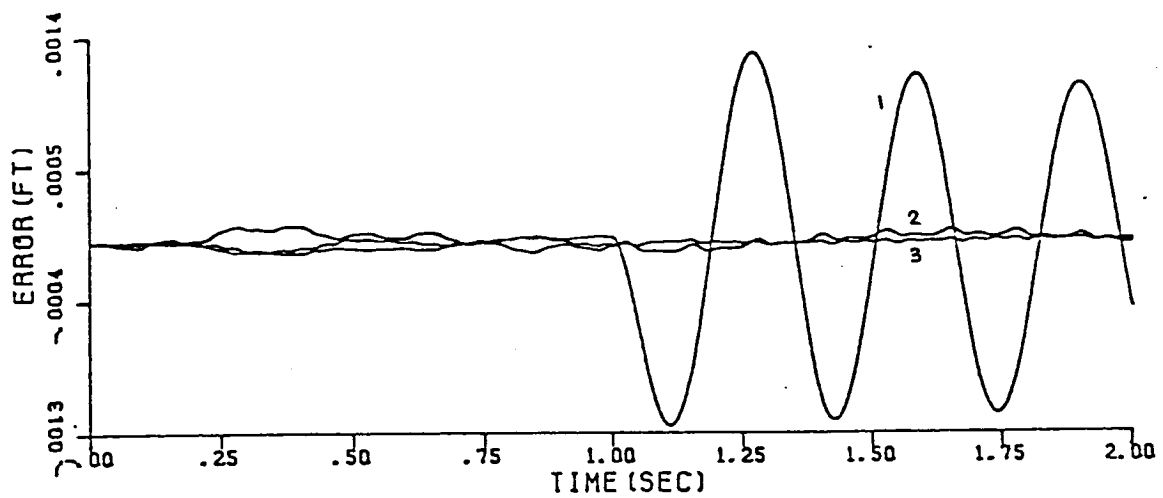


(c) real output error for actuator #2 failure.

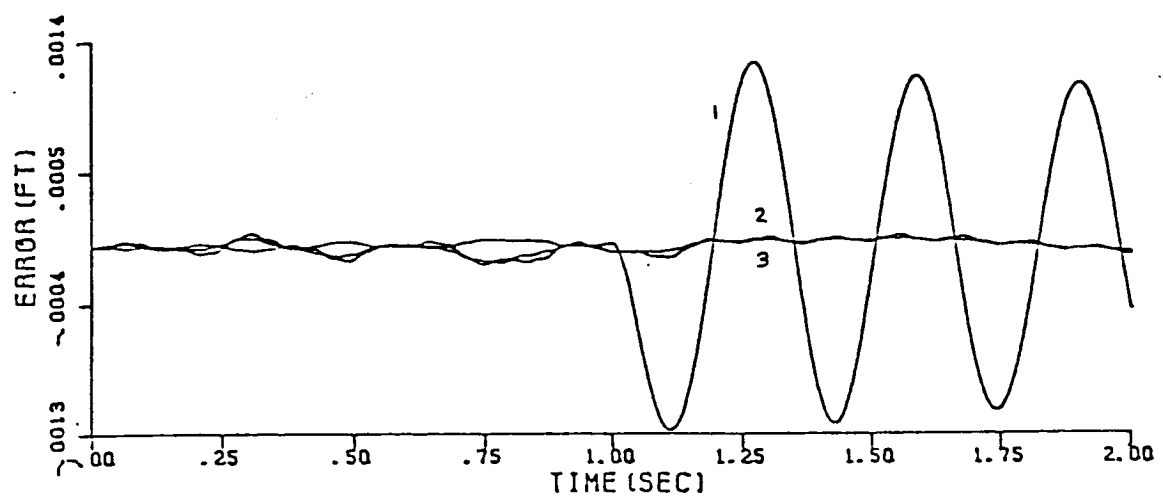
Figs.4.5a-c: Actuator failure for matched models.



(a) 4-mode filter



(b) 5-mode filter



(c) 6-mode filter

Figs.4.6a-c: Model error effect for different filter models.

the unmodeled fifth mode with a natural frequency of 61 rad/sec is being excited heavily by the input frequency of 50 rad/sec. This excitation is much less for the five-mode filter of Fig. 4.6b since the mode at 61 rad/sec is now included in the model, and the effect in Fig. 4.6c for the six-mode filter is barely noticeable. Therefore, one should include in his model at least the first mode whose natural frequency lies beyond the highest input frequency.

The results of an eight-mode system/five-mode filter set of tests for various input frequencies and bandwidths are shown in Table 4.2. The peak failure signal for actuator #1 is given along with the peak signal-to-noise ratio—the peak noise is the peak signal achieved in direction \hat{e}_2 and \hat{e}_3 . It appears that for a constant filter bandwidth, the performance of the filter drops off sharply as the input frequency is pushed farther past the filter poles. This is due to faster attenuation of the failure signal than the spillover noise outside the filter bandwidth. For a fixed input frequency, the signal-to-noise ratio reaches a maximum of 45 for a bandwidth of 15 rad/sec and input frequency of 5 rad/sec and a maximum of 36 for a bandwidth of 25 rad/sec and $\omega_u = 20$ rad/sec. Results for three filter bandwidths and three input frequencies are plotted in Figs. 4.7 to 4.9.

It is interesting to note that when the input frequency is being held constant, the trends we are observing are for

TABLE 4.2: Peak failure signals and signal-to-noise ratios for various input frequencies and filter bandwidths in actuator failure tests.

FILTER POLES (rad/sec)	INPUT FREQUENCY (rad/sec)					
	5		20		50	
	*PS	+S/N	PS	S/N	PS	S/N
5	.0158	16	.00181	4	-	-
10	.00595	40	.00150	21	.000284	5
15	.00297 ^x	45	.00119	31	.000255	5
20	.00175	41	.000925	35	.000238	5
25	.00114	35	.000709	36	-	-
30	.000804	29	.000562	23	-	-

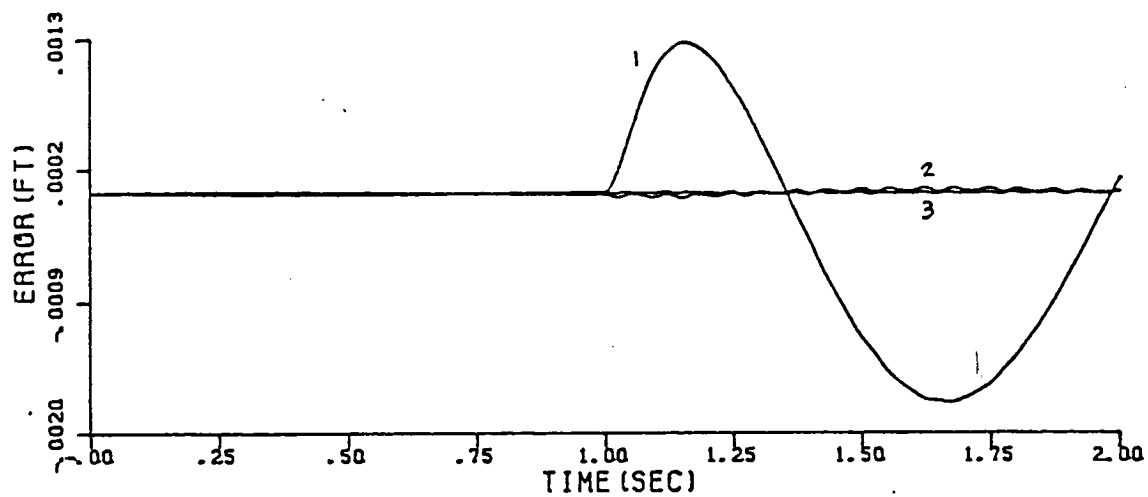
*peak failure signal in 1.5-2.0 sec interval

+peak failure signal divided by peak noise in other two output directions (1.5-2.0 sec)

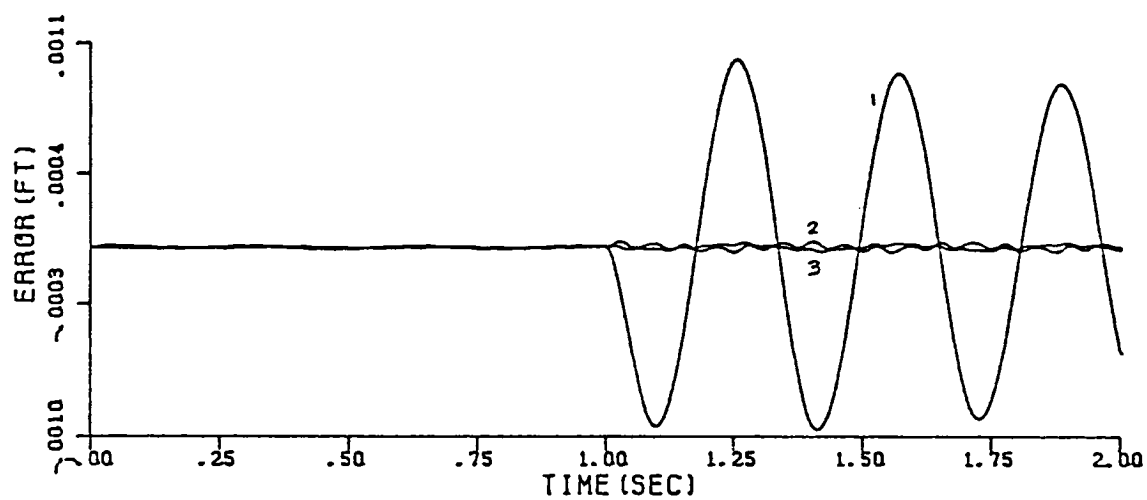
^xthe corresponding results with the detector gain designed for detecting only actuator#1 failures were: PS=0.00121, S/N=1.5

TABLE 4.3: Normalized mode shape values at sensor and actuator locations (taken from reference[5]).

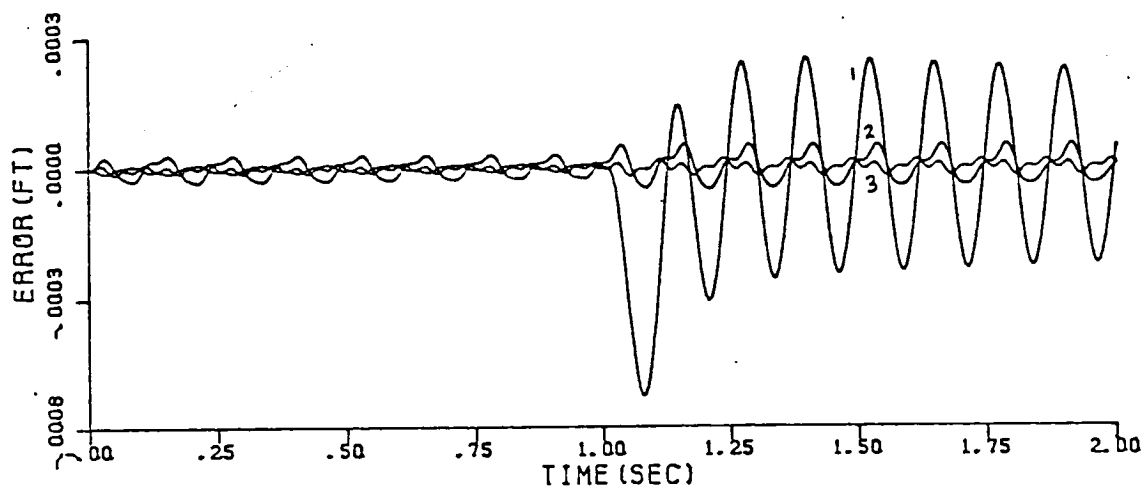
MODE SHAPE	MODE SHAPE VALUE at		
	x=0.5 ft	x=2.5 ft	x=6.0 ft
ϕ_1	1.00	1.00	1.00
ϕ_2	-1.59	-1.01	0.00
ϕ_3	-1.60	-0.123	1.21
ϕ_4	1.32	-0.876	0.00
ϕ_5	1.04	-1.30	1.41
ϕ_6	-0.753	1.09	0.00
ϕ_7	-0.465	0.356	1.40
ϕ_8	-0.181	-0.553	0.00



(a) $\omega_u = 5$ rad/sec

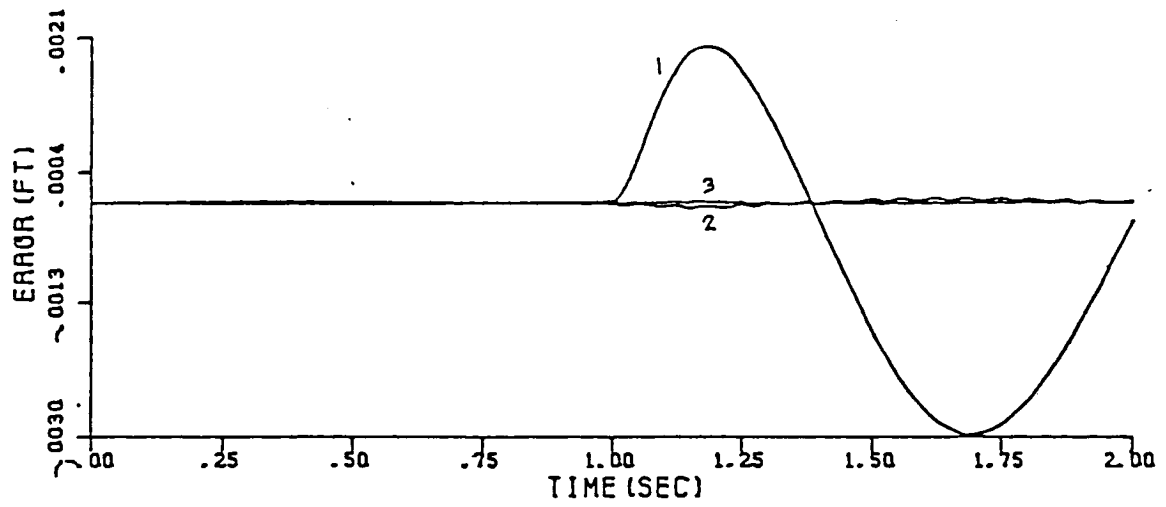


(b) $\omega_u = 20$ rad/sec

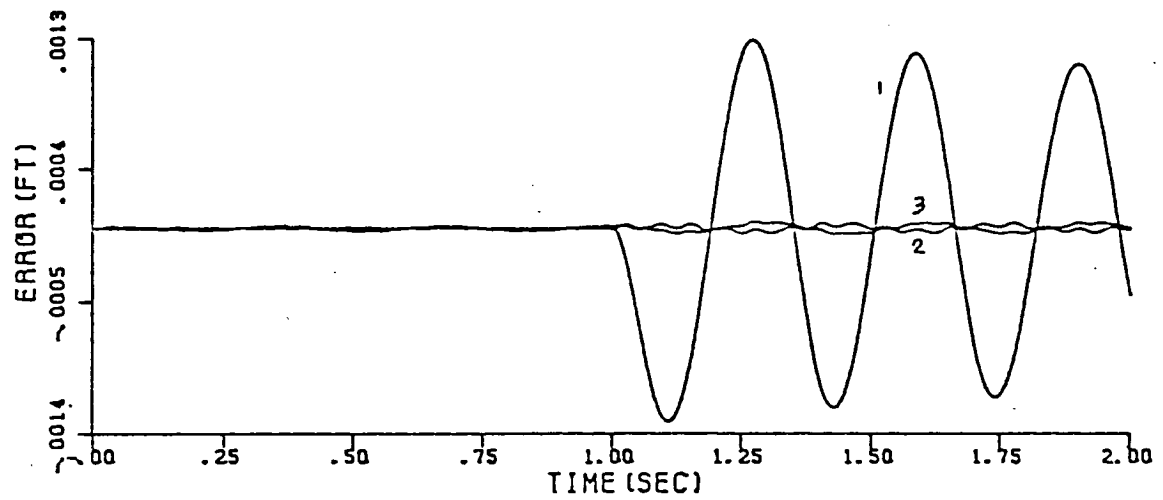


(c) $\omega_u = 50$ rad/sec

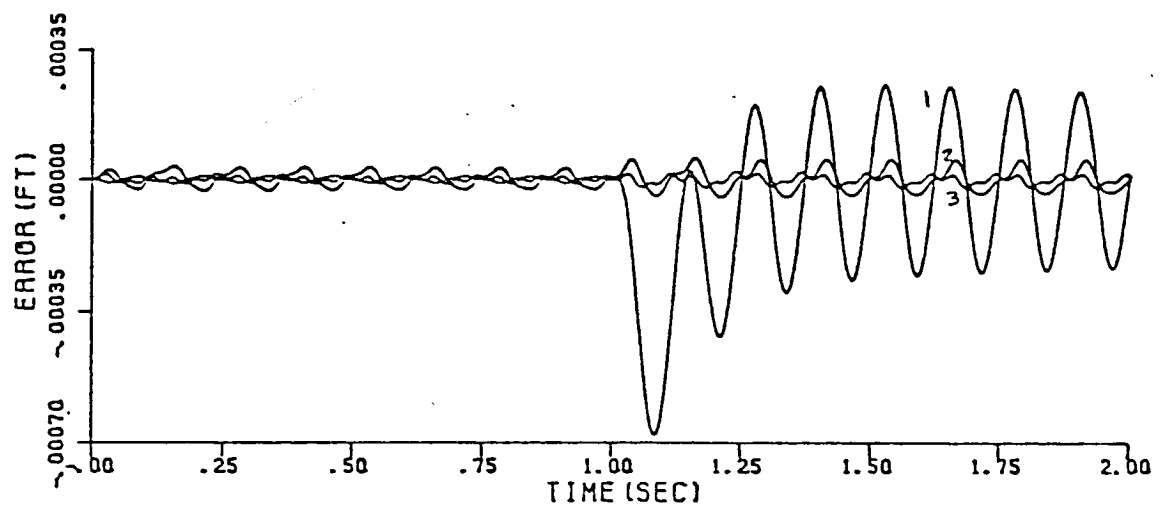
Figs.4.7a-c: Actuator tests for $\lambda = -10$ rad/sec.



(a) $\omega_u = 5$ rad/sec

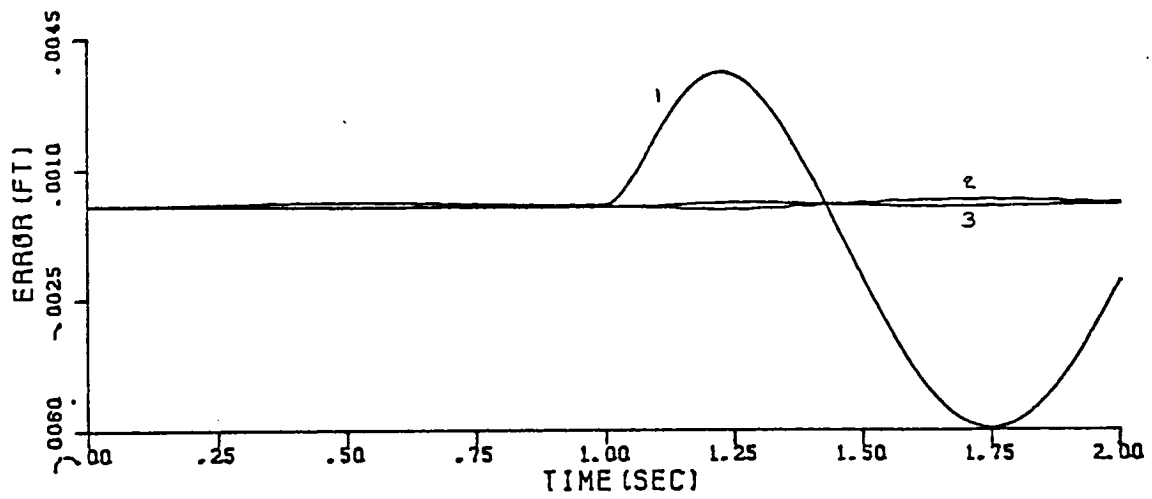


(b) $\omega_u = 20$ rad/sec

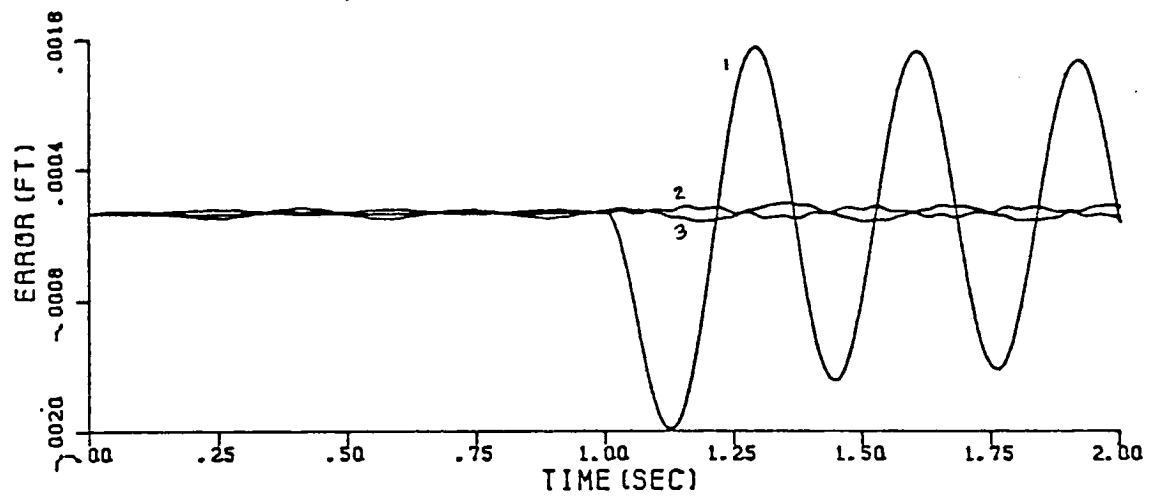


(c) $\omega_u = 50$ rad/sec

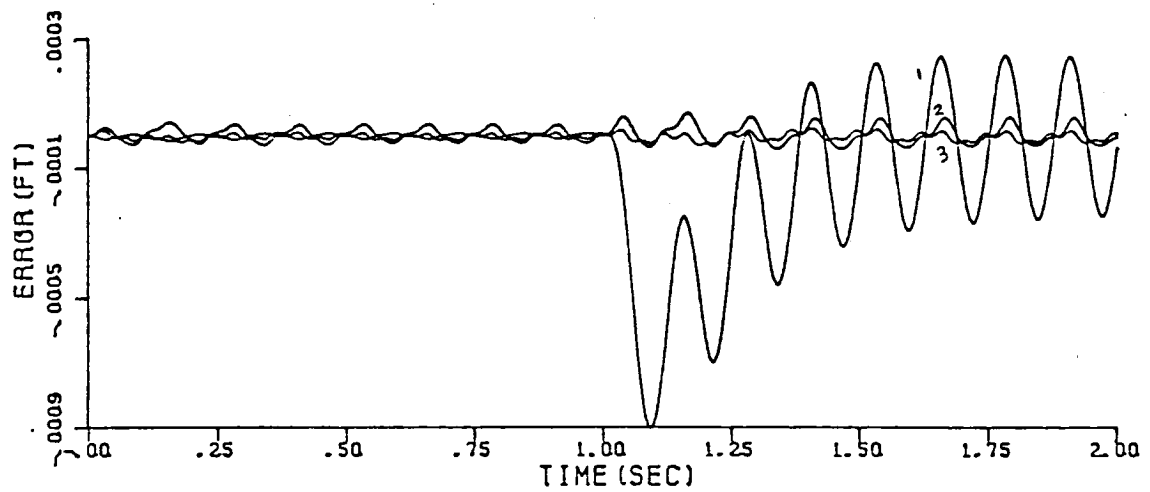
Figs.4.8a-c: Actuator tests for $\lambda = -15$ rad/sec.



(a) $\omega_u = 5$ rad/sec



(b) $\omega_u = 20$ rad/sec



(c) $\omega_u = 50$ rad/sec

Figs.4.9a-c: Actuator tests for $\lambda = -20$ rad/sec.

constant control spillover—however, the observation spillover coefficient DC_u in (4.4-5) changes since D and the filter poles change. But even if the filter poles are held constant and D is changed, the effects can be quite dramatic. For instance, if the detector gain is designed to monitor failures of just actuator #1 instead of both actuators, the signal-to-noise ratios for $\omega_u = 5$ rad/sec between filter poles of 15 and 20 rad/sec are about two rather than 40 to 50. The failure signal itself, however, is relatively unaffected.

A set of simulations was also run for detection of complete failure (zero signal) of the sensor colocated with actuator #1. Instead of driving the system with actuator inputs, initial amplitudes were placed directly on the various modes in order to excite them. Since the output transformation for the sensor case is a pure rotation of coordinate axes, the magnitude of the outputs will actually be in feet if normalized mode shapes are used. Thus, the transformed output errors have physical significance, whereas their meaning was obscured by the transformation in the actuator case.

The results of the sensor failure simulations for filter poles at 15 rad/sec and varying initial conditions are given in Table 4.4 and Fig. 10. In all cases, the two rigid body modes had no initial conditions, and the amplitudes on the first three flex modes were 0.12 ft, 0.09 ft, and 0.06 ft, respectively. The corresponding filter initial conditions

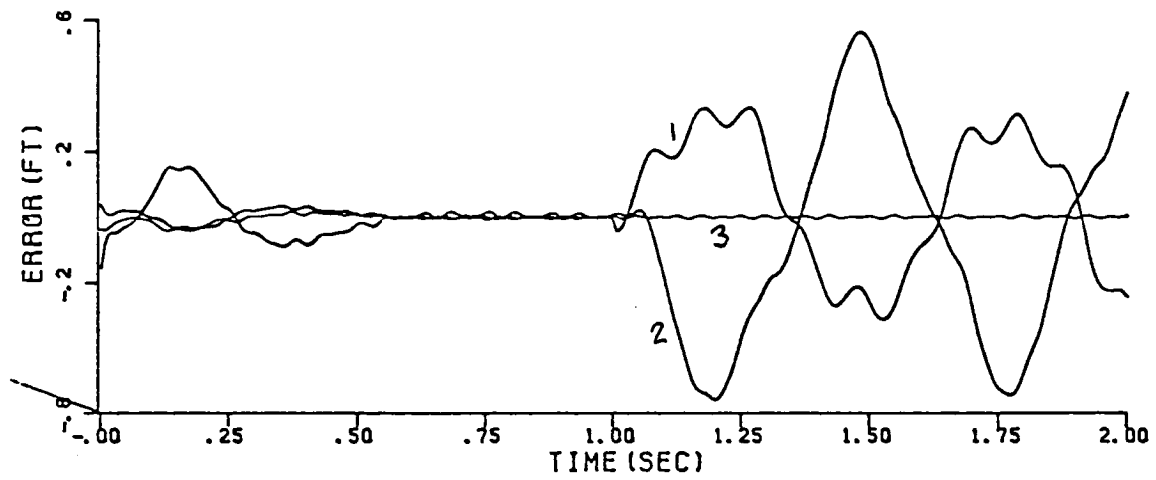
TABLE 4.4: Sensor failure results for filter poles at 15 rad/sec and various initial conditions.

INITIAL AMPLITUDES (ft)			PEAK OUTPUT SIGNALS (ft)			$\times S/N$
ψ_{60}	ψ_{70}	ψ_{80}	${}^+PS_1$	$*PS_2$	${}^-PN$	
.0045	.0030	.0015	.317	.561	5.92×10^{-3}	95
.0030	.0020	.0010	.317	.561	3.95×10^{-3}	142
.0015	.0010	.0005	.317	.561	1.97×10^{-3}	285
.0003	.0002	.0001	.317	.561	3.13×10^{-4}	1790 ⁵
0	0	0	.317	.561	5.36×10^{-6}	10

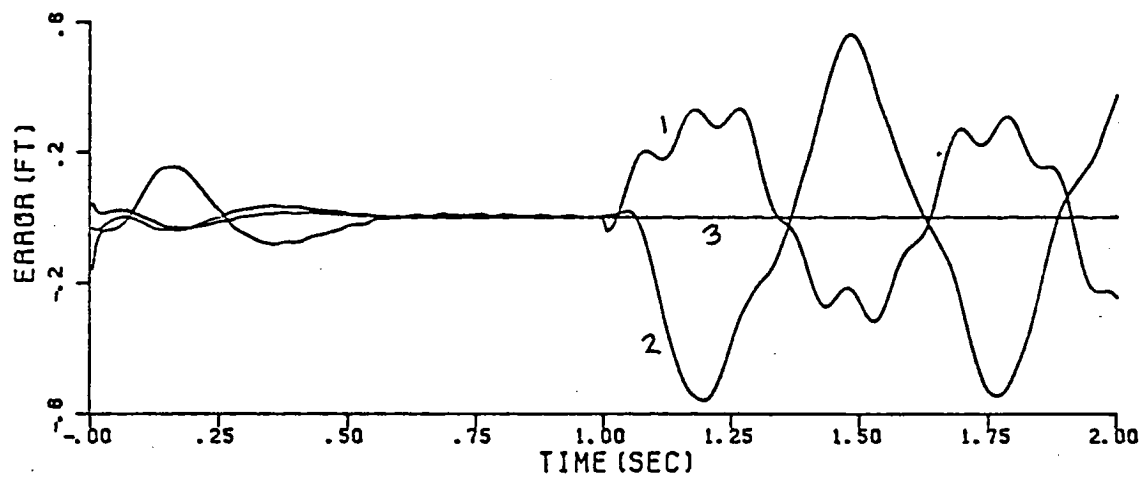
TABLE 4.5: Sensor failure results for various filter bandwidths and fixed initial conditions ($\psi_{60}=.003\text{ft}$, $\psi_{70}=.002\text{ft}$, $\psi_{80}=.001\text{ft}$).

FILTER POLES (rad/sec)	PEAK OUTPUT SIGNALS (ft)			$\times S/N$
	${}^+PS_1$	$*PS_2$	${}^-PN$	
5	.781	1.191	.00810	147
10	.491	.800	.00456	175
15	.316	.561	.00395	142
20	.224	.396	.00394	100
25	.177	.286	.00288	99
30	.144	.211	.00287	74

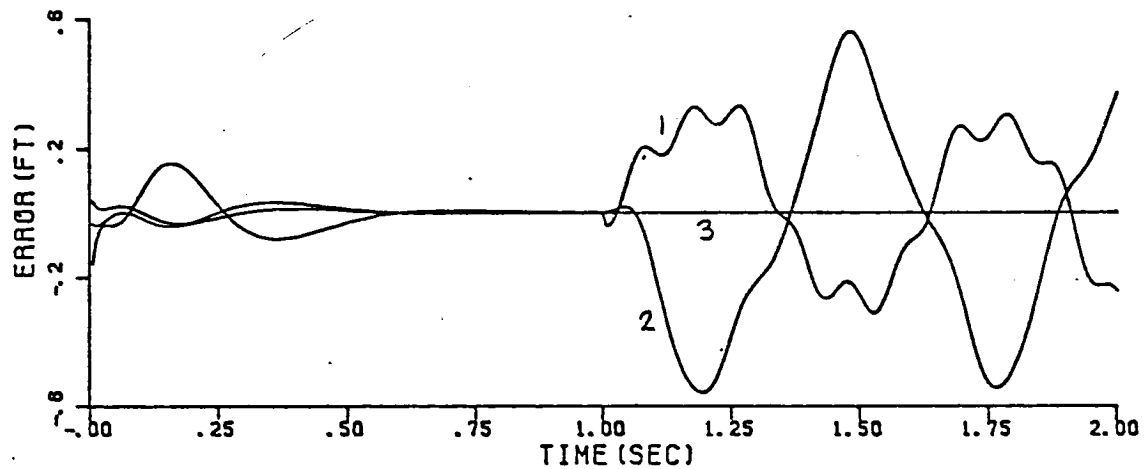
⁺ peak signal in direction #1 (1.5-2.0 sec)
^{*} same for direction #2
⁻ same for direction #3
^x peak signal in direction #1 and #2 divided by peak noise in direction #3



(a) $\psi_{60} = .0045$ ft

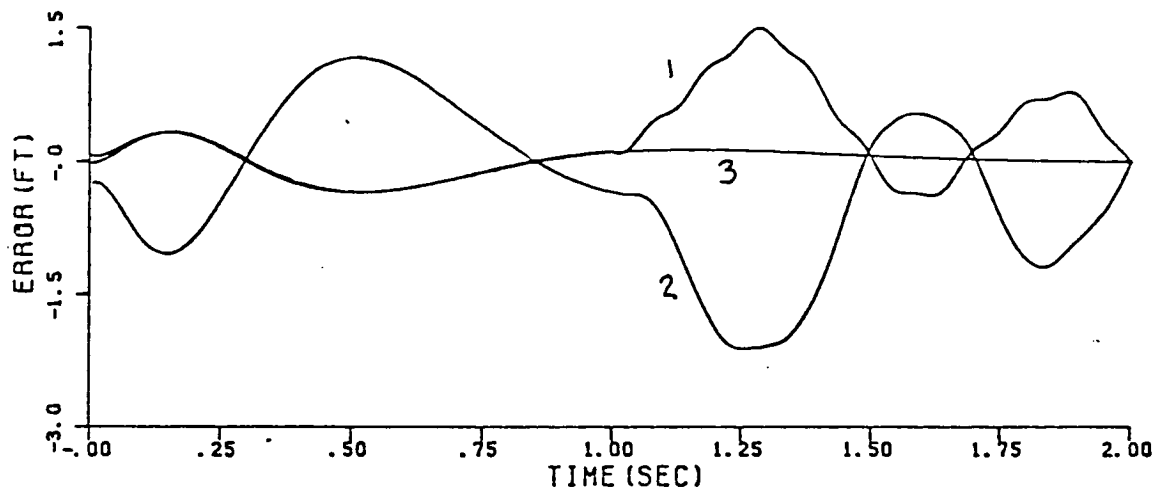


(b) $\psi_{60} = .0015$ ft

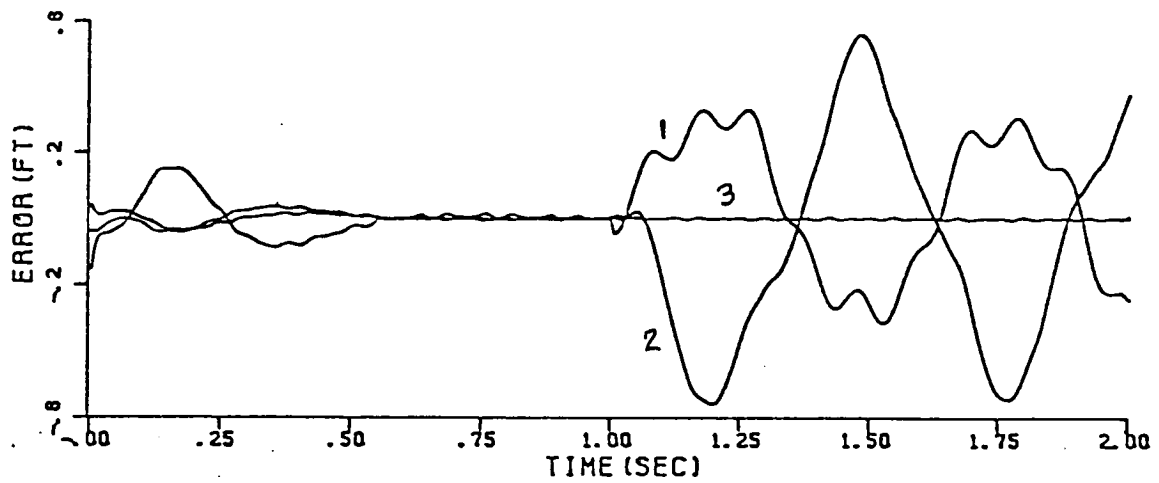


(c) $\psi_{60} = .0003$ ft

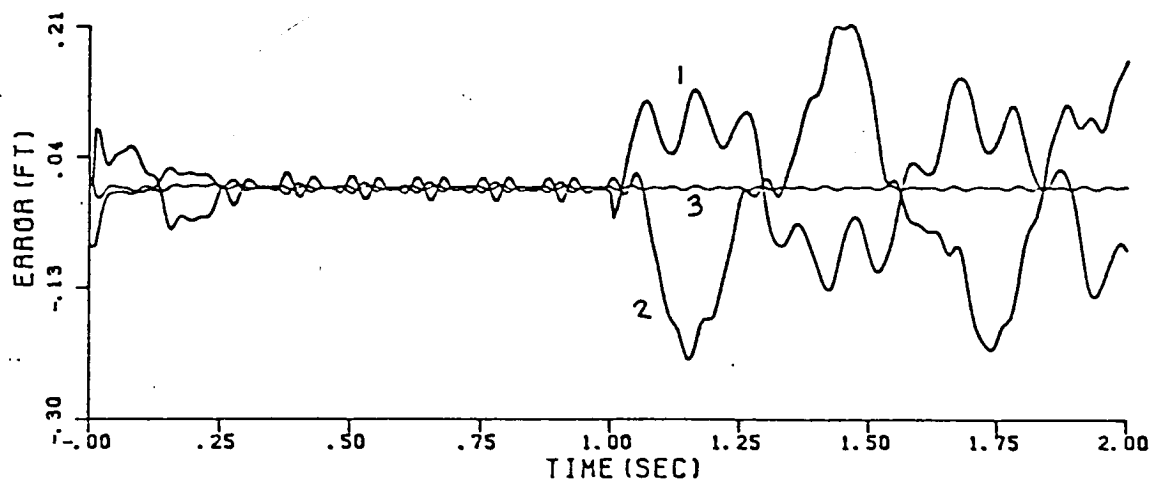
Figs.4.10a-c: Sensor tests for various initial conditions.



(a) 5 rad/sec



(b) 10 rad/sec



(c) 20 rad/sec

Figs.4.11a-c: Sensor tests for various filter bandwidths.

were all zero. The amplitudes on the three unmodeled modes (next three flex modes) are given in the table. The failure signal plane is $\hat{\underline{e}}_1 \times \hat{\underline{e}}_2$. The model error noise is very sensitive to initial conditions on the unmodeled modes, varying almost proportionally. The failure signal itself though is unaffected.

Table 4.5 shows results when the amplitudes on the three unmodeled modes are held constant at 0.003, 0.002, and 0.001 ft and the filter bandwidth is varied. The signal-to-noise ratio reaches a peak near 10 rad/sec where the attenuation of the spillover noise relative to the failure signal is greatest. Between 25 and 30 rad/sec, there was almost no attenuation of noise whereas there was a 25% reduction in the failure signal resulting in loss of signal-to-noise ratio. Plots for several cases appear in Fig. 4.11.

4.4.2 Sampled-data systems

Instead of monitoring a system continuously, it is usually the case because of computational considerations that sensor data is taken at regular intervals and the output held constant between sampling periods. This scheme is depicted in Fig. 4.4 for the detection filter. The switch at #1 closes once every sampling period to receive an update, and the signal stays constant between sampling times. Switch #2 closes at the same instant switch #1 closes, and

is shown in order to emphasize that the output error to the filter remains constant between sampling updates.

The effect of data sampling on filter performance in detection of actuator #1 failures for filter poles at 15 rad/sec and input frequencies of 20 rad/sec is shown in Table 4.6. As expected, the signal-to-noise ratio increases with sampling rate, but even at 160 hz, it is still a long way from the continuous sampling case where it is 31 (see Table 4.2). As illustrated in Fig. 4.12, the failure signal remains constant for different sampling rates, whereas the noise decreases for faster rates.

As a final illustration of data sampling, consider the case where the sampling rate is held constant at 64 hz, and filter bandwidth is varied. Table 4.7 shows results for filter poles between 5 and 20 rad/sec. At 5 rad/sec, the error signal due to spillover noise reached values nearly equal to the failure signal. Between 10 and 20 rad/sec the signal-to-noise ratio increased as it did for the continuous case. Finally, at 25 rad/sec the filter became unstable because the filter time constants were too fast for the sampled-error feedback to have a stabilizing effect. Plots for several cases appear in Fig. 4.13.

It is important to understand that these data-sampling results are for a case in which the detection filter was designed on a continuous data basis, and then data sampling

TABLE 4.6: Data-sampling results for input frequencies of 20 rad/sec, filter poles at 15 rad/sec, and various sampling rates.

SAMPLING FREQUENCY (hz)	PEAK OUTPUT ERROR SIGNALS ($\cdot 10^4$)			$x_{S/N}$
	+PS	*PN ₂	-PN ₃	
50	11.7	3.41	2.21	3.4
64	11.7	2.17	0.70	5.4
96	11.7	1.53	0.43	7.6
160	11.7	1.02	0.25	11.5

TABLE 4.7: Data-sampling results for input frequencies of 20 rad/sec, 64 hz sampling rate, and various filter bandwidths.

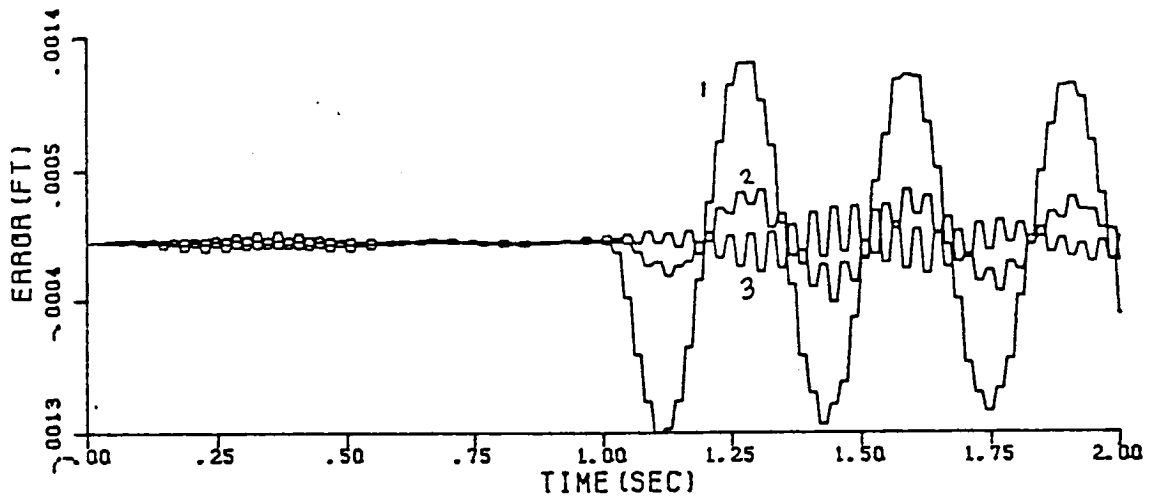
FILTER POLES (rad/sec)	PEAK OUTPUT ERROR SIGNALS ($\cdot 10^4$)			S/N
	PS	PN ₂	PN ₃	
5	17.9	7.49	12.5	1.4
10	14.0	3.53	2.0	4.0
15	11.7	1.53	0.4	5.4
20	9.3	1.35	0.3	6.8

+peak signal in direction #1 (1.5-2.0 sec)

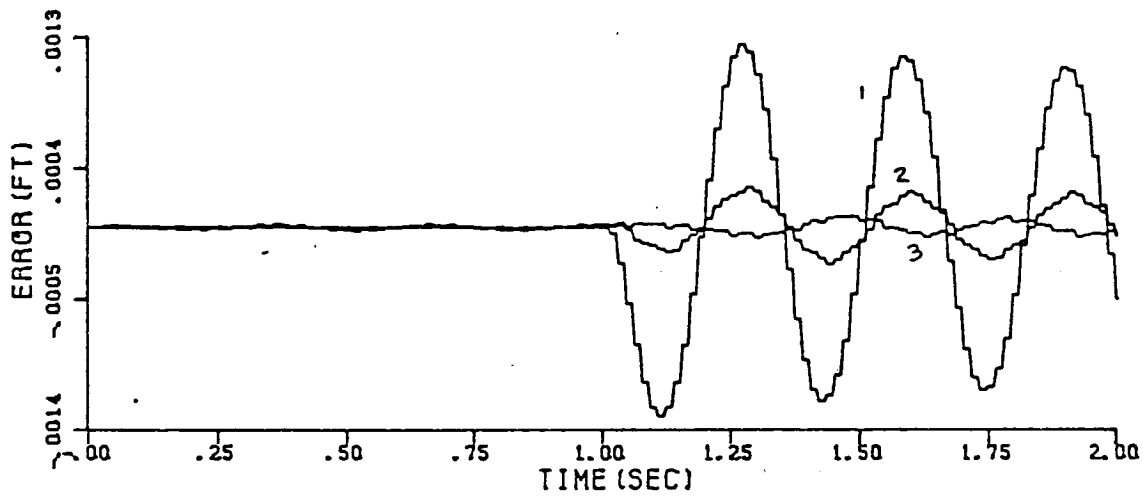
*same for direction #2

-same for direction #3

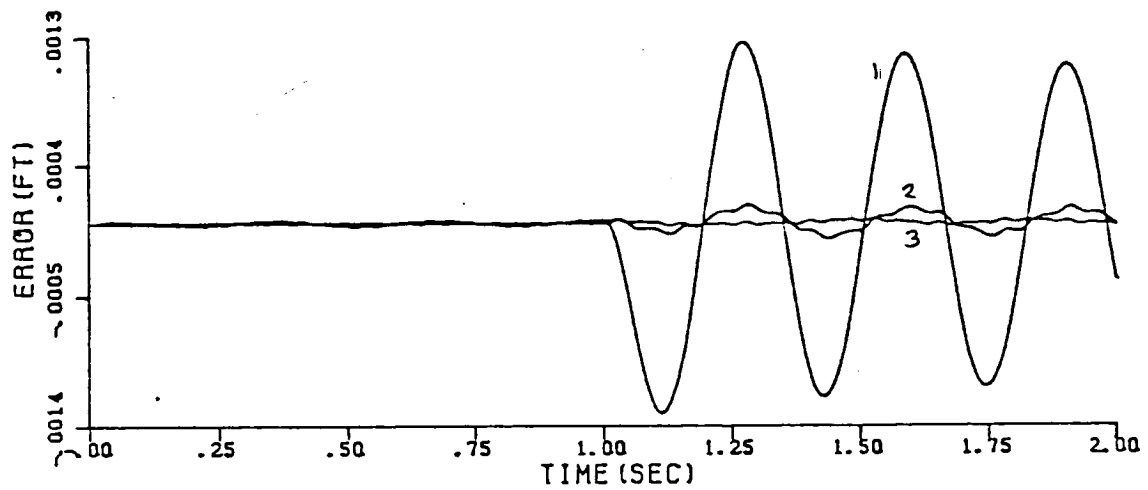
x peak signal in direction #1 divided by peak signal in direction #2 and #3 (1.5-2.0 sec)



(a) 50 hz

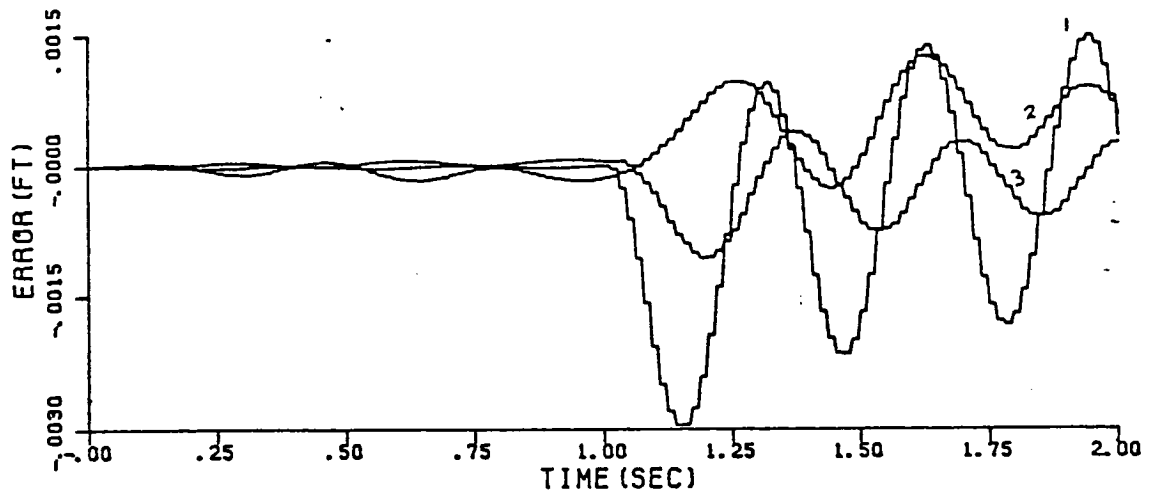


(b) 64 hz

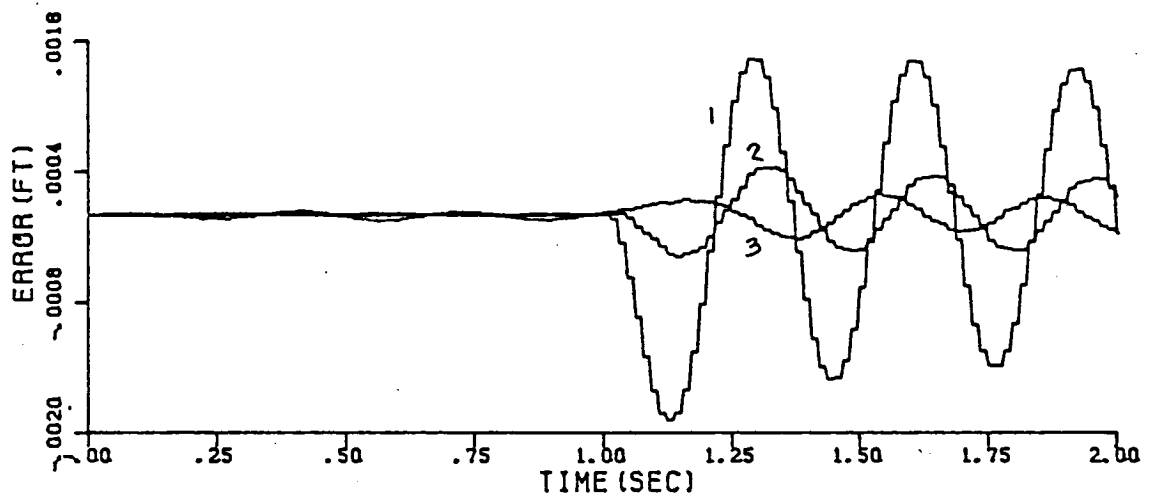


(c) 160 hz

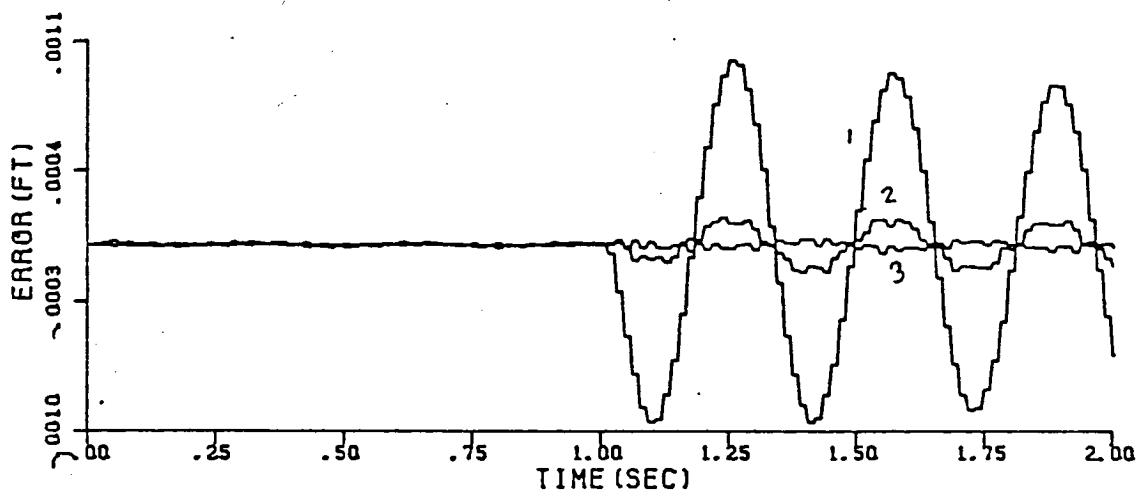
Figs.4.12a-c: Data sampling tests for various sampling rates(filter bandwidth is 15 rad/sec).



(a) 5 rad/sec



(b) 10 rad/sec



(c) 20 rad/sec

Figs.4.13a-c: Data sampling tests for various filter bandwidths(sampling rate = 64 hz).

was imposed on the resulting filter. It is possible to design the failure detection filter on the basis of a sampled-data description of the dynamics. This protects against the instability observed in these results, but data sampling fundamentally limits the ability of the filter to restrict a continuous failure signature to a single direction or plane in the output space.

CHAPTER V

SUMMARY AND CONCLUSIONS

The failure detection filter performs very well in the context of flexible structure dynamics when the dynamic model in the filter matches that of the system it is monitoring. It was found that the filter usually works quite well even when the description of the system includes modes which are not modeled in the filter. This performance rapidly diminishes, however, as the input frequencies become close to the natural frequencies of the unmodeled modes. For a given input frequency, an optimum filter bandwidth for maximum signal-to-noise ratio usually exists not far beyond the input frequency.

It is not always the case, however, that the filter will perform satisfactorily in the presence of modeling error. Sometimes two different detector gains capable of detecting the same failure event and designed with the same filter poles will yield grossly different detection performances—in one case the signal-to-noise ratio might be 50 and in the other case it might be less by an order of magnitude. This effect is caused by the direct appearance of the detector gain in the filter input due to observation spillover, the same phenomenon encountered when designing control systems for flexible structures.

The filter worked well for sensor failures, even when the initial amplitudes on the unmodeled modes were a significant fraction of those on the modeled modes (up to 7.5% were tested).

By varying filter bandwidth, it was possible to obtain very high signal-to-noise ratios for fixed initial conditions.

As expected, satisfactory performance of the filter designed for continuous data processing when used in a sampled-data mode depended strongly on a very high sampling rate. Only when the sampling rate reached five times the natural frequency of the last system mode did the signal-to-noise ratio surpass 10. As can be anticipated, when the sampling rate to filter bandwidth ratio is too low, the phase lag caused by sampling tended to destabilize the system.

These observations bring to mind several suggestions with regard to both the actual beam experiment and areas for further study:

- (1) To ensure adequate filter performance, it may be necessary to eliminate observation spillover as much as possible—it might be possible to accomplish this using a phase lock loop¹⁰ to comb out only the modeled modes from the output or by reducing the bandwidth of sensor data (one must be careful in doing this, however, not to attenuate the failure signal as well).
- (2) It may be necessary to use a sampling rate of at least 64 hz in order to get stable and adequate performance from the filter—this will depend upon the degree of excitation of the higher modes.
- (3) Even after specifying D to be a detector gain and assign-

ing all the filter eigenvalues, there is still a lot of freedom left in D (especially when D is designed to detect only one event) that could be used to reduce spillover noise—using this freedom would require a more analytic approach to solving for D and involve solving a set of nonlinear simultaneous equations when assigning eigenvalues.

- (4) The whole issue of stochastic failure detection filter theory has not even been addressed here—this will be an additional consideration in designing the filter when optimizing signal-to-noise ratios in the presence of plant, actuator, and sensor noise.

APPENDIX A

FILE: FDFIL FORTRAN A VM/SP CONVERSATIONAL MONITOR SYSTEM

```

C*****FDF00010
C                                             FDF00020
C      PROGRAM FDFIL COMPUTES THE DETECTOR GAIN      FDF00030
C      OF THE FAILURE DETECTION FILTER              FDF00040
C      FOR BOTH ACTUATOR AND SENSOR FAILURE EVENTS  FDF00050
C                                                    FDF00060
C*****FDF00070
C      INPUT:  N - NUMBER OF SYSTEM STATES          FDF00080
C              NS - NUMBER OF SENSORS              FDF00090
C              NF - NUMBER OF FAILURE EVENTS        FDF00100
C              IFAL - (=1) TO INPUT EVENT VECTORS FOR SENSOR CASE FDF00110
C                  (=0) THEN CF=I IS GENERATED FOR ALL SENSORS FDF00120
C              IAS - (=1) FOR ACTUATOR EVENTS      FDF00130
C                  (=2) FOR SENSOR EVENTS          FDF00140
C              EV - FILTER EIGENVALUES             FDF00150
C              A - SYSTEM MATRIX                   FDF00160
C              C - MEASUREMENT MATRIX              FDF00170
C              FALL - MATRIX OF EVENT VECTORS      FDF00180
C                  (COLUMNS ARE EVENTS)           FDF00190
C                                                    FDF00200
C      OUTPUT: D -DETECTOR GAIN                    FDF00210
C              DPR - AUXILIARY DETECTOR GAIN       FDF00220
C              MU - ARRAY OF SEPARABILITY ORDERS   FDF00230
C              NU - ARRAY OF DETECTION ORDERS      FDF00240
C              NUMOD - ARRAY OF MODIFIED DETECTION ORDERS FDF00250
C              IQ - ARRAY OF COMPLETED STATE SPACE ORDERS FDF00260
C              CF - MATRIX OF OUTPUT ERROR DIRECTIONS FOR FDF00270
C                  ACTUATOR FAILURES (COLUMNS ARE VECTORS) FDF00280
C              CZKLAF - THIS VECTOR AND THE UNIT VECTOR IN THE FDF00290
C                  ITH DIRECTION SPAN THE PLANE OF OUTPUT FDF00300
C                  ERRORS FOR SENSOR FAILURES      FDF00310
C                                                    FDF00320
C      IMSL SUBROUTINES THAT ARE USED:              FDF00330
C      VMULFM(A,B,C) - C=A(TRANPOSE)*B             FDF00340
C      VMULFP(A,B,C) - C=A*B(TRANPOSE)             FDF00350
C      VMULFF(A,B,C) - C=A*B                       FDF00360
C      LINV1F(A,AI) - AI=A(INVERSE)                 FDF00370
C      EIGRF(A,EV) - EV=EIGENVALUES(A)              FDF00380
C                                                    FDF00390
C*****FDF00400
C                                             FDF00410
C                                             FDF00420
C                                             FDF00430
C* THIS IS THE MAIN PROGRAM FOR ACTUATOR EVENT FILTER FDF00440
C                                                    FDF00450
C      INTEGER NU(10),ICAT(10)                      FDF00460
C      REAL DOUT(20,10)                             FDF00470
C      DOUBLE PRECISION                             FDF00480
C      &      A(20,20),C(10,20),FALL(20,10),CF(10,10),G(20,10), FDF00490
C      &      ZKF(20,20),CPF(10,20),ZMF(200,20),D(20,10), FDF00500
C      &      DC(20,20),ADC(20,20),WK(440),REVAL(40),REVEC(800), FDF00510
C      &      DPR(20,10),AP(20,20),EV,EPS,TOL FDF00520
C      COMPLEX*16 EVAL(20),EVEC(20,20) FDF00530
C      EQUIVALENCE(EVAL(1),REVAL(1)),(EVEC(1,1),REVEC(1)) FDF00540
C      DATA IN,IO/7,8/ FDF00550

```

```

      READ(IN,10) N,NS,NF,IFAL,IAS,EV
      READ(IN,20) ((A(I,J),J=1,16),I=1,16),
&                ((C(I,J),J=1,16),I=1,8),
&                ((FALL(I,J),J=1,8),I=1,16)
10  FORMAT(5I5/E14.4)
20  FORMAT(32(8F10.3/),16(8F10.3/),15(8F10.3/),8F10.3)
      WRITE(10,25) N,NS,NF,IFAL,IAS,EV
25  FORMAT('N=',I2,5X,'NS=',I2,5X,'NF=',I2,5X,'IFAL=',I2,5X,
&         'IAS=',I2/'EV=',E14.4/)
      WRITE(10,26) ((A(I,J),J=1,8),I=1,8),
&                ((C(I,J),J=1,8),I=1,8),
&                ((FALL(I,J),J=1,8),I=1,8)
26  FORMAT(///'A='/'8(8F10.4//)'C='/'8(8F10.4//)'FALL='/'8(8F10.4//))
      IF(IAS.EQ.2) GO TO 27
      CALL SEPDET(A,C,FALL,N,NF,NS,ISEP,IDET,IDIR,C,CF,G,NU,NUMOD,
&               ZKF,CPF,ZMF)
      IF((ISEP.EQ.1).OR.(IDET.EQ.1)) GO TO 100
      CALL DGAIN(C,A,EV,G,CF,CPF,NU,NUMOD,N,NF,NS,O,O,DPR,
&              ZKF,ZMF,AP,D)
      GO TO 28
C
C*  CALL THE MAIN PROGRAM FOR SENSOR EVENT FILTER
C
27  CALL SENSOR(C,A,EV,G,NU,CF,CPF,N,NF,NS,
&             ZKF,ZMF,FALL,IFAL,IDET,ICAT,D)
      DO 271 I=1,10
      IF(ICAT(I).EQ.3) STOP
271  CONTINUE
      IF(IDET.EQ.0) GO TO 28
      WRITE(10,277) IDET,((FALL(I,J),J=1,4),I=1,6)
277  FORMAT('IDET=',I1/'FALL='/'6(4E14.4//))
      GO TO 200
28  CALL VMULFF(D,C,N,NS,N,20,10,DC,20,IER)
      CALL MATSUB(A,DC,20,20,N,N,ADC)
      WRITE(10,29) ((ADC(I,J),J=1,4),I=1,4)
29  FORMAT('A-DC='/'4(4E14.4//))
C*  VERIFY THE PLACEMENT OF FILTER EIGENVALUES
      CALL EIGRF(ADC,N,20,O,REVAL,REVEC,20,WK,IER)
      WRITE(10,30) (EVAL(I),I=1,16)
30  FORMAT('CLOSED-LOOP EVS ARE: '/'16(2F10.4//))
      WRITE(10,40) ((D(I,J),J=1,3),I=1,16)
40  FORMAT('GAIN MATRIX D='/'16(3E16.6//))
      DO 48 I=1,N
      DO 48 J=1,NS
      DOUT(I,J)=SNGL(D(I,J))
48  CONTINUE
      WRITE(11,50) ((DOUT(I,J),J=1,3),I=1,16)
50  FORMAT(15(3E16.6/),3E16.6)
      GO TO 200
100 WRITE(10,110) ISEP,IDET
110 FORMAT('THE SYSTEM IS NOT SEPARABLE OR DETECTABLE: '/'
&         'ISEP=',I1,10X,'IDET=',I1)
200 STOP
      END
C

```

FDF00560
 FDF00570
 FDF00580
 FDF00590
 FDF00600
 FDF00610
 FDF00620
 FDF00630
 FDF00640
 FDF00650
 FDF00660
 FDF00670
 FDF00680
 FDF00690
 FDF00700
 FDF00710
 FDF00720
 FDF00730
 FDF00740
 FDF00750
 FDF00760
 FDF00770
 FDF00780
 FDF00790
 FDF00800
 FDF00810
 FDF00820
 FDF00830
 FDF00840
 FDF00850
 FDF00860
 FDF00870
 FDF00880
 FDF00890
 FDF00900
 FDF00910
 FDF00920
 FDF00930
 FDF00940
 FDF00950
 FDF00960
 FDF00970
 FDF00980
 FDF00990
 FDF01000
 FDF01010
 FDF01020
 FDF01030
 FDF01040
 FDF01050
 FDF01060
 FDF01070
 FDF01080
 FDF01090
 FDF01100

```

C* SEPDET DETERMINES SEPARABILITY AND DETECTABILITY OF EVENTS
C
      SUBROUTINE SEPDET(A,C,FALL,N,NF,NS,ISEP,IDET,IDIR,CSYS,CF,G,NU,
&          NUMOD,ZKF,CPF,ZMF)
      INTEGER MU(10),NU(10),IQ(10),NUMOD(10)
      DOUBLE PRECISION
&          A(20,20),C(10,20),FALL(20,10),CF(10,10),CPF(10,20),
&          G(20,10),ZKF(20,20),ZMF(200,20),F(20),CAJ(10,20),
&          CAJF(10),OM(10,10),OMSUB(10,10),WL(20),WF(20,10),
&          CFTC(10,20),CFTCF(10,10),CFTCFI(10,10),WKAR(460),
&          CFTTI(10,20),AFALL(20,10),AFCF(20,20),CFCF(10,20),
&          ZMFNUL(20,20),AJ(20,20),ZMFSUB(20,20),FALL2(20,10),
&          ZMFSB(10,20),ZMFSB2(10,20),AJ2(20,20),AMUF(20),
&          CSYS(10,20),EPS,TOL,CAJEPS,ZKNU1
      DATA EPS,IO/1.D-4,8/
      ISEP=0
      IDET=0
      DO 3 I=1,N
        DO 3 J=1,NF
          FALL2(I,J)=FALL(I,J)
3      CONTINUE
      DO 20 K=1,NF
        DO 5 I=1,N
          F(I)=FALL(I,K)
5      CONTINUE
        MU(K)=0
        CALL MATID(AJ,20,N)
6      CALL VMULFF(C,AJ,NS,N,N,10,20,CAJ,10,IER)
        CALL MATVEC(CAJ,F,10,20,NS,N,CAJF)
        TOL=0.00
        DO 7 I=1,NS
          DO 7 J=1,N
            CAJEPS=CAJ(I,J)*EPS
            TOL=DABS(DMAX1(TOL,CAJEPS))
7      CONTINUE
        NZERO=0
        DO 10 I=1,NS
          IF(DABS(CAJF(I)).LT.TOL) NZERO=NZERO+1
10     CONTINUE
        IF(NZERO.NE.NS) GO TO 12
        MU(K)=MU(K)+1
        CALL VMULFF(A,AJ,N,N,N,20,20,AJ2,20,IER)
        DO 11 I=1,N
          DO 11 J=1,N
            AJ(I,J)=AJ2(I,J)
11     CONTINUE
        GO TO 6
12     WRITE(IO,13) K,MU(K)
13     FORMAT('K=',I2,5X,'MU=',I2)
        CALL MATVEC(AJ,F,20,20,N,N,AMUF)
        DO 15 I=1,N
          FALL(I,K)=AMUF(I)
          CF(I,K)=CAJF(I)
15     CONTINUE
20     CONTINUE

```

```

FDF01110
FDF01120
FDF01130
FDF01140
FDF01150
FDF01160
FDF01170
FDF01180
FDF01190
FDF01200
FDF01210
FDF01220
FDF01230
FDF01240
FDF01250
FDF01260
FDF01270
FDF01280
FDF01290
FDF01300
FDF01310
FDF01320
FDF01330
FDF01340
FDF01350
FDF01360
FDF01370
FDF01380
FDF01390
FDF01400
FDF01410
FDF01420
FDF01430
FDF01440
FDF01450
FDF01460
FDF01470
FDF01480
FDF01490
FDF01500
FDF01510
FDF01520
FDF01530
FDF01540
FDF01550
FDF01560
FDF01570
FDF01580
FDF01590
FDF01600
FDF01610
FDF01620
FDF01630
FDF01640
FDF01650

```

```

205  WRITE(IO,205) ((CF(I,J),J=1,3),I=1,3)
      FORMAT('CF='//3(3E16.6//))
      CALL MATID(OM,10,NS)
      CALL ORTRED(CF,10,10,NS,NF,OM,NS,O,OM,OMSUB,
&             IRKCF,ICODE3,ZKNU1,WL,IQ,WF)
      WRITE(IO,207) IRKCF
207  FORMAT('RANK CF IS ',I2)
      IF(IRKCF.EQ.NF) GO TO 21
      ISEP=1
      WRITE(IO,209)
209  FORMAT('THE EVENTS ARE NOT SEPARABLE')
      RETURN
21  CALL VMULFM(CF,C,NS,NF,N,10,10,CFTC,10,IER)
      CALL VMULFM(CF,CF,NS,NF,NF,10,10,CFTCF,10,IER)
      CALL LINV1F(CFTCF,NF,10,CFTCFI,O,WKAR,IER)
      CALL VMULFF(CFTCFI,CFTC,NF,NF,N,10,10,CFTTI,10,IER)
      CALL VMULFF(A,FALL,N,N,NF,20,20,AFALL,20,IER)
      CALL VMULFF(AFALL,CFTTI,N,NF,N,20,10,AFCF,20,IER)
      CALL MATSUB(A,AFCF,20,20,N,N,ZKF)
      CALL VMULFF(CF,CFTTI,NS,NF,N,10,10,CFCF,10,IER)
      CALL MATSUB(C,CFCF,10,20,NS,N,CPF)
      CALL MATGEN(CPF,ZKF,10,20,200,NS,N,N,ZMFSB,ZMFSB2,ZMF)
      WRITE(IO,303) ((ZKF(I,J),J=1,4),I=1,4),
&             ((CPF(I,J),J=1,4),I=1,3)
303  FORMAT('ZKF='//4(4E14.4//)'CPF='//3(4E14.4//))
      CALL MATID(ZMFNUL,20,N)
      CALL ORTRED(ZMF,200,20,NS=N,N,ZMFNUL,NS,O,ZMFNUL,ZMFSUB,
&             IRKZMF,ICODE3,ZKNU1,WL,IQ,WF)
      CALL DETGEN(MU,FALL,FALL2,IDIR,CSYS,A,C,N,NS,NF,ZKF,NU,NUMOD,G)
      WRITE(IO,315) IRKZMF,(NU(I),I=1,2)
315  FORMAT('IRKZMF=',I2,10X,'NU1-2=',2I5//)
      NUG=N-IRKZMF
      INUSUM=0
      DO 25 I=1,NF
          INUSUM=INUSUM+NU(I)
25  CONTINUE
      IF(INUSUM.EQ.NUG) GO TO 30
      IDET=1
30  RETURN
      END

C
C*  DETGEN FINDS THE DETECTION ORDER AND GENERATOR FOR THE EVENTS
C
      SUBROUTINE DETGEN(MU,FALL,FALL2,IDIR,CSYS,A,C,N,NS,NF,ZKF,
&             NU,NUMOD,G)
      INTEGER MU(10),NU(10),IQ(10),NUMOD(10),LEXP(10)
      DOUBLE PRECISION
&             FALL(20,10),A(20,20),C(10,20),CSUB(10,20),
&             G(20,10),F(20),CSF(10),CSFTC(20),CT(20,10),
&             ASF(20),ASUB(20,20),ZK(20,20),CP(10,20),ZMP(200,20),
&             ZMK(200,20),ZMKNUL(10,10),CI(20),AMU(20,20),
&             WL(20),WF(20,10),ZKF(20,20),ZMPNUL(20,20),ZMKSUB(20,20),
&             ZMPSUB(20,20),ZMPSB(10,20),ZMKSB(10,20),
&             ZMPSB2(10,20),ZMKSB2(10,20),AMU2(20,20),
&             AF(20),FALL2(20,10),ZKL(20,20),CZKL(10,20),

```


&	CZKLAF(10),ZKL2(20,20),CSYS(10,20),CZKEPS,	FDF02210
&	CFTCF,ZKNU1,CIAMUF,EPS,TOL	FDF02220
	DATA IO,EPS/8,1.0-4/	FDF02230
	DO 45 K=1,NF	FDF02240
	DO 5 I=1,N	FDF02250
	F(I)=FALL(I,K)	FDF02260
5	CONTINUE	FDF02270
	CALL MATVEC(C,F,10,20,NS,N,CSF)	FDF02280
	DO 3 I=1,NS	FDF02290
	DO 3 J=1,N	FDF02300
	CT(J,I)=C(I,J)	FDF02310
3	CONTINUE	FDF02320
	CALL MATVEC(CT,CSF,20,10,N,NS,CSFTC)	FDF02330
	CFTCF=0.	FDF02340
	DO 10 I=1,NS	FDF02350
	CFTCF=CFTCF+CSF(I)**2	FDF02360
10	CONTINUE	FDF02370
	DO 15 I=1,N	FDF02380
	CSFTC(I)=CSFTC(I)/CFTCF	FDF02390
15	CONTINUE	FDF02400
	CALL MATVEC(A,F,20,20,N,N,ASF)	FDF02410
	DO 17 I=1,N	FDF02420
	DO 17 J=1,N	FDF02430
	ASUB(I,J)=ASF(I)*CSFTC(J)	FDF02440
17	CONTINUE	FDF02450
	DO 18 I=1,NS	FDF02460
	DO 18 J=1,N	FDF02470
	CSUB(I,J)=CSF(I)*CSFTC(J)	FDF02480
18	CONTINUE	FDF02490
	CALL MATSUB(A,ASUB,20,20,N,N,ZK)	FDF02500
	CALL MATSUB(C,CSUB,10,20,NS,N,CP)	FDF02510
	CALL MATGEN(CP,ZK,10,20,200,NS,N,N,ZMP)	FDF02520
	CALL MATID(ZMPNUL,20,N)	FDF02530
	CALL ORTRED(ZMP,200,20,NS*N,N,ZMPNUL,NS,0,ZMPNUL,ZMPSUB,	FDF02540
&	IRKZMP,ICODE3,ZKNU1,WL,IQ,WF)	FDF02550
	WRITE(IO,206) IRKZMP	FDF02560
206	FORMAT('RANK OF ZMP IS ',I2)	FDF02570
	NU(K)=N-IRKZMP	FDF02580
	CALL MATGEN(C,ZK,10,20,200,NS,N,NU(K),ZMKS, ZMKS2,ZMK)	FDF02590
	CALL ORTRED(ZMK,200,20,NS*N,N,ZMPNUL,NS,0,ZMKNUL,ZMKS,	FDF02600
&	IRKZMK,ICODE3,ZKNU1,WL,IQ,WF)	FDF02610
	NUMOD(K)=IRKZMK	FDF02620
	WRITE(IO,216) NUMOD(K)	FDF02630
216	FORMAT('NUMOD=',I2)	FDF02640
	DO 20 J=1,N	FDF02650
	CI(J)=C(ICODE3,J)	FDF02660
20	CONTINUE	FDF02670
	CIAMUF=0.DO	FDF02680
	DO 25 I=1,N	FDF02690
	CIAMUF=CIAMUF+CI(I)*F(I)	FDF02700
25	CONTINUE	FDF02710
	DO 40 I=1,N	FDF02720
	G(I,K)=(CIAMUF/ZKNU1)*WL(I)	FDF02730
40	CONTINUE	FDF02740
43	WRITE(IO,225) (G(I,K),I=1,4)	FDF02750

225	FORMAT('G=' /4E14.4)	FDF02760
	IF(IDIR.NE.1) GO TO 45	FDF02770
	LEXP(K)=0	FDF02780
	DO 441 I=1,N	FDF02790
	AF(I)=FALL2(I,K)	FDF02800
441	CONTINUE	FDF02810
	CALL MATID(ZKL,20,N)	FDF02820
442	CALL VMULFF(CSYS,ZKL,NS,N,N,10,20,CZKL,10,IER)	FDF02830
	CALL MATVEC(CZKL,AF,10,20,NS,N,CZKLAF)	FDF02840
	TOL=0.DO	FDF02850
	DO 443 I=1,NS	FDF02860
	DO 443 J=1,N	FDF02870
	CZKEPS=CZKL(I,J)*EPS	FDF02880
	TOL=DABS(DMAX1(TOL,CZKEPS))	FDF02890
443	CONTINUE	FDF02900
	NZERO=0	FDF02910
	DO 444 I=1,NS	FDF02920
	IF(DABS(CZKLAF(I)).LT.TOL) NZERO=NZERO+1	FDF02930
444	CONTINUE	FDF02940
	IF(NZERO.NE.NS) GO TO 446	FDF02950
	LEXP(K)=LEXP(K)+1	FDF02960
	CALL VMULFF(ZK,ZKL,N,N,N,20,20,ZKL2,20,IER)	FDF02970
	DO 445 I=1,N	FDF02980
	DO 445 J=1,N	FDF02990
	ZKL(I,J)=ZKL2(I,J)	FDF03000
445	CONTINUE	FDF03010
	GO TO 442	FDF03020
446	WRITE(10,447) LEXP(K),(CZKLAF(I),I=1,NS)	FDF03030
447	FORMAT('L=',I2,5X,'CZKLAF=',3E16.6)	FDF03040
45	CONTINUE	FDF03050
	RETURN	FDF03060
	END	FDF03070
C		FDF03080
C*	DGAIN DETERMINES THE DETECTOR GAIN FOR THE FILTER	FDF03090
C		FDF03100
	SUBROUTINE DGAIN(C,A,EV,GEN,CF,CPF,NU,NUMOD,N,NF,NS,IAP,IDPR,DPR,	FDF03110
	& ZKF,ZMF,AP,D)	FDF03120
	INTEGER NU(10),IQ(10),NUMOD(10)	FDF03130
	DOUBLE PRECISION	FDF03140
	& C(10,20),A(20,20),GEN(20,10),CF(10,10),CPF(10,20),	FDF03150
	& G(20),D(20,10),P(20),Q(20),AJ(20,20),AJG(20),	FDF03160
	& QD(20,10),CFTCF(10,10),CFTCFI(10,10),WK(460),	FDF03170
	& CFTTI(10,10),DP(20,10),ZMF(200,20),ZMFNUL(20,20),	FDF03180
	& WL(20),WF(20,10),AP(20,20),DPC(20,20),PSI(20),	FDF03190
	& APJ(20,20),WFI(20),APJWF(20),PSIW(20,10),ZKF(20,20),	FDF03200
	& ZKFQ(20,20),ZKFWF(20),W(20,10),CPFW(10,10),CPFWT(10,10),	FDF03210
	& CPFWTI(10,10),CFWTI(10,10),DPR(20,10),CF2TTI(10,10),	FDF03220
	& DPRSUB(20,10),DH(20,10),OMSUB(10,10),AJ2(20,20),	FDF03230
	& APJ2(20,20),ZKFQ2(20,20),ZMFSUB(20,20),EV,EPS,TOL	FDF03240
	DATA 10/8/	FDF03250
	DO 35 K=1,NF	FDF03260
	DO 5 I=1,N	FDF03270
	G(I)=GEN(I,K)	FDF03280
5	CONTINUE	FDF03290
	CALL EVAS(20,NUMOD(K),EV,P)	FDF03300

```

DO 10 I=1,N
  Q(I)=P(1)*G(I)
10 CONTINUE
  NUMOD1=NUMOD(K)-1
  IF(NUMOD1.EQ.O) GO TO 21
  DO 20 J=1,NUMOD1
    CALL MATPOW(A,20,N,J,AJ2,AJ)
    CALL MATVEC(AJ,G,20,20,N,N,AJG)
    DO 15 I=1,N
      Q(I)=Q(I)+P(J+1)*AJG(I)
15 CONTINUE
20 CONTINUE
21 CALL MATPOW(A,20,N,NUMOD(K),AJ2,AJ)
  CALL MATVEC(AJ,G,20,20,N,N,AJG)
  DO 25 I=1,N
    Q(I)=Q(I)+AJG(I)
25 CONTINUE
  DO 30 I=1,N
    QD(I,K)=Q(I)
30 CONTINUE
35 CONTINUE
  CALL VMULFM(CF,CF,NS,NF,NF,10,10,CFTCF,10,IER)
  CALL LINV1F(CFTCF,NF,10,CFTCF1,O,WK,IER)
  CALL VMULFP(CFTCF1,CF,NF,NF,NS,10,10,CFTTI,10,IER)
  CALL VMULFF(QD,CFTTI,N,NF,NS,20,10,DP,20,IER)
  CALL VMULFF(DP,C,N,NS,N,20,10,DPC,20,IER)
  CALL MATSUB(A,DPC,20,20,N,N,AP)
  WRITE(IO,391) ((DP(I,J),J=1,3),I=1,4),
& ((AP(I,J),J=1,4),I=1,4)
391 FORMAT('DP='//4(3E14.4)//'AP='//4(4E14.4)//)
  NUSUM=O
  DO 40 K=1,NF
    NUSUM=NUSUM+NU(K)
40 CONTINUE
  IF(IDPR.EQ.1) GO TO 90
  IF((N-NUSUM.NE.O).AND.(IAP.NE.1)) GO TO 50
  DO 45 I=1,N
    DO 45 J=1,NS
      D(I,J)=DP(I,J)
45 CONTINUE
  RETURN
50 CALL MATID(ZMFNUL,20,N)
  CALL ORTRED(ZMF,200,20,NS*N,N,ZMFNUL,NS,1,ZMFNUL,ZMFSUB,
& IRKZMF,ICODE3,ZKNU1,WL,IQ,WF)
  WRITE(IO,411) (IQ(I),I=1,4)
411 FORMAT('IQ='//4I4)
  ICP=O
  DO 85 I=1,NS
    IF(IQ(I).EQ.O) GO TO 85
    ICP=ICP+1
    CALL EVAS(20,IQ(I),EV,P)
    DO 55 L=1,N
      WFI(L)=WF(L,I)
55 CONTINUE
    DO 60 J=1,N

```

```

FDF03310
FDF03320
FDF03330
FDF03340
FDF03350
FDF03360
FDF03370
FDF03380
FDF03390
FDF03400
FDF03410
FDF03420
FDF03430
FDF03440
FDF03450
FDF03460
FDF03470
FDF03480
FDF03490
FDF03500
FDF03510
FDF03520
FDF03530
FDF03540
FDF03550
FDF03560
FDF03570
FDF03580
FDF03590
FDF03600
FDF03610
FDF03620
FDF03630
FDF03640
FDF03650
FDF03660
FDF03670
FDF03680
FDF03690
FDF03700
FDF03710
FDF03720
FDF03730
FDF03740
FDF03750
FDF03760
FDF03770
FDF03780
FDF03790
FDF03800
FDF03810
FDF03820
FDF03830
FDF03840
FDF03850

```

```

        PSI(J)=P(1)*WFI(J)                                FDF03860
60      CONTINUE                                           FDF03870
        IQIM1=IQ(I)-1                                       FDF03880
        IF(IQIM1.EQ.0) GO TO 71                             FDF03890
        DO 70 J=1,IQIM1                                     FDF03900
            CALL MATPOW(AP,20,N,J,APJ2,APJ)                 FDF03910
            CALL MATVEC(APJ,WFI,20,20,N,N,APJWF)            FDF03920
            DO 65 K=1,N                                       FDF03930
                PSI(K)=PSI(K)+P(J+1)*APJWF(K)               FDF03940
            CONTINUE                                         FDF03950
70      CONTINUE                                           FDF03960
71      CALL MATPOW(AP,20,N,IQ(I),APJ2,APJ)                 FDF03970
        CALL MATVEC(APJ,WFI,20,20,N,N,APJWF)              FDF03980
        DO 75 K=1,N                                         FDF03990
            PSI(K)=PSI(K)+APJWF(K)                          FDF04000
75      CONTINUE                                           FDF04010
        CALL MATPOW(ZKF,20,N,IQ(I)-1,ZKFQ2,ZKFQ)           FDF04020
        CALL MATVEC(ZKFQ,WFI,20,20,N,N,ZKFWF)              FDF04030
        DO 80 L=1,N                                         FDF04040
            PSIW(L,ICP)=PSI(L)                              FDF04050
            W(L,ICP)=ZKFWF(L)                               FDF04060
80      CONTINUE                                           FDF04070
85      CONTINUE                                           FDF04080
        CALL VMULFF(CPF,W,NS,N,ICP,10,20,CPFW,10,IER)      FDF04090
        CALL VMULFM(CPFW,CPFW,NS,ICP,ICP,10,10,CPFWT,10,IER) FDF04100
        CALL LINV1F(CPFWT,ICP,10,CPFWTI,0,WK,IER)           FDF04110
        CALL VMULFP(CPFWTI,CPFW,ICP,ICP,NS,10,10,CFWTTI,10,IER) FDF04120
        CALL VMULFF(PSIW,CFWTTI,N,ICP,NS,20,10,DPR,20,IER) FDF04130
90      WRITE(10,457) ((DPR(I,J),J=1,3),I=1,4)            FDF04140
457     FORMAT('DPR='//4(3E14.4//))                        FDF04150
        CALL VMULFF(CF,CFTTI,NS,NF,NS,10,10,CF2TTI,10,IER) FDF04160
        CALL VMULFF(DPR,CF2TTI,N,NS,NS,20,10,DPRSUB,20,IER) FDF04170
        CALL MATSUB(DPR,DPRSUB,20,10,N,NS,DH)               FDF04180
        CALL MATADD(DP,DH,20,10,N,NS,D)                    FDF04190
        RETURN                                              FDF04200
        END                                                FDF04210
C                                                        FDF04220
C*  SENSOR IS THE MAIN PROGRAM FOR SENSOR EVENT FILTER DESIGN FDF04230
C                                                        FDF04240
        SUBROUTINE SENSOR(C,A,EV,G,NU,CF,CPF,N,NF,NS,      FDF04250
&          ZKF,ZMF,FALL,IFAL,IDET,ICAT,D)                 FDF04260
        INTEGER NU(10),IQ(10),NUMOD(10),ICAT(10)          FDF04270
        DOUBLE PRECISION                                     FDF04280
&          A(20,20),C(10,20),G(20,10),CF(10,10),CPF(10,20), FDF04290
&          ZKF(20,20),ZMF(200,20),FALL(20,10),D(20,10),CCT(10,10), FDF04300
&          CCTI(10,10),AP(20,20),WOSUB(10,20),WOSUB2(10,20), FDF04310
&          WO(200,20),F(20),AF(20),WOAF(200),APAF(20),WK(40), FDF04320
&          APAF2(20),CAPAF(10),CAAFN1(10,20),CAFNUL(20,20), FDF04330
&          CAFSUB(20,20),WL(20),WF(20,10),AFALL(20,10), FDF04340
&          DPR(20,10),CPF2(10,20),AP2(20,20),AFALL2(20,10), FDF04350
&          EPS,TOL,WOEPS                                   FDF04360
        DATA IO,EPS/8,1.D-4/                               FDF04370
        IDIR=0                                               FDF04380
        IF(IFAL.EQ.1) GO TO 5                                FDF04390
        CALL VMULFP(C,C,NS,N,NS,10,10,CCT,10,IER)          FDF04400

```

	CALL LINV1F(CCT,NS,10,CCTI,O,WK,IER)	FDF04410
	CALL VMULFM(C,CCTI,NS,N,NS,10,10,FALL,20,IER)	FDF04420
	WRITE(IO,121) ((FALL(I,J),J=1,4),I=1,4)	FDF04430
	FORMAT('FALL='//4(4E14.4//))	FDF04440
121	5 CALL SEPDET(A,C,FALL,N,NF,NS,ISEP,IDET,IDIR,C,CF,G,NU,NUMOD,	FDF04450
	& ZKF,CPF,ZMF)	FDF04460
	IF(IDET.EQ.1) RETURN	FDF04470
	CALL DGAIN(C,A,EV,G,CF,CPF,NU,NUMOD,N,NF,NS,1,O,DPR,	FDF04480
	& ZKF,ZMF,AP,D)	FDF04490
	CALL MATGEN(CPF,AP,10,20,200,NS,N,N,WOSUB,WOSUB2,WO)	FDF04500
	WRITE(IO,132) ((WO(I,J),J=1,4),I=1,12)	FDF04510
132	FORMAT('WO='//12(4E14.4//))	FDF04520
	NSN=NS*N	FDF04530
	TOL=O.	FDF04540
	DO 10 I=1,NS	FDF04550
	DO 10 J=1,N	FDF04560
	WOEPS=WO(I,J)*EPS	FDF04570
	TOL=DABS(DMAX1(TOL,WOEPS))	FDF04580
	10 CONTINUE	FDF04590
	WRITE(IO,143) TOL	FDF04600
143	FORMAT('TOL=',E14.4/)	FDF04610
	DO 60 K=1,NF	FDF04620
	DO 15 I=1,N	FDF04630
	F(I)=FALL(I,K)	FDF04640
	15 CONTINUE	FDF04650
	CALL MATVEC(A,F,20,20,N,N,AF)	FDF04660
	CALL MATVEC(WO,AF,200,20,NS*N,N,WOAF)	FDF04670
	WRITE(IO,156) (WOAF(I),I=1,8)	FDF04680
156	FORMAT('WOAF='//2(4E14.4//))	FDF04690
	NO=O	FDF04700
	DO 20 I=1,NSN	FDF04710
	IF(DABS(WOAF(I)).LT.TOL) NO=NO+1	FDF04720
	20 CONTINUE	FDF04730
	IF(NO.EQ.NSN) GO TO 25	FDF04740
	ICAT(K)=1	FDF04750
	GO TO 60	FDF04760
	25 ICNT=O	FDF04770
	DO 30 I=1,N	FDF04780
	APAF(I)=AF(I)	FDF04790
	30 CONTINUE	FDF04800
	ICNT=ICNT+1	FDF04810
35	CALL MATVEC(C,APAF,10,20,NS,N,CAPAF)	FDF04820
	DO 40 I=1,NS	FDF04830
	CAAFN1(I,ICNT)=CAPAF(I)	FDF04840
	40 CONTINUE	FDF04850
	IF(ICNT.EQ.N) GO TO 50	FDF04860
	CALL MATVEC(AP,APAF,20,20,N,N,APAF2)	FDF04870
	DO 45 I=1,N	FDF04880
	APAF(I)=APAF2(I)	FDF04890
	45 CONTINUE	FDF04900
	GO TO 35	FDF04910
50	CALL MATID(CAFNUL,20,N)	FDF04920
	CALL ORTRED(CAAFN1,NS,N,10,20,CAFNUL,NS,O,CAFNUL,	FDF04930
	& CAFSUB,IRKCAF,ICODE3,ZKNU1,WL,IQ,WF)	FDF04940
	IF(IRKCAF.NE.1) GO TO 55	FDF04950

	ICAT(K)=2	FDF04960
	GO TO 60	FDF04970
55	ICAT(K)=3	FDF04980
60	CONTINUE	FDF04990
	WRITE(IO,166) (ICAT(K),K=1,4)	FDF05000
166	FORMAT('ICAT=',4I3/)	FDF05010
	DO 65 K=1,NF	FDF05020
	IF(ICAT(K).EQ.3) RETURN	FDF05030
65	CONTINUE	FDF05040
	CALL VMULFF(A,FALL,N,N,NF,20,20,AFALL,20,IER)	FDF05050
	WRITE(IO,177) ((AFALL(I,J),J=1,4),I=1,6)	FDF05060
177	FORMAT('AFALL=''/6(4E14.4/)/)/)	FDF05070
	DO 68 I=1,NS	FDF05080
	DO 68 J=1,N	FDF05090
	CPF2(I,J)=CPF(I,J)	FDF05100
68	CONTINUE	FDF05110
	DO 69 I=1,N	FDF05120
	DO 69 J=1,N	FDF05130
	AP2(I,J)=AP(I,J)	FDF05140
69	CONTINUE	FDF05150
	IDIR=1	FDF05160
C*	IF AFALL2 IS INPUTTED TO PROGRAM.	FDF05170
C*	DELETE THESE NEXT 5 STATEMENTS	FDF05180
	NF2=NF	FDF05190
	DO 70 I=1,N	FDF05200
	DO 70 J=1,NF2	FDF05210
	AFALL2(I,J)=AFALL(I,J)	FDF05220
70	CONTINUE	FDF05230
	CALL SEPDET(AP2,CPF2,AFALL2,N,NF2,NS,ISEP,IDET,IDIR,C,CF,G,	FDF05240
	& NU,NUMOD,ZKF,CPF,ZMF)	FDF05250
	IF(IDET.EQ.1) RETURN	FDF05260
	CALL DGAIN(CPF2,AP2,EV,G,CF,CPF,NU,NUMOD,N,NF2,NS,O,O,DPR,	FDF05270
	& ZKF,ZMF,AP,DPR)	FDF05280
	WRITE(IO,127) ((DPR(I,J),J=1,4),I=1,6)	FDF05290
127	FORMAT('DPR=''/6(4E14.4/)/)/)	FDF05300
	IDIR=0	FDF05310
	CALL SEPDET(A,C,FALL,N,NF,NS,ISEP,IDET,IDIR,C,CF,G,NU,NUMOD,	FDF05320
	& ZKF,CPF,ZMF)	FDF05330
	CALL DGAIN(C,A,EV,G,CF,CPF,NU,NUMOD,N,NF,NS,O,1,DPR,	FDF05340
	& ZKF,ZMF,AP,D)	FDF05350
	RETURN	FDF05360
	END	FDF05370
C		FDF05380
C*	ORTRED PERFORMS ORTHOGONAL REDUCTION ON MATRIX V	FDF05390
C		FDF05400
	SUBROUTINE ORTRED(V,M1V,N1V,MV,NV,OMI,NS,ICODE4,OM,OMSUB,	FDF05410
	& IRANK,ICODE3,ZKNU1,WL,IO,WF)	FDF05420
	INTEGER IQ(10),ICODE1(10)	FDF05430
	DOUBLE PRECISION	FDF05440
	& V(M1V,N1V),OMI(N1V,N1V),OM(N1V,N1V),OMSUB(N1V,N1V),	FDF05450
	& VK(20),W(20),WL(20),WF(20,10),WTVK,ZKNU1,EPS,TOL,VKEPS	FDF05460
	DATA IO,EPS/8,1.D-4/	FDF05470
	ICNT=0	FDF05480
	IRANK=0	FDF05490
	ICODE2=0	FDF05500

ICCODE3=0	FDF05510
WRITE(10,205)	FDF05520
205 FORMAT('ENTERING ORTRD')	FDF05530
DO 5 I=1,NS	FDF05540
IQ(I)=0	FDF05550
ICCODE1(I)=0	FDF05560
5 CONTINUE	FDF05570
DO 10 I=1,MV	FDF05580
DO 10 J=1,NV	FDF05590
OM(I,J)=OMI(I,J)	FDF05600
10 CONTINUE	FDF05610
DO 95 K=1,MV	FDF05620
TOL=0.	FDF05630
DO 20 J=1,NV	FDF05640
VK(J)=V(K,J)	FDF05650
VKEPS=VK(J)*EPS	FDF05660
TOL=DABS(DMAX1(TOL,VKEPS))	FDF05670
20 CONTINUE	FDF05680
IF(TOL.LT.EPS) TOL=EPS	FDF05690
ICCODE2=ICCODE2+1	FDF05700
IARG=ICCODE2-((ICCODE2-1)/NS)*NS	FDF05710
IF(ICCODE1(IARG).NE.O) GO TO 95	FDF05720
CALL MATVEC(OM,VK,N1V,N1V,NV,NV,W)	FDF05730
NZERO=0	FDF05740
DO 25 I=1,NV	FDF05750
IF(DABS(W(I)).LT.TOL) NZERO=NZERO+1	FDF05760
25 CONTINUE	FDF05770
WTVK=0.	FDF05780
DO 29 I=1,NV	FDF05790
WTVK=WTVK+W(I)*VK(I)	FDF05800
29 CONTINUE	FDF05810
IF(NZERO.NE.NV) GO TO 28	FDF05820
ICCODE1(IARG)=1	FDF05830
GO TO 95	FDF05840
28 IF(DABS(WTVK).GT.TOL) GO TO 30	FDF05850
ICCODE1(IARG)=1	FDF05860
GO TO 95	FDF05870
30 IF(ICCODE3.NE.O) GO TO 35	FDF05880
ICCODE3=K	FDF05890
35 DO 40 I=1,NV	FDF05900
WL(I)=W(I)	FDF05910
40 CONTINUE	FDF05920
IF(ICCODE4.NE.1) GO TO 80	FDF05930
IQ(IARG)=IQ(IARG)+1	FDF05940
DO 60 I=1,NV	FDF05950
WF(I,IARG)=W(I)	FDF05960
60 CONTINUE	FDF05970
80 IRANK=IRANK+1	FDF05980
WTVK=0.	FDF05990
DO 85 I=1,NV	FDF06000
WTVK=WTVK+W(I)*VK(I)	FDF06010
85 CONTINUE	FDF06020
ZKNU1=WTVK	FDF06030
DO 90 I=1,NV	FDF06040
DO 90 J=1,NV	FDF06050

	OMSUB(I,J)=W(I)*W(J)/WTVK	FDF06060
90	CONTINUE	FDF06070
	CALL MATSUB(OM,OMSUB,N1V,N1V,NV,NV,OM)	FDF06080
95	CONTINUE	FDF06090
	RETURN	FDF06100
	END	FDF06110
C		FDF06120
C*	MATGEN GENERATES LARGER MATRIX C FROM A AND B	FDF06130
C		FDF06140
	SUBROUTINE MATGEN(A,B,M1A,N1A,M1C,MA,NA,N,CSUB,CSUB2,C)	FDF06150
	DOUBLE PRECISION A(M1A,N1A),B(N1A,N1A),C(M1C,N1A),	FDF06160
	& CSUB(M1A,N1A),CSUB2(M1A,N1A),EPS	FDF06170
	DATA EPS/1.D-5/	FDF06180
	DO 5 I=1,MA	FDF06190
	DO 5 J=1,NA	FDF06200
	IF(DABS(A(I,J)).LT.EPS) A(I,J)=0.DO	FDF06210
	C(I,J)=A(I,J)	FDF06220
	CSUB(I,J)=C(I,J)	FDF06230
5	CONTINUE	FDF06240
	IF(N.EQ.1) RETURN	FDF06250
	NM1=N-1	FDF06260
	DO 15 K=1,NM1	FDF06270
	CALL VMULFF(CSUB,B,MA,NA,NA,M1A,N1A,CSUB2,M1A,IER)	FDF06280
	DO 10 I=1,MA	FDF06290
	DO 10 J=1,NA	FDF06300
	CSUB(I,J)=CSUB2(I,J)	FDF06310
	C(MA*K+I,J)=CSUB(I,J)	FDF06320
10	CONTINUE	FDF06330
15	CONTINUE	FDF06340
	RETURN	FDF06350
	END	FDF06360
C		FDF06370
C*	EVAS DETERMINES COEFFICIENTS P IN CHARACTERISTIC EQUATION	FDF06380
C		FDF06390
	SUBROUTINE EVAS(N1,N,EV,P)	FDF06400
	REAL PDUM(10)	FDF06410
	DOUBLE PRECISION P(N1),EV	FDF06420
	EVSNGL=SNGL(EV)	FDF06430
	DO 5 K=1,N	FDF06440
	I=N-K+1	FDF06450
	BETA=(FLOAT(IFACT(N))/(FLOAT(IFACT(N-1))*FLOAT(IFACT(I))))	FDF06460
	& *(EVSNGL**I)	FDF06470
	PDUM(K)=((-1.O)**I)*BETA	FDF06480
	P(K)=DBLE(PDUM(K))	FDF06490
5	CONTINUE	FDF06500
	RETURN	FDF06510
	END	FDF06520
C		FDF06530
C*	MULTIPLIES MATRIX BY VECTOR	FDF06540
C		FDF06550
	SUBROUTINE MATVEC(ARRAY,V,M1,N1,M,N,RET)	FDF06560
	DOUBLE PRECISION ARRAY(M1,N1),V(N1),RET(M1)	FDF06570
	DO 10 I=1,M	FDF06580
	RET(I)=0.DO	FDF06590
	DO 10 J=1,N	FDF06600

RET(I)=RET(I)+ARRAY(I,J)*V(J)	FDF06610
10 CONTINUE	FDF06620
RETURN	FDF06630
END	FDF06640
C	FDF06650
C* ADDS MATRIX B TO MATRIX A	FDF06660
C	FDF06670
SUBROUTINE MATADD(A,B,M1,N1,M,N,RET)	FDF06680
DOUBLE PRECISION A(M1,N1),B(M1,N1),RET(M1,N1)	FDF06690
DO 10 I=1,M	FDF06700
DO 10 J=1,N	FDF06710
RET(I,J)=A(I,J)+B(I,J)	FDF06720
10 CONTINUE	FDF06730
RETURN	FDF06740
END	FDF06750
C	FDF06760
C* SUBTRACTS MATRIX B FROM A	FDF06770
C	FDF06780
SUBROUTINE MATSUB(A,B,M1,N1,M,N,RET)	FDF06790
DOUBLE PRECISION A(M1,N1),B(M1,N1),RET(M1,N1)	FDF06800
DO 10 I=1,M	FDF06810
DO 10 J=1,N	FDF06820
RET(I,J)=A(I,J)-B(I,J)	FDF06830
10 CONTINUE	FDF06840
RETURN	FDF06850
END	FDF06860
C	FDF06870
C* GENERATES THE IDENTITY MATRIX	FDF06880
C	FDF06890
SUBROUTINE MATID(A,N1,N)	FDF06900
DOUBLE PRECISION A(N1,N1)	FDF06910
DO 20 I=1,N	FDF06920
DO 10 J=1,N	FDF06930
A(I,J)=0.00	FDF06940
10 CONTINUE	FDF06950
A(I,I)=1.000	FDF06960
20 CONTINUE	FDF06970
RETURN	FDF06980
END	FDF06990
C	FDF07000
C* RAISES MATRIX A TO POWER K	FDF07010
C	FDF07020
SUBROUTINE MATPOW(A,N1,N,K,AK2,AK)	FDF07030
DOUBLE PRECISION A(N1,N1),AK(N1,N1),AK2(N1,N1)	FDF07040
CALL MATID(AK,N1,N)	FDF07050
IF(K.EQ.0) RETURN	FDF07060
DO 10 IDUM=1,K	FDF07070
CALL VMULFF(A,AK,N,N,N,N1,N1,AK2,N1,IER)	FDF07080
DO 5 I=1,N	FDF07090
DO 5 J=1,N	FDF07100
AK(I,J)=AK2(I,J)	FDF07110
5 CONTINUE	FDF07120
10 CONTINUE	FDF07130
RETURN	FDF07140
END	FDF07150

C		FDF07160
C*	FINDS FACTORIAL OF N	FDF07170
C		FDF07180
	INTEGER FUNCTION IFACT(N)	FDF07190
	IFACT=1	FDF07200
	IF(N.LE.1) RETURN	FDF07210
	DO 10 J=2,N	FDF07220
	IFACT=IFACT*J	FDF07230
10	CONTINUE	FDF07240
	RETURN	FDF07250
	END	FDF07260

```

          +++++
        ++++++
      ++++++
    ++++++
  ++++++
-----
I---MASSACHUSETTS INSTITUTE OF TECHNOLOGY---I
-----
III      III      III      III      III
III      III      III      III      III
III      III      III      III      III
III      III      III      III      III
III      III      III      III      III
III      III      III      III      III
-----
=====
===== IPC
=====

```

VM/SP CONVERSATIONAL MONITOR SYSTEM

98

APPENDIX B

FILE: FDSIM FORTRAN A VM/SP CONVERSATIONAL MONITOR SYSTEM

```

C*****FDS00010
C                                           FDS00020
C                                           FDS00030
C           PROGRAM FDSIM SIMULATES CONTINUOUS      FDS00040
C           SYSTEM AND FILTER DYNAMICS              FDS00050
C           FOR FAILURE DETECTION AND IDENTIFICATION FDS00060
C*****FDS00070
C                                           FDS00080
C                                           FDS00090
C INPUT: NSYS - NUMBER OF SYSTEM STATES           FDS00100
C        NFIL - NUMBER OF FILTER STATES           FDS00110
C        NS - NUMBER OF SENSORS                   FDS00120
C        NA - NUMBER OF ACTUATORS                 FDS00130
C        NF - NUMBER OF FAILURE EVENTS            FDS00140
C        IAS - (=1) FOR ACTUATOR FAILURES         FDS00150
C              (=2) FOR SENSOR FAILURES          FDS00160
C        OMU - ACTUATOR INPUT FREQUENCY           FDS00170
C        ISR - SAMPLING RATE (HZ)                 FDS00180
C        NTSEC - INTEGRATION FREQUENCY (HZ)       FDS00190
C        IFAIL - # OF FAILED ACTUATOR OR SENSOR   FDS00200
C        TFAIL - TIME OF FAILURE (SEC)            FDS00210
C        TLAST - TIME OF SIMULATION               FDS00220
C        A - SYSTEM MATRIX                       FDS00230
C        BS - CONTROL EFFECTIVENESS MATRIX FOR SYSTEM FDS00240
C        CS - MEASUREMENT MATRIX FOR SYSTEM      FDS00250
C        CF1 - MATRIX OF OUTPUT ERROR DIRECTIONS FOR FDS00260
C              ACTUATOR FAILURES (COLUMNS ARE VECTORS)
C        D - DETECTOR GAIN                       FDS00270
C        X - INITIAL STATES                      FDS00280
C                                           FDS00290
C                                           FDS00300
C OUTPUT: RE - TRANSFORMED OUTPUT ERROR VECTOR   FDS00310
C*****FDS00320
C                                           FDS00330
C                                           FDS00340
C                                           FDS00350
C        DIMENSION A(20,20),BS(20,10),BF(20,10),CS(10,20),U(10),
&        D(20,10),CF1(10,10),X(40),XDOT(40),E(10),S(10,10),
&        R(10,10),CFTCF(10,10),CFTCFI(10,10),CFTTI(10,10),
&        WK(40),WK1(40,9),RE(10),CIA(24),CF(10,20),
&        XS(20),XF(20),YS(10),YF(10),
&        TIME(5000),RE1(5000),RE2(5000),RE3(5000)
C        EXTERNAL FCN
C        DATA IN,IO,IND,TOL,EPS,NW/9,10,1,0.001,1.E-4,40/
C        COMMON A,BS,BF,CS,CF,D,E,U,OMU,NSYS,NFIL,NA,NS
C        CALL PLOTS(IDUM,IDUM,18)
C        READ(IN,5) NSYS,NFIL,NS,NA,NF,IAS,OMU,ISR,NTSEC,IFAIL,TFAIL,TLAST,
&        ((A(I,J),J=1,16),I=1,16),
&        ((BS(I,J),J=1,8),I=1,16),
&        ((CS(I,J),J=1,16),I=1,8),
&        ((CF1(I,J),J=1,3),I=1,8),
&        ((D(I,J),J=1,3),I=1,16),
&        (X(I),I=1,32)
5  FORMAT(6I3/F10.4/I3/2I3,2F10.4/32(8F10.4/),16(8F10.4/),
&        16(8F10.4/),8(3E16.6/),16(3E16.6/),4(8F10.4/))
C        WRITE(IO,7) NSYS,NFIL,NS,NA,NF,NTSEC,IFAIL,TFAIL,TLAST,
&        ((CF1(I,J),J=1,4),I=1,4).
C                                           FDS00460
C                                           FDS00470
C                                           FDS00480
C                                           FDS00490
C                                           FDS00500
C                                           FDS00510
C                                           FDS00520
C                                           FDS00530
C                                           FDS00540
C                                           FDS00550

```

```

&          ((D(I,J),J=1,4),I=1,4)
7 FORMAT('NSYS=',I2,'NFIL=',I2,5X,'NS=',I2,5X,'NA=',I2,5X,'NF=',I2,5X,
&        'NTSEC=',I3,5X,'IFAIL=',I2,5X,'TFAIL=',F8.3,5X,'TLAST=',
&        F8.3/'CF1='/'4(4E14.4)/'/'D='/'4(4E14.4)/')
NE=NSYS+NFIL
DO 10 I=1,NFIL
  DO 10 J=1,NA
    BF(I,J)=BS(I,J)
10 CONTINUE
  DO 12 I=1,NS
    DO 12 J=1,NFIL
      CF(I,J)=CS(I,J)
12 CONTINUE
  DO 20 I=1,NS
    DO 15 J=1,NF
      S(I,J)=0.
15 CONTINUE
  S(I,I)=1.0
20 CONTINUE
  IF(IAS.EQ.2) GO TO 21
  CALL VMULFM(CF1,CF1,NS,NF,NF,10,10,CFTCF,10,IER)
  CALL LINVF(CFTCF,NF,10,CFTCFI,0,WK,IER)
  CALL VMULFP(CFTCFI,CF1,NF,NF,NS,10,10,CFTTI,10,IER)
  CALL VMULFF(S,CFTTI,NS,NF,NS,10,10,R,10,IER)
  GO TO 24
21 COSGAM=CF1(2,1)/SQRT(CF1(2,1)**2+CF1(3,1)**2)
  SINGAM=CF1(3,1)/SQRT(CF1(2,1)**2+CF1(3,1)**2)
  R(1,1)=1.0
  R(1,2)=0.
  R(1,3)=0.
  R(2,1)=0.
  R(2,2)=COSGAM
  R(2,3)=SINGAM
  R(3,1)=0.
  R(3,2)=-SINGAM
  R(3,3)=COSGAM
24 T=0.
  CALL FCN(NE,T,X,XDOT)
  WRITE(10,25)
25 FORMAT(2X,'TIME',16X,'E1',12X,'E2',12X,'E3'/)
  WRITE(10,30) T,(RE(I),I=1,3)
30 FORMAT(2X,F6.3,10X,3E14.4)
  ILAST=INT(TLAST)*NTSEC
  IPLOT=ILAST
  NFE=NTSEC/ISR
  INDEXE=0
  IWRT=0
  DO 50 K=1,ILAST
    TEND=FLOAT(K)/FLOAT(NTSEC)
C* NEXT STATEMENTS FOR DATA-SAMPLING ONLY
C   INDEXE=INDEXE+1
C   IF(INDEXE.NE.NFE) GO TO 38
C   NP1=NSYS+1
C   DO 32 I=1,NSYS
C     XS(I)=X(I)

```

FDS00560
FDS00570
FDS00580
FDS00590
FDS00600
FDS00610
FDS00620
FDS00630
FDS00640
FDS00650
FDS00660
FDS00670
FDS00680
FDS00690
FDS00700
FDS00710
FDS00720
FDS00730
FDS00740
FDS00750
FDS00760
FDS00770
FDS00780
FDS00790
FDS00800
FDS00810
FDS00820
FDS00830
FDS00840
FDS00850
FDS00860
FDS00870
FDS00880
FDS00890
FDS00900
FDS00910
FDS00920
FDS00930
FDS00940
FDS00950
FDS00960
FDS00970
FDS00980
FDS00990
FDS01000
FDS01010
FDS01020
FDS01030
FDS01040
FDS01050
FDS01060
FDS01070
FDS01080
FDS01090
FDS01100

C	32	CONTINUE	FDSO1110
C		DO 34 I=NP1,NE	FDSO1120
C		XF(I-NSYS)=X(I)	FDSO1130
C	34	CONTINUE	FDSO1140
C		CALL MATVEC(CS,XS,10,20,NS,NSYS,YS)	FDSO1150
C		CALL MATVEC(CF,XF,10,20,NS,NFIL,YF)	FDSO1160
C		CALL VEC(SYS,YF,10,NS,E)	FDSO1170
C		INDEXE=0	FDSO1180
C			FDSO1190
	38	IF(T.LT.TFAIL) GO TO 41	FDSO1200
		IF(IFLAG.EQ.1) GO TO 41	FDSO1210
		IFLAG=1	FDSO1220
		IF(IAS.EQ.2) GO TO 415	FDSO1230
		DO 40 I=1,NSYS	FDSO1240
		BS(I,IFAIL)=0.	FDSO1250
	40	CONTINUE	FDSO1260
		GO TO 41	FDSO1270
	415	DO 416 J=1,NSYS	FDSO1280
		CS(IFAIL,J)=0.	FDSO1290
	416	CONTINUE	FDSO1300
	41	CALL DVERK(NE,FCN,T,X,TEND,TOL,IND,C1A,NW,WK1,IER)	FDSO1310
		IF(IND.LT.0 .OR. IER.GT.0) GO TO 62	FDSO1320
		CALL MATVEC(R,E,10,10,NS,NS,RE)	FDSO1330
		TIME(K)=T	FDSO1340
		RE1(K)=RE(1)	FDSO1350
		RE2(K)=RE(2)	FDSO1360
		RE3(K)=RE(3).	FDSO1370
		IWRT=IWRT+1	FDSO1380
		IF(IWRT.NE.5) GO TO 50	FDSO1390
		WRITE(IO,45) T,(RE(I),I=1,3)	FDSO1400
	45	FORMAT(2X,F6.3,10X,3E14.4)	FDSO1410
		IWRT=0	FDSO1420
	50	CONTINUE	FDSO1430
		CALL PICTUR(8.0,3.0,'TIME(SEC)',9,'ERROR(FT)',9,	FDSO1440
		& TIME,RE1,IPL0T,0.,0.	FDSO1450
		& TIME,RE2,IPL0T,0.,1.	FDSO1460
		& TIME,RE3,IPL0T,0.,2)	FDSO1470
		CALL ENDPLOT(12.0,0.0,999)	FDSO1480
		GO TO 100	FDSO1490
	62	WRITE(IO,75)	FDSO1500
	75	FORMAT('IND<0 OR IER>0')	FDSO1510
	100	STOP	FDSO1520
		END	FDSO1530
C			FDSO1540
C			FDSO1550
C			FDSO1560
		SUBROUTINE FCN(NE,T,X,XDOT)	FDSO1570
		DIMENSION X(NE),XDOT(NE),U(10),BS(20,10),BF(20,10),CS(10,20),	FDSO1580
		& XS(20),XSDOT(20),XF(20),XFDOT(20),YS(10),YF(10),	FDSO1590
		& E(10),D(20,10),A(20,20),AXS(20),AXF(20),BSU(20),	FDSO1600
		& BFU(20),DE(20),AXFBFU(20),CF(10,20)	FDSO1610
		COMMON A,BS,BF,CS,CF,D,E,U,OMU,NSYS,NFIL,NA,NS	FDSO1620
		U(1)=EXP(-0.2*T)*SIN(OMU*T)	FDSO1630
		U(2)=EXP(-0.2*T)*SIN(OMU*T)	FDSO1640
		U(3)=EXP(-0.2*T)*SIN(OMU*T)	FDSO1650
		NP1=NSYS+1	

DO 5 I=1,NSYS	FDS01660
XS(I)=X(I)	FDS01670
XSDOT(I)=XDOT(I)	FDS01680
5 CONTINUE	FDS01690
DO 10 I=NP1,NE	FDS01700
XF(I-NSYS)=X(I)	FDS01710
XFDOT(I-NSYS)=XDOT(I)	FDS01720
10 CONTINUE	FDS01730
CALL MATVEC(A,XS,20,20,NSYS,NSYS,AXS)	FDS01740
CALL MATVEC(BS,U,20,10,NSYS,NA,BSU)	FDS01750
CALL VECP(AXS,BSU,20,NSYS,XSDOT)	FDS01760
CALL MATVEC(A,XF,20,20,NFIL,NFIL,AXF)	FDS01770
CALL MATVEC(CS,XS,10,20,NS,NSYS,YS)	FDS01780
CALL MATVEC(CF,XF,10,20,NS,NFIL,YF)	FDS01790
CALL VEC(SYS,YF,10,NS,E)	FDS01800
CALL MATVEC(D,E,20,10,NFIL,NS,DE)	FDS01810
CALL MATVEC(BF,U,20,10,NFIL,NA,BFU)	FDS01820
CALL VECP(AXF,BFU,20,NFIL,AXFBFU)	FDS01830
CALL VECP(AXFBFU,DE,20,NFIL,XFDOT)	FDS01840
DO 15 I=1,NSYS	FDS01850
XDOT(I)=XSDOT(I)	FDS01860
15 CONTINUE	FDS01870
DO 20 I=NP1,NE	FDS01880
XDOT(I)=XFDOT(I-NSYS)	FDS01890
20 CONTINUE	FDS01900
RETURN	FDS01910
END	FDS01920
C	FDS01930
C	FDS01940
C	FDS01950
SUBROUTINE MATVEC(ARRAY,V,M1,N1,M,N,RET)	FDS01960
DIMENSION ARRAY(M1,N1),V(N1),RET(M1)	FDS01970
DO 10 I=1,M	FDS01980
RET(I)=0.	FDS01990
DO 10 J=1,N	FDS02000
RET(I)=RET(I)+ARRAY(I,J)*V(J)	FDS02010
10 CONTINUE	FDS02020
RETURN	FDS02030
END	FDS02040
C	FDS02050
C	FDS02060
C	FDS02070
SUBROUTINE VECP(V1,V2,N1,N,VADD)	FDS02080
DIMENSION V1(N1),V2(N1),VADD(N1)	FDS02090
DO 5 I=1,N	FDS02100
VADD(I)=V1(I)+V2(I)	FDS02110
5 CONTINUE	FDS02120
RETURN	FDS02130
END	FDS02140
C	FDS02150
C	FDS02160
C	FDS02170
SUBROUTINE VEC(S,V1,V2,N1,N,VSUB)	FDS02180
DIMENSION V1(N1),V2(N1),VSUB(N1)	FDS02190
DO 5 I=1,N	FDS02200
VSUB(I)=V1(I)-V2(I)	FDS02210
5 CONTINUE	FDS02220
RETURN	FDS02230
END	FDS02240

VM/SP CONVERSATIONAL MONITOR SYSTEM

103

FILE: FDSIMS DATA A

VM/SP CONVERSATIONAL MONITOR SYSTEM

-1.30	0.	1.09	0.	0.356	0.	-0.553	0.
1.00	0.	0.00	0.	1.21	0.	0.00	0.
1.41	0.	0.00	0.	1.40	0.	0.00	0.
0.							
0.							
0.							
0.							
0.							
0.							
0.							
0.							
0.							
0.							
0.177572E+02		0.584335E+00		0.105736E+01			
0.584315E+00		0.894988E+01		-0.195613E+01			
0.105725E+01		-0.195635E+01		0.886879E+01			
0.							
0.							
0.							
0.							
0.							
0.214951E+01		0.981505E+01		0.149971E+02			
0.193940E+02		0.627022E+02		0.635415E+02			
-0.560015E+01		-0.487336E+01		0.688610E+01			
-0.383867E+02		-0.486003E+02		-0.240117E+01			
-0.586796E+01		0.119337E+01		0.746371E+01			
-0.207824E+02		0.113480E+02		0.575569E+02			
0.575753E+01		-0.985363E+01		-0.165995E+02			
-0.884495E+02		0.587169E+02		-0.434314E+03			
0.294047E-01		0.362257E+01		0.562981E+02			
-0.484272E+03		0.117701E+04		0.569748E+03			
0.0		0.0		0.0			
0.0		0.0		0.0			
0.0		0.0		0.0			
0.0		0.0		0.0			
0.0		0.0		0.0			
0.0		0.0		0.0			
0.0		0.0		0.0			
0.	0.	0.	0.	0.	0.	0.	0.
0.	0.	0.	0.	0.	0.	0.	0.
0.	0.	0.	0.	0.	0.	0.	0.
0.	0.	0.	0.	0.	0.	0.	0.
0.							

References

1. Beard, R.V., "Failure Accommodation in Linear Systems Through Self-Reorganization," Ph.D. Thesis, Dept. of Aeronautics and Astronautics, M.I.T. Cambridge MA, Feb. 1971.
2. Jones, H.L., "Failure Detection in Linear Systems," Ph.D. Thesis, Dept. of Aeronautics and Astronautics, M.I.T. Cambridge MA, Aug. 1973.
3. Meserole, J.S., "Detection Filters for Fault-Tolerant Control of Turbofan Engines," Ph.D. Thesis, Dept. of Aeronautics and Astronautics, M.I.T., Cambridge MA, June 1981.
4. Cole, S.R., Horner, G., and Montgomery, R., "Finite Element Analysis of Experimental Beam," NASA Langley Research Center, 1980.
5. Major, C.S., "A Demonstration of the Use of Generalized Parity Relations for Detection and Identification of Instrument Failures on a Free-free Beam," M.I.T. Space Systems Lab., Report #28-81, Sept. 1981.
6. VanderVelde, W.E., and Carignan, C.R., "A Dynamic Measure of Controllability and Observability for the Placement of Actuators and Sensors on Large Space Structures," M.I.T. Space Systems Lab., Report #2-82, Jan. 1982.
7. Balas, M.J., "Active Control of Flexible Systems," Proc. of Dynamics and Control of Large Flexible Spacecraft Symposium, Blacksburg VA, June 1977.

8. VanderVelde, W.E., "Application of Failure Detection Filter Theory to Reliable Longitudinal Control of Guideway Vehicles," Report for U.S. Dept. of Transportation Contract No. DOT-TSC-1445, M.I.T. Cambridge MA, March 1979.
9. Gerard, J.P., "Application of Failure Detection Theory to Longitudinal Control of Guideway Vehicles," M.S. Thesis, Dept. of Aeronautics and Astronautics, M.I.T., Cambridge MA, June 1978.
10. Gustafson, D.E., and Speyer, J.L., "Linear Minimum Variance Filters Applied to Carrier Tracking," Trans. on Auto. Control, Vol. AC-21, No. 1, Feb. 1976.
11. VanderVelde, W.E., "Reliability Issues in Active Control of Flexible Space Structures," Workshop on Structural Dynamics and Control of Large Space Structures, NASA Langley Research Center, Oct. 1980.

